Assessment of the Fate of Manganese in Oxide-Coated Filtration Systems

by

Andrea L. Crowe

Thesis submitted to the Faculty of the

Virginia Polytechnic Institute and State University

in partial fulfillment of the requirements for the degree of

MASTER OF SCIENCE

IN

ENVIRONMENTAL ENGINEERNG

APPROVED:

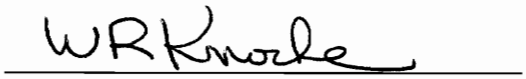

Dr. William Knocke, Chairman

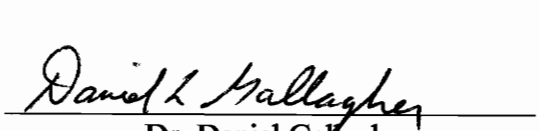

Dr. Daniel Gallagher

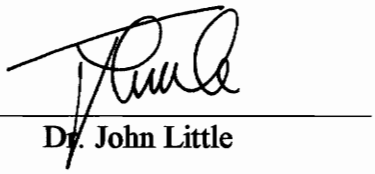

Dr. John Little

January 24, 1997

Blacksburg, Virginia

Keywords: Manganese, Oxide, Coating, Filter, Media, Backwash, Water Treatment

ASSESSMENT OF THE FATE OF MANGANESE IN OXIDE-COATED FILTRATION SYSTEMS

by

Andrea L. Crowe

Dr. William Knocke, Chairman

Department of Environmental Engineering

(ABSTRACT)

This study examined the fate of manganese in manganese oxide ($MnO_x(s)$) coated filter media. Specific objectives of the project included the following:

1. Determination of the effect of influent pH upon Mn(II) sorption and oxidation and upon the physical characteristics of the coating on the media.
2. Determination of the effect of backwash rate upon $MnO_x(s)$ coatings.
3. Examination of the effect of air scour upon $MnO_x(s)$ coatings.
4. Observation of the effect of an increasing $MnO_x(s)$ coating on the physical characteristics of anthracite coal filter media.
5. Development of an overall mass balance on manganese loading and accumulation on the filter media.

Resolution of the stated objectives involved construction, optimization, and continuous operation of a pilot-scale filtration system for the purpose of removing manganese from filter-applied water. The pilot-scale filter system functioned like a typical water treatment plant filtration system with similar hydraulic loading rates, influent manganese concentrations, free chlorine dosage, filter media bed depths, filter run times, and backwash rates.

With regard to the fate of manganese in $MnO_x(s)$-coated filter media, it was determined that as long as free chlorine was present to oxidize sorbed manganese, manganese continued to accumulate and remained on the media in sufficient

concentrations to promote continual removal of soluble Mn(II). While oxide coating that was susceptible to breakage was removed in backwash, some portion of coating remained on the media. The combination of $MnO_x(s)$ accumulation during filtration and its partial removal during backwash maintained a net amount of $MnO_x(s)$ coating optimal for catalyzing further manganese removal and, yet, did not hinder filtration for turbidity by significantly altering the size of the media.

The results of the pilot-scale study also indicated the following pertinent conclusions:

1. Neutral or slightly acidic pH conditions ($7 \geq pH \geq 6$) inhibited Mn(II) oxidation before filtration and, instead, promoted sorption and oxidation of Mn(II) on $MnO_x(s)$-coated media. Alkaline filter influent pH ($pH > 7$) allowed some Mn(II) oxidation before filtration, resulting in significant manganese removal by $MnO_x(s)$ particle filtration.
2. Although the intent of $MnO_x(s)$-coating on the filter media was to remove influent Mn(II) from filter-applied water, $MnO_x(s)$ that was removed by particle filtration also provided $MnO_x(s)$ surface area within the filter and, thus, additional sorption sites for Mn(II) removal.
3. Increases in fluid backwashing rate tended to produce greater amounts of $MnO_x(s)$ release from filter media for the duration of these backwash operations. However, backwashing did not result in complete $MnO_x(s)$ release from the media surface; rather, there was always sufficient $MnO_x(s)$ retained to permit efficient soluble Mn(II) removal after the filtration operations were restarted.

Removal of soluble Mn(II) by sorption and oxidation proved to be a dependable, low-maintenance Mn(II) removal technique that worked well within a wide range of raw water influent conditions. Because the process is cost-effective and easily integrated into new or existing water treatment facilities, it is an economical and competitive alternative for removal of soluble Mn(II).

Acknowledgments

My sincere thanks goes to Dr. Knocke for his support as my major advisor. His enduring patience and timely assistance throughout the duration of the research and thesis composition have been very much appreciated. Thanks also to my other committee members: Dr. Gallagher, whose tremendous computer knowledge saved me in many a computer crisis; and Dr. Little, whose unfailing eagerness in gaining new knowledge was an encouragement just to keep working.

Thanks to the National Science Foundation for funding the entire project entitled *Development and Field Verification of Sorption/Oxidation Models for Soluble Manganese Removal by Oxide-Coated Filtration Systems*, of which this portion was the examination of the fate of surface adsorbed/oxidized Mn(II). Thanks also to the Trustees of the Edna Bailey Sussman Fund, who graciously provided the funds for research during the summer of 1994.

I am especially grateful to the Blacksburg, Christiansburg, VPI Water Authority for providing the facilities necessary for the pilot-size apparatus. Jerry Higgins, Manager, and all the Operators provided the water, filter media, and space needed for the project, as well as an immense amount of help and materials in the construction of the apparatus. Everyone helped me watch over the system throughout the duration of the project, and they allowed me to use their facilities as if I was a regular employee. They also taught me much of what I know about operating a water treatment plant. My best friends in graduate school were at the water treatment plant. I miss you guys.

I also wish to acknowledge my family, whose attentive love and support gave me the strength and encouragement to carry the project to completion. I consider myself blessed from birth with more than I ever could have hoped for in a family.

Lastly and most importantly, I thank the LORD for these many blessings and successes. I dedicate all to His glory and honor.

Table of Contents

List of Figures

Page

Page

List of Tables

Page

List of Exhibits

Introduction

Manganese found in water sources such as groundwater and the hypolimnetic regions of lakes and reservoirs frequently exceeds the secondary maximum contaminant level (SMCL) of 0.05 $^{mg}/_{L}$ for potable finished water (Coffey, *et al.*, 1993; Knocke, *et al.*, 1988; Knocke *et al.*, 1989). Concerns with manganese are predominantly aesthetic concerns that include taste, color, and odor problems, staining of plumbing fixtures and laundry, and increased turbidity. More serious but less likely problems include clogging of pipelines and promotion of biological growth within distribution systems. In addition to encouraging biological growth, the biological activity within a treatment plant or distribution system, in turn, may release more reduced (dissolved) manganese into solution in an anaerobic environment and further cultivate the reaction (Knocke, *et al.*, 1989). Although manganese is not directly responsible for adverse health effects due to poor water quality, it certainly contributes to public scrutiny of the water supply industry and may be an indicator of inadequate water treatment.

Removal of soluble manganese (Mn(II)) by adsorption onto manganese oxide ($MnO_x(s)$) coated filter media and subsequent oxidation by free chlorine to $MnO_x(s)$ is an effective continuous removal technique for manganese-laden waters. However, previous research has not addressed the fate of surface adsorbed/oxidized manganese or its physical effects upon filter media. In full-scale water treatment facilities that practice this type of Mn(II) removal during filtration, the sorption/oxidation process has produced neither cementing effects nor noticeable media growth due to continuous layering of manganese oxides. Since manganese breakthrough does not seem to be a problem when removing Mn(II) in this manner, filter backwashing has been proposed as the reason for a relatively slight accumulation of $MnO_x(s)$ upon the media in comparison to the amount of manganese removed from the influent water. Agitation during backwash may remove the

oxide coating from the media, or manganese may desorb and redissolve in manganese-free backwash water, resulting in little net oxide accumulation.

The main objective of the research presented herein was to assess the fate of surface adsorbed/oxidized Mn(II) on MnO_x(s) coated filter media. Several of the operating parameters under investigation were varied, however, resulting in the following components of the main objective:

1. Determination of the effect of influent pH upon Mn(II) sorption and oxidation and upon the physical characteristics of the coating on the media.
2. Determination of the effect of backwash rate upon the MnO_x(s) coating.
3. Examination of the effect of air scour upon the MnO_x(s) coating.
4. Observation of the effect of an increasing MnO_x(s) coating on the physical characteristics of anthracite coal filter media.
5. Development of an overall mass balance on manganese loading and accumulation on the filter media.

Resolution of the stated objectives aided in identifying treatment techniques and operating procedures for a variety of water treatment plants and water treatment schemes. The operational flexibility afforded in the design of a typical water treatment facility allows optimization for manganese removal with few changes in chemical dosage and in location of chemical addition. For this reason, soluble Mn(II) removal by sorption and oxidation onto MnO_x(s) coated filter media may be easily integrated into the water treatment process at virtually any utility.

Literature Review

The literature review chapter presents a compilation of previous research by others that deals with topics similar to those included in the scope of the present study. Much of the information presented is essential for understanding the hypotheses and objectives for the project. The methods of operation, experimentation, and testing presented in the methods and materials chapter were based upon previous studies and experimental methods that indicated the chemistry of manganese removal by sorption and oxidation and the mechanics involved in operating and backwashing filters.

Specific subsections of the literature review include solid and aqueous phase manganese species, conventional treatment options for manganese removal, manganese removal by sorption and oxidation within filters, pH effects on sorption and oxidation, oxidants, the role of manganese oxide ($MnO_x(s)$) coatings in soluble manganese (Mn(II)) removal, physical characteristics of $MnO_x(s)$ coatings, natural $MnO_x(s)$ coatings in the geological environment, the effect of $MnO_x(s)$ coatings on filter media, mechanics of filter backwashing, and the effects of air scour on $MnO_x(s)$ coatings.

Solid and Aqueous Phase Manganese Species

Forms of manganese within raw water sources span a broad range of oxidation states, species, and sizes from strictly soluble electroactive manganese (Mn(II)) to non-electroactive colloidal oxyhydroxides of various sizes and oxidation states to the larger highly oxidized particulate forms (De Vitre *et al.*, 1988; Knocke *et al.*, 1988; La Zerte and Burling, 1990). In most freshwaters with pH 7-8, manganese is predominantly present as soluble $Mn(II)_{aq}$ (De Vitre *et al.*, 1988); in fact, the aqueous Mn(II) form is the most common valence found within the entire pE-pH range of typical natural waters (Knocke *et*

al., 1988). However, geological research identifies other manganese species and valence states dependent on the aerobic status of various depth regions in lakes and reservoirs.

Particulate and colloidal species usually inhabit the upper portions of a lake or reservoir while colloidal and electroactive (soluble) species dominate the lower regions (De Vitre *et al.*, 1988). The metalimnion contains mostly colloidal manganese species (La Zerte and Burling, 1990). Within the colloidal speciation, though, particle size decreases with increasing depth to the point where some of the colloidal manganese passes a 0.45 micron filter, and, yet, is non-electroactive as compared to electroactive Mn(II). Generally, most literature sources term the amount of manganese passing through a 0.45 micron filter as soluble and, thus, electroactive Mn(II) (De Vitre *et al.*, 1988).

De Vitre *et al.* (1988) used a polarographic technique to distinguish between electroactive manganese, which they termed soluble, and non-electroactive manganese, which they termed colloidal, up to a maximum diameter of 0.45 microns. The size of fifty nanometers became the distinction between soluble and colloidal manganese species. The authors compared polarographic data with those concentrations determined by syringe filtration and subsequent atomic absorption spectrophotometric analysis (detection limit 2 $^{\mu g}/_{L}$) to find that "field filtration, using syringes, yields size distributions which do not really correspond to the true particle sizes, because of retention factors other than particle diameter. However, filtration may be used as an operational tool to define two broad size classes."

Particulate manganese oxide ($MnO_x(s)$) forms as a result of soluble manganese diffusion into the upper oxygenated regions of a lake (i.e. autochthoneous regions). The maximum concentration of manganese particulates occurs at the depth at which photosynthesis (oxygen production) is most intense. Conversely, $MnO_x(s)$ redissolves as it settles back into decreasing pE regimes containing limited dissolved oxygen ($O_2(aq)$). Therefore, another manganese concentration peak results at a greater depth where reducing conditions promote dissolution to Mn(II). Raw water intakes are commonly

located at or near one of these two manganese concentration peak depths (De Vitre *et al.*, 1988).

Conventional Treatment Options for Manganese Removal

Conventional treatment of waters for manganese removal or mitigation includes the following options: oxidation and settling of the manganese precipitate followed by filtration of any residual manganese precipitate; removal by manganese greensand; or sequestering soluble manganese by addition of polyphosphates or sodium silicate. In the oxidation/settling/filtration process, a strong oxidant such as potassium permanganate ($KMnO_4$), chlorine dioxide (ClO_2) or ozone (O_3) is added at the outset of treatment under alkaline pH conditions to oxidize the manganese to an insoluble form that settles during sedimentation and/or filters out (Knocke *et al.*, 1988; Knocke *et al.*, 1989). Failure in this sort of removal is often due to colloidal $MnO_x(s)$ penetrating the filters and escaping into the distribution system (Knocke *et al.*, 1988). However, other treatment plant difficulties result from this type of treatment approach. Excessive amounts of $MnO_x(s)$ precipitates tend to bind filter media (Bratby, 1988). Also, the oxidation efficiency of potassium permanganate is adversely affected in the presence of high total organic carbon, low oxidation pH, or low temperatures (Knocke *et al.*, 1989); however, the increased desire for organics removal at acidic pH values and with lower oxidant doses makes manganese removal necessary under these conditions (Knocke *et al.*, 1988). Also, if anaerobic reducing conditions develop within the sedimentation basin, oxidized manganese will reduce again to the soluble Mn(II) form for transport out of the sedimentation basin (Hoehn *et al.*, 1987), and, possibly, through the filters into the distribution system.

Manganese greensand is a zeolite mineral that has become popular for removing soluble Mn(II) by one of two mechanisms that are briefly described here (Knocke *et al.*, 1989). Usually, $KMnO_4$ is the oxidant of choice for Mn(II) treatment by pressure filtration through greensand. Upon contact with $KMnO_4$, soluble Mn(II) rapidly oxidizes

to $MnO_x(s)$, of which even the colloidal fraction is removed in the tiny pore spaces of manganese greensand. Residual $KMnO_4$ then regenerates occupied sorption sites within the greensand. Alternatively, if the $KMnO_4$ dose is less than that stoichiometrically required, the manganese greensand provides sites for soluble manganese Mn(II) sorption and removal. A combination of these two mechanisms is necessary for continuous manganese removal because occupied greensand sites must be regenerated in order to continue effective removal, or intermittent regeneration with $KMnO_4$ is required (Griffin, 1960; Knocke *et al.*, 1989).

Sequestering of soluble manganese by polyphosphate (Griffin, 1960; Knocke *et al.*, 1989; Robinson *et al.*, 1987) or sodium silicate (Robinson *et al.*, 1987) addition is a viable alternative to removal but is generally used only when the water supply is unfiltered (O'Connor, 1971). These chemicals stabilize both soluble Mn(II) and soluble iron (Fe(II)) in solution so that they do not oxidize in the distribution system and precipitate out of solution as solid brown particles (Griffin, 1960; Knocke *et al.*, 1989). However, treatment of this sort is appropriate only when total metal concentrations do not exceed 1 $^{mg}/_{L}$. Polyphosphate addition must take place before any oxidants are applied because it will not stabilize precipitated ferric hydroxide. Polyphosphate dosage should also not be greater than 10 $^{mg}/_{L}$ because of the potential for the phosphorus to stimulate bacteria growth in the distribution system. The chlorine residual concentration must also be great enough to control the bacteria. Also, when water is heated, the polyphosphate turns to orthophosphate and loses its sequestering power, introducing the possibility for sedimentation in hot water heaters and generators (O'Connor, 1971).

Manganese Removal by Sorption and Oxidation Within Filters

Sorption

Stumm and Morgan (1970) reported that highly oxidized forms of manganese were characterized by high specific surface areas, such as 300 m^2/g for δMnO_2. These hydrous oxides are able to interact with cations, especially at alkaline pH values above the zero point of charge. The authors determined that sorption of Mn(II) to manganese oxides was surface complex formation or ion exchange, where hydrogen ions or other cations were released while Mn(II) was adsorbed.

Soluble Mn(II) has an increased opportunity to adsorb onto filter media as a result of hydrodynamic retardation, which is the deceleration of a particle as it approaches a collector (Amirtharajah, 1988). As the fluid channel narrows, the velocity of fluid flow decreases (Tobriason and O'Melia, 1988), and this phenomenon provides a momentary quiescent environment for sorption to take place.

When no oxidant is present, Mn(II) removal is accomplished by adsorption alone, until all the available sorption sites are occupied (Knocke *et al.*, 1989). As early as 1946, manganese removal upon oxide-coated media was observed at the Montebello Filters, Baltimore, Maryland. Using 18 inches of coated sand, they removed manganese from raw water without any other treatment for 24 to 36 hours. Afterwards, they used a strong chlorine solution to regenerate the media and, again, removed manganese in the filters for 24 to 36 hours before exhaustion in an effort to prove that catalysis was responsible for soluble manganese removal (Edwards and McCall, 1946). Also, Knocke *et al.* (1991) reported that standard filters of depths of 24 to 30 inches may remove Mn(II) for a month or longer before exhaustion.

Concern has been expressed about the reliability of hydrous oxide coatings to retain soluble manganese due to its slow oxidation rate (Robinson *et al.*, 1987). However, sorption capacity is a direct function of the number of available sorption sites upon the

media (Knocke *et al.*, 1989). In the most recent experiments involving manganese uptake rates and sorption capacity within continuously regenerated media, media depth profiles indicate that the majority of influent manganese is removed within the first 3 to 6 inches of filter depth, even during rapid filtration (Knocke *et al.*, 1988; Knocke *et al.*, 1991). Depth profiles of manganese solution concentrations as they pass through a filter indicate the same solution concentration profile within the filter after several hours of filtration as at the beginning of the filter cycle (Coffey *et al.*, 1993). Figure 1 shows manganese concentrations in the influent, effluent, and 3-inch media depth sample port (top port). The throughput volume of 200 L corresponds to a loading period of 3.5 hours at a filtration rate of 5.1 $^{gpm}/_{ft^2}$. If the manganese coating was not sufficiently regenerated, the solution concentration profiles would increase with depth as filtration progressed. Also, media depth profiles would indicate increasing amounts of $MnO_x(s)$ coating at greater depths within the filter.

The following increased the rate of manganese uptake: an increased number of sorption sites, an increase in solution pH, an increase in surface $MnO_x(s)$ concentration, and the presence of free chlorine. The Mn(II) sorption uptake rate constant increases with increasing pH, possibly because of the increased negative surface charge on $MnO_x(s)$ which makes available more sites for adsorption. Knocke *et al.* (1989) found that the removal capacity of $MnO_x(s)$-coated media was not a function of the amount of oxide coating on the media but was a function of the number of sites available for sorption. However, larger amounts of coating had a greater removal efficiency for a longer time than lesser amounts of coating subjected to the same loading conditions. Highly oxidized forms of manganese coating also had greater removal efficiency than those manganese forms not completely oxidized. Acidic pH values were detrimental to soluble Mn(II) uptake. The authors also illustrated experimentally that a similar number of sorption sites could be available under the following two contrasting conditions: operation at a fairly low pH with a large surface oxide concentration, or operation at a higher pH with a smaller surface oxide concentration. Decreased temperatures did not affect the Mn(II)

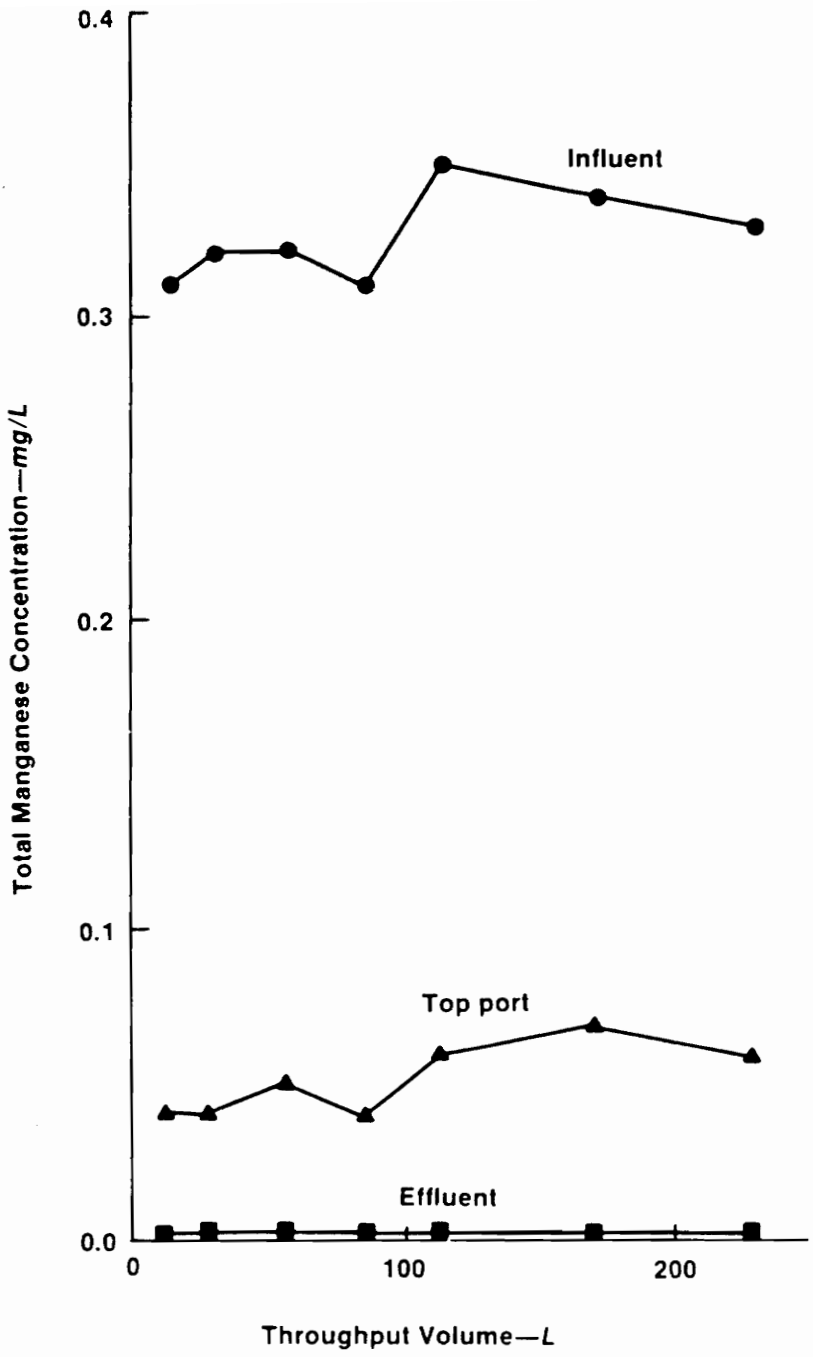

Figure 1. Mn removal characteristics under high-rate loading conditions (pH = 8.0; HOCl = 1 mg as Cl_2/L; 5.1 $^{gpm}/_{ft^2}$; filter medium from plant 1)
(After Knocke *et al.*, 1988)

sorption rate onto the oxide-coated media, although it did hinder bulk solution Mn(II) oxidation to the colloidal $MnO_x(s)$ form with strong oxidants.

Equations Describing Mn(II) Sorption and Oxygenation

The equations following describe first soluble Mn(II) oxidation to form an original oxide coating; second, sorption of soluble Mn(II) onto the original coating; and, third, oxidation of the sorbed manganese to form additional $MnO_x(s)$ coating (Coffey *et al.*, 1993; Knocke *et al.*, 1989):

$$Mn^{2+} + {}^1/_2\, O_2 + H_2O \longrightarrow MnO_2(s) + 2H^+ \qquad (1)$$

$$Mn^{2+} + MnO_2(s) \longrightarrow Mn^{2+}{\cdot}MnO_2(s) \qquad (2)$$

$$Mn^{2+}{\cdot}MnO_2(s) + {}^1/_2\, O_2 + H_2O \longrightarrow 2MnO_2(s) + 2H^+ \qquad (3)$$

The first and last reactions are the rate determining reactions because of the slow oxidation rate of manganese. The second reaction, which is the sorption reaction, is the rapid, autocatalytic phase of manganese removal.

Coffey *et al.* (1993) found that Nakanishi modeled manganese removal in a slightly different format with the following reactions:

$$Mn^{2+} + MnO(OH)_2(s) \longleftrightarrow MnO_2MnO(s) + 2H^+ \qquad (4)$$

$$MnO_2MnO(s) + HOCl \longleftrightarrow 2MnO_2(s) + H^+ + Cl^- \qquad (5)$$

Coffey *et al.* (1993) then developed a model for the reaction rate of overall soluble manganese removal described by the following:

$$-d[Mn^{2+}]/dt = k_0[Mn^{2+}] + k_1[Mn^{2+}][MnO_2(s)] \quad (6)$$

where k_0 = oxidation rate constant
k_1 = adsorption rate constant

Aqueous Mn(II) transforms completely to MnO_2 with the use of oxidants by the following process (Stumm and Morgan, 1970) :

$$\underset{}{Mn(II)(aq)} \longrightarrow \underset{\text{(hausmannite)}}{Mn_3O_4} \longrightarrow \underset{\text{(feitknechtite)}}{\beta MnOOH} \rightarrow \underset{\text{(manganite)}}{\gamma MnOOH} \rightarrow \underset{\text{(manganate)}}{\delta MnO_2} \longrightarrow \underset{\text{(nsutite)}}{\gamma MnO_2}$$

pH Effects on Sorption and Oxidation

Previous research indicates that Mn(II) sorption is intimately dependent upon the pH of manganese-containing influent waters. Alkaline pH conditions promote efficient removal of Mn(II) by sorption with or without addition of an oxidant (Knocke *et al.*, 1988). Effective removal by oxidation with chlorine and filtration by particle removal, however, requires influent pH values of at least 8.0 to 8.5 (DeVitre *et al.*, 1988; Knocke *et al.*, 1988) and up to 9.5 (Bratby, 1988).

Under acidic conditions and without the presence of an oxidant, manganese removal by sorption ceases once available sorption sites are saturated (Knocke *et al.*, 1988; Knocke *et al.*, 1989). The ability of $MnO_x(s)$ to remove soluble Mn(II) decreases significantly even at pH 5 to 7; the removal rate slows by 80% at pH 6 as compared to pH 8. Decreasing pH for treating organics, then, may be detrimental to soluble Mn(II) removal when no oxidant is present. Also, the removal potential of oxide-coated media decreases when the coating is in the low-oxidized form [$MnO_{1.4\text{-}1.6}(s)$] found under acidic

pH conditions rather than the highly oxidized form [$MnO_{1.8\text{-}2.0}$(s)]. This removal potential decrease is referred to as exhausting the sorptive removal capacity. The capacity may be restored by simply contacting the media with a strong oxidant such as $KMnO_4$ (Knocke *et al.*, 1988). If a filter is out of service for some time, reducing conditions may develop causing MnO_x(s) to redissolve into Mn(II) so that the first water through the filter contains soluble manganese. If such reducing conditions are suspected, the filter should be backwashed before use (Knocke *et al.*, 1991).

Manganese removal capacity increases with increasing pH. Above pH 7, removal capacities approach 0.5 moles Mn(II) per mole of MnO_x(s) coating (Knocke *et al.*, 1989; Morgan and Stumm, 1964). The manganese uptake rate intensifies with increasing pH due to the enhanced negative charge upon the oxide surface. Also, as influent water pH increases, the decreased hydrogen ion concentration in the water forces the oxide coating to release H^+, providing additional sorption sites for the Mn(II) (Knocke *et al.*, 1989).

Morgan and Stumm (1964) observed the stability of MnO_2 colloidal suspensions by alkalimetric pH adjustment procedures. They determined a zero point of charge of 2.8 $\pm$ 0.3, above which the surface charge becomes progressively more negative. An increase in pH decreases the concentration of the competing H^+ ion, thus improving the affinity of the MnO_x(s) surface for Mn(II) sorption (Knocke *et al.*, 1991).

Oxidants

Comparison of Chlorine and Other Oxidants

Although chlorine is the oxidant of choice for manganese removal by sorption and oxidation within filters, the following oxidants are also used: potassium permanganate, chlorine dioxide, and ozone (Knocke *et al.*, 1989). Because these oxidants are stronger than chlorine, they oxidize manganese immediately to a colloidal form which is more likely to penetrate filters, especially just after backwashing before the filter is ripe (Knocke *et al.*, 1988). Combined chlorine residuals, on the other hand, will not oxidize manganese

because of their low oxidizing potential. If manganese oxidation is not desired, weak oxidants like chloramines are beneficial (Griffin, 1960).

When chlorine is the oxidant during filtration, backwashing reclaims only a small part of the manganese deposited on the anthracite filter media. However, when a stronger oxidant oxidizes the manganese, a greater percentage of the deposited manganese is released during backwash. Table 1 illustrates the relationship between oxidant strength, the species of manganese accompanying that oxidant to the filter, and the percent of manganese recovered during the subsequent backwash. Evidently, chlorine oxidizes soluble Mn(II) after it has sorbed onto the existing oxide coating, whereas stronger oxidants oxidize much of the manganese before contact with the filter, which results in particle deposition instead of sorption. Trapped $MnO_x(s)$ particles backwash easily out of the filter as compared to the $MnO_x(s)$ coating that is attached to the filter media (Knocke *et al.*, 1988).

Chlorine

Although chlorine aids in manganese removal within a filter at pH $\geq$ 6.1, chlorine does not routinely oxidize manganese (Mn(II)) before filtration (Knocke *et al.*, 1988; Knocke *et al.*, 1989). Instead, chlorine oxidizes previously sorbed manganese on the oxide coating and regenerates the media for further sorption (Knocke *et al.*, 1989). According to Knocke *et al.* (1988), filter-applied water in chlorine oxidation studies typically contains more than 98 percent soluble manganese in separation by ultrafiltration.

The theoretical stoichiometric amount of chlorine required for manganese oxidation is 1.3 milligrams free chlorine as Cl_2 per milligram Mn(II) (Knocke *et al.*, 1988). However, soluble manganese sorption is rapid with filter influent chlorine concentrations between 1 and 2 $^{mg}/_{L}$ as Cl_2 (Knocke *et al.*, 1989). Studies using both greater and less than stoichiometrically required chlorine concentrations showed that the greater-than-required chlorine concentrations exhibited a greater-than-required oxidant demand,

Table 1. Manganese Recovery During Backwash

(After Knocke *et al*., 1988)

Oxidant	Mn Applied to Filter	Percent Mn Recovered
HOCl	> 98% soluble	Average = 15 Range = 2 - 37
KMnO4	20% soluble 80% oxidized	Average = 59 Range = 40-91

whereas the less-than-required chlorine concentrations (< 1 $^{mg}/_{L}$ as Cl_2) exhibited a less-than-required oxidant demand evident from residual chlorine in the effluent. In the first case, the increased free chlorine was regenerating the $MnO_x(s)$ coating to higher oxidation states. In the second case, the sorptive capacity of the media was removing manganese without complete oxidation. Neither situation allowed manganese to escape in the effluent (Knocke *et al.*, 1988).

In a study of sorption kinetics, as the free chlorine concentration increased, the manganese uptake rate constant (k) also increased approximately linearly to the chlorine concentration. According to Knocke *et al.* (1989), an increased chlorine concentration more quickly oxidizes sorbed manganese, which keeps the maximum number of surface sites available for adsorption. The enhanced adsorptive capability causes the momentary concentration of Mn(II) near the media surface to be lower compared to that of the surrounding solution. The resultant gradient established attracts Mn(II) to the media surface, enhancing the overall rate of removal. In other words, the sooner an occupied sorption site is regenerated, the sooner it is again available for sorption, and the increased Mn(II) concentration gradient between the oxide coated media and the influent water promotes earlier removal within the filter. Manganese removed in this manner tends to remain on the media without significant removal during backwash (Knocke *et al.*, 1988).

The Role of Manganese Oxide Coatings in Mn(II) Removal

As early as 1960, the water treatment industry began to realize that a manganese dioxide coating was necessary for manganese removal by filtration (Griffin, 1960). When water treatment facilities replace filter media, they should consider treating the new media to add a synthetic oxide coating by contact first with a soluble manganous sulfate solution and then a highly concentrated hypochlorite or potassium permanganate solution (Knocke *et al.*, 1988). In this way, the media will remove manganese during the first several weeks

or months of treatment instead of merely forming the initial oxide coating during this time and allowing manganese to escape the filters as would normally occur.

A treatment facility in Brazil that was removing high concentrations of manganese and iron in the filters tried to chemically clean the media with sodium sulfite ($NaSO_3$), sodium hydroxide (NaOH), hydroxylamine hydrochloride ($NH_2OH{\cdot}HCl$), and sulfuric acid (H_2SO_4) at pH < 1.0. They observed no effect with $NaSO_3$ or NaOH, but both $NH_2OH{\cdot}HCl$ at >0.01% solution and four-hour contact with H_2SO_4 at pH < 2.0 successfully removed much of the oxide coating. However, that treatment facility also claimed that it was unnecessary and undesirable to remove all of the oxide coating because of its benefit in catalyzing the precipitation reactions within the filter (Bratby, 1988).

Physical Characteristics of $MnO_x(s)$ Coatings

A $MnO_x(s)$ coating upon filter media changes the physical appearance and color of the media. The effect is more obvious on sand than on anthracite coal because the original light sand color is covered with black $MnO_x(s)$, referred to as filter seasoning or aging (Griffin, 1960). Efficient Mn(II) removal does not take place until this coating exists (Knocke *et al.*, 1988).

Both physical and chemical sorption characteristics potentially vary according to the type of oxidant used to oxidize the sorbed manganese. Knocke *et al.* (1989) found a decreased sorption capacity for a $MnO_x(s)$ surface generated by permanganate oxidation as compared to Morgan and Stumm who produced a manganese dioxide coating ($MnO_2(s)$) under increased alkaline pH conditions with oxygen. It should be noted that the oxide surface does not auto oxidize sorbed Mn(II); the oxidant present or added later oxidizes the sorbed Mn(II) to $MnO_x(s)$. Physical characteristics of the $MnO_x(s)$ coating may vary by thickness, strength, and configuration (i.e. layered or patchy).

Figure 2 illustrates the effect of the $MnO_x(s)$ coating on anthracite coal filter media. Photograph A is a $MnO_x(s)$-coated anthracite grain. Photograph B is a similar

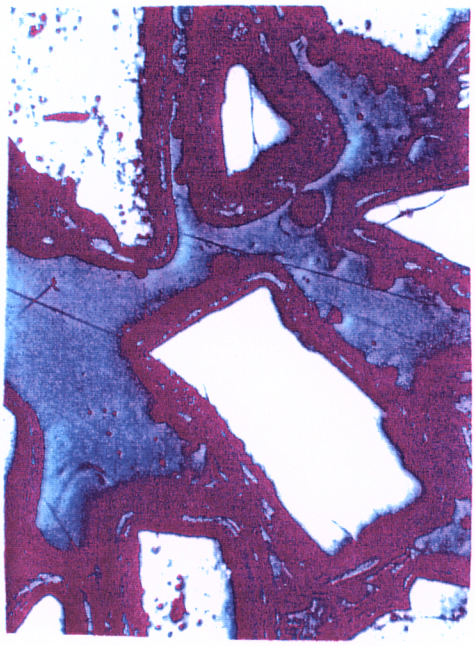

Photograph A. Filter Media with $MnO_x(s)$ Coating.

Photograph B. Filter Media with $MnO_x(s)$ Coating Chemically Removed.

Figure 2. $MnO_x(s)$ Coating on Anthracite Filter Media. (After Merkle *et al.*, 1996).

anthracite grain from which the $MnO_x(s)$ coating has been chemically removed.

Natural Manganese Oxide Coatings in the Geological Environment

Geological studies have shown that natural manganese oxide coatings develop at a retarded rate when soluble manganese is available for sorption. In a natural setting, manganese deposition has a similar pH dependency in that an increased precipitate thickness corresponds to an increase in pH (Junta and Hochella, 1994).

Original sorption is most likely to occur at the "top or base of steps" or discontinuities in the substrate accepting the manganese as illustrated in Figure 3. After initial sorption and oxidation, that coated site becomes the most reactive site for further sorption. According to Junta and Hochella (1994), manganese precipitate growth may be controlled by the substrate or the precipitate. In substrate-controlled growth, a $MnO_x(s)$ layer forms and covers the substrate before the oxide coating itself begins to adsorb Mn(II) and increase in thickness. In precipitate controlled growth, the substrate has minimal appropriate sorption and growth sites. The initial precipitate forms in a discontinuity and continues sorption and oxidation upon itself to form patches of manganese oxide. Evidently, the geometric character of the substrate instead of the surface composition determines the rate of Mn(II) sorption and oxidation during the initial stages of deposition.

The major difference in the geological manganese studies and in filter media studies is the strength of the oxidant and the resulting oxidation state of the manganese oxide coating. In geological studies, atmospheric $O_2(g)$ and dissolved $O_2(aq)$ are the primary oxidants, which are both weaker than the free chlorine employed in filtration studies. As a result, the highest manganese oxidation state found in the geological studies was Mn(III) as in the oxyhydroxide form (MnOOH) (Junta and Hochella, 1994). A

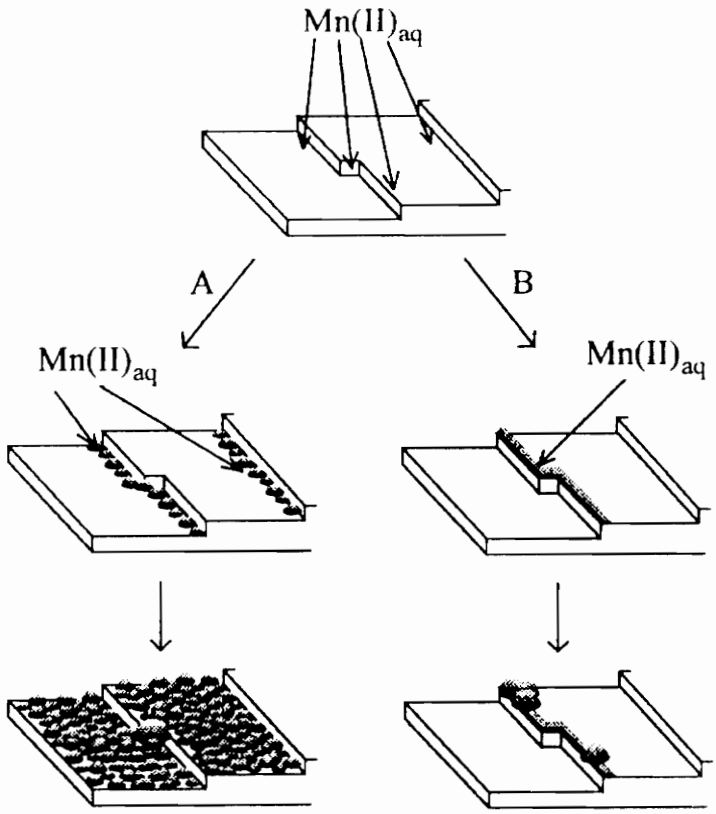

Figure 3. Schematic showing the two pathways through which manganese precipitates develop over time. (The reaction starts with adsorption of Mn(II) to sites along steps. Pathway A represents substrate controlled growth. Pathway B represents precipitate controlled growth. Active adsorption-oxidation sites have been indicated by arrows in the first two steps of the schematic, from Junta and Hochella, 1994).

natural manganese oxide coating transforms from an initial Mn_3O_4 coating to γMnOOH by the following process:

Mn_3O_4	⟶	βMnOOH	⟶	γMnOOH
hausmannite		feitknechtite		manganite
(initial)		(intermediate dominant phase)		(final and complete transformation)

The geological process does not favor transformation to γMnO_2, the highest and most desirable oxidation state for manganese sorption in water treatment (Murray *et al.*, 1985).

Effect of $MnO_x(s)$ Coatings on Filter Media

Most of the literature on manganese coatings reports that the oxide coating has little effect on media size, shape, density, and specific gravity. One direct filtration utility in Brazil, though, reported heavy black stains on their sand after two or three filter cycles. The plant was removing high concentrations of both manganese and iron and attributed a prominent filter bed depth increase to manganese. They claimed that after backwash, the filter bed rose two inches, meaning that manganese deposits build up continuously on the sand grains and are not removed by normal washing, "Over time, these gelatinous deposits agglomerate and eventually form mudballs that could serve to severely disrupt the filters (Bratby, 1988)." They contacted a pilot filter with sulfuric acid (H_2SO_4) at pH 2.0 for four hours and reported that the sand grains retained their stained appearance but that the bed depth decreased five inches to its original position. However, they mentioned nothing about the iron coating that should also have been present on the media, strengthening the total oxide coating and contributing to the agglomeration. The black color of the manganese oxide coating obviously predominated over the yellowish brown iron oxide so that the total coating appeared to be manganese.

All other available literature that addressed the effect of the $MnO_x(s)$ coating upon the media emphasized the unnoticeable effect of a coating in comparison to uncoated

media. Knocke *et al.* (1989) showed that $MnO_x(s)$ coatings have no significant impact on media size and shape or density and, therefore, do not affect filter characteristics such as media depth or porosity. Table 2 contains data from four treatment plants in support of these findings. The specific gravity of manganese oxides ranges from 4.8 to 5.2 as compared to the specific gravity of anthracite of 1.5, but the relatively small amount of oxide coating in comparison to the media grain volume offsets any increase in specific gravity. Therefore, concerns involving changes in specific gravity of coated anthracite such as increased mixing with sand during backwash, changes in clean bed headloss, and increasing filter bed depth appear unwarranted. Water treatment plants that practice Mn(II) removal by sorption and oxidation confirm that the oxide coating is not detrimental to filtration even though the media may slightly increase in size (Griffin, 1960).

Mechanics of Filter Backwashing

After soluble manganese has sorbed and oxidized on the media, the subsequent backwash removes some of the manganese coating. Since particle collisions and abrasions in a fluidized bed are negligible, hydrodynamic shear at the water-grain interface is the primary cleaning mechanism (Amirtharajah, 1978; Cleasby *et al.*, 1975). Increased fluid shear is the result of the increased drag forces necessary to keep the media grains in a fluidized state (Fitzpatrick, 1991), and it is the drag forces rather than interparticle collisions that clean the grains (Cleasby *et al.*, 1977).

The bulk of previous backwash literature testifies that backwashing with water alone is inadequate because of the lack of particle abrasion (Cleasby *et al.*, 1975).

Table 2: Results of Size and Density Studies With and Without a Surface Coating on the Media

Media Source (Sample Number)	Surface Coating	Specific Gravity	Uniformity Coefficient U.C. = D_{60}/D_{10}	Effective Size (D_{10}) (mm)
Durham (#4) (coal)	Yes	1.90	1.82	0.55
Durham (#4) (coal)	No	1.95	1.88	0.48
Portsmouth (#6) (coal)	Yes	1.61	1.55	0.76
Portsmouth (#6) (coal)	No	1.59	1.60	0.74
Ruckersville (#7) (sand)	Yes	2.62	-	-
Ruckersville (#7) (sand)	No	2.64	-	-
Blacksburg (#12) (coal)	Yes	1.63	1.59	0.82
Blacksburg (#12) (coal)	No	1.62	1.50	0.80
Typical values for: Sand*		2.65	1.35 - 1.75	0.40 - 0.55
Anthracite*		1.50	< 1.70	0.45 - 0.80

* Values taken from Clark *et al.* 1987, p. 391.

(After Knocke *et al.*, 1989).

Evidence in support of this limited contact includes the following from Fitzpatrick (1991):

1. During laboratory experiments there is no abrasion of plexiglass filter columns,
2. In order to maintain the grains in a fluidized state, a thin film of liquid must continue to flow around each grain, and
3. If the grains actually collided, then there would be an upwardly decreasing particle density instead of the abrupt change seen at the top of the bed. Also, almost all of the wash water energy is used in suspending the grains so that none is available to support particle friction (Camp *et al.*, 1971).

Fluidized particles must maintain a field of flow around their perimeter in order to remain suspended. Buevich and Markov (1970) claimed that very few collisions actually occur in a fluidized homogeneous particle bed because, as particles approach each other, the liquid pressure between the particles increases, continually decreasing the velocity of approach of the particles toward each other and preventing them from colliding. According to Amirtharajah (1978), Adler and Happel indicated that solid-solid frictional effects are insignificant in the low porosity range of fluidized beds where they should be dominant. Johnson and Cleasby (1966) also stated that over a fourteen-year period, sand sizes in some filters increased from 0.43 mm to 0.65 mm due to deposited layers resulting from insufficient recarbonation and lack of particle contact during backwash in sand filters of small grain size. However, the supposition at that time was that the larger grain sizes would not fluidize as well as small sand grain sizes, thus promoting a greater number of collisions and an increase in scour action.

Observational studies using boroscope and HSV techniques to film and photograph the fluidization process reveal that many deposits are detached during the gradual bed expansion before fluidization. When the grains initially become mobile, they rotate and move relative to each other which may result in some abrasion and release of attached deposits (Fitzpatrick, 1991).

Hydraulics of Fluidized Beds

During the partially fluidized/low porosity phase of bed expansion when many deposits are detached, turbulence is fluid-generated (Amirtharajah, 1978; Fitzpatrick, 1991). However, above the critical fluidized porosity of 0.70, turbulence decreases to particle-generated turbulence (Amirtharajah, 1978). It is during full fluidization that "grain movement is erratic, showing brief temporal and spatial phases of immobility followed by rapid movement and circulatory motion (Fitzpatrick, 1991)."

As fluid velocity increases, the hydraulic resistance of a stationary bed increases until the hydraulic resistance is equal to the bed weight. When the hydraulic resistance is equal to the bed weight, any further increase in velocity causes the bed to expand, corresponding to the limit of stability of a fixed bed. Generally, the top layers of a stationary bed fluidize and expand before the bottom layers because the hydraulic resistance coefficient is higher and because the hydraulic resistance becomes equal to the upper bed weight earlier. Instead of a single critical velocity and limit of stability, then, a range of velocities is associated with bed expansion from initial fluidization to a fully expanded bed (Zabrodsky, 1966).

Original fluidization follows a typical pressure curve OAB as shown in Figure 4. When fluid velocities decrease, the resulting pressure drop follows curve BCO without the pressure peak at A. If, after fluidization, a bed settles without vibration or disturbance, it rests in a more expanded state so that subsequent fluidizations will follow the pressure curve OCB more closely. More compact beds display higher pressure peaks during initial fluidization. The upward pressure in the bed must initially exceed the equivalent weight of the bed (i.e. the product of the bulk weight and bed height) producing a pressure peak similar to A. After the bed expands, the fluidization pressure theoretically settles back to the bed equivalent weight as shown in the line from C to B (Zabrodsky, 1966).

Sometimes, fluidization begins at the bottom of a bed because the friction between the bed and walls is minimal, hydraulic resistance at the top of the bed is great, the velocity

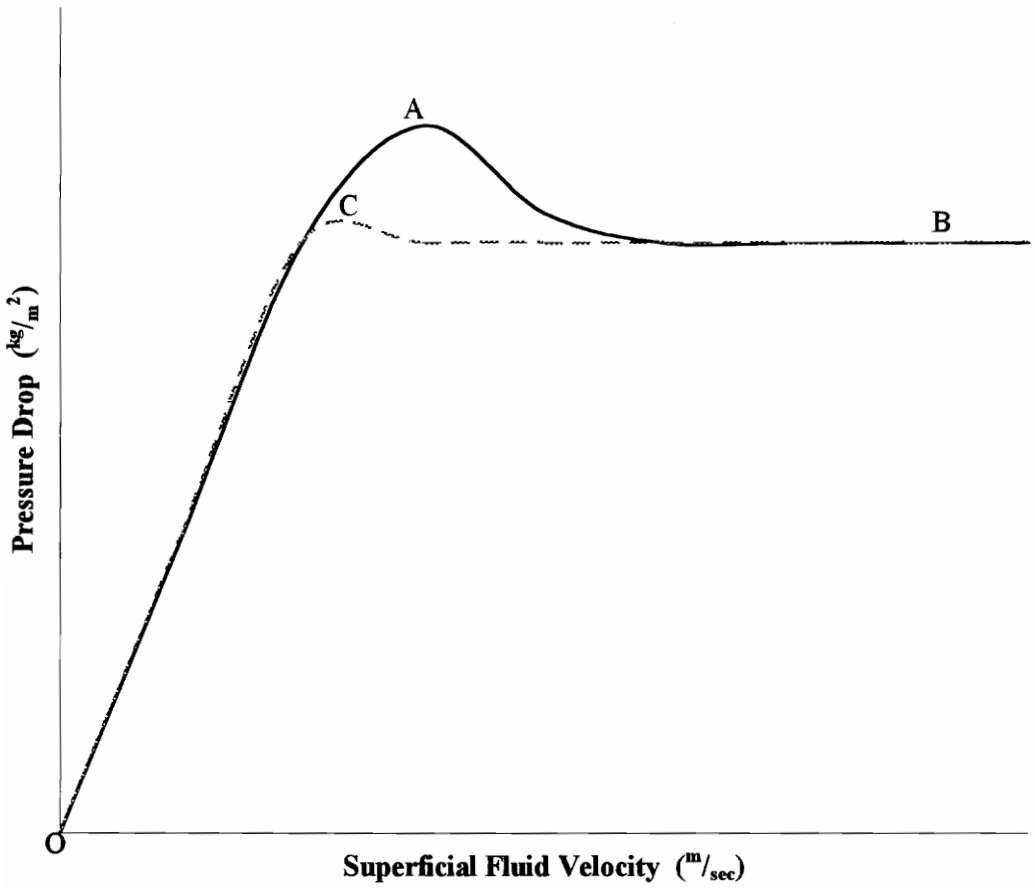

Figure 4. Lines of initial fluidization (OAB) and the reverse process (BCO). (After Zabrodsky, 1966).

of fluid is 30-70% greater at the walls than at the middle of the bed due to less dense packing, and velocity increases such that it lifts the entire bed. The true velocity around the particles projecting from the raised bed is much smaller than the velocity around the individual particles within the bed. Therefore, particles fall from the bottom of the bed, causing it to fluidize from the bottom up (Zabrodsky, 1966).

The two-fold role of particle roughness negates itself as a factor in determining fluidization velocity. Rough particles do not compact as well as smooth particles because friction between the particles hinders settling of the bed, causing an indirect decrease in hydraulic resistance. However, particle roughness directly increases the resistance coefficient in the transitional and turbulent flow regimes, essentially neutralizing the effect of the more expanded settled state (Zabrodsky, 1966).

Optimum Bed Expansion

Most literature on backwashing states that the desired porosity of a fluidized bed is approximately 0.70. Maximum hydraulic shear and the most active particle motion provide optimum cleaning at porosities between 0.68 and 0.71 (Amirtharajah, 1988; Cleasby *et al.*, 1977; Huang and Basagoiti, 1989).

The properties of fluidized beds that maximize at a porosity of 0.7 are turbulence, heat transfer, mixing, and mass transfer (Cleasby *et al.*, 1975). McCume and Wilhelm measured mass transfer characteristics by observing the partial dissolution of spherical and flake-shaped napthol particles in a fluidized bed to find that mass transfer did, indeed, maximize around a porosity of 0.70 to 0.75 (Amirtharajah, 1978).

A greater bed expansion is necessary to remove more adhesive floc particles from media grains (Huang and Basagoiti, 1989). A direct filtration plant in Brazil claimed backwash rates greater than 35 $^{gpm}/_{ft^2}$ were necessary to clean the filters to the point where only 10 percent of the dirty particles originally in a filter remained after backwash (Bratby, 1988).

Air Scour

Air scour has become the most recent breakthrough in filter backwashing technology. The flow of bubbles up through media causes increased particle contact that promotes abrasion and release of attached materials. Air application during backwash provides more efficient cleaning, especially for solids with high adhesive forces (Amirtharajah, 1988). Long-term air scour studies indicate that air scour is harmless to media because of the observance of negligible anthracite loss due to abrasion and an unchanged media size gradation (Cleasby *et al.*, 1975).

Cleasby *et al.* (1977) describe air bubble action as follows:

> "When the air is introduced at the bottom of the filter, the bubbles travel upward carrying some water and dirt particles as they pass through the bed and burst at the surface, where the maximum scouring action appears to be produced. Substantial agitation of the medium near the bed's surface occurs, and it is this action that provides the basis for air scour use in sand filters where minimum solids penetration occurs."

Several air scour procedures exist according to media type, plant operation capability and preference, and popularity according to geographical location. Typical air application rate is 3 - 5 $^{scfm}/_{ft^2}$ of filter area (Robinson *et al.*, 1987). The order of application of air and water, though, differs for various water treatment facilities. Some air scour operations involve application of air alone for approximately 5 minutes followed by a combination of air and water such that the air flow decreases as the backwash water flow increases to a typical backwash rate of around 15 $^{gpm}/_{ft^2}$. Wash water, alone, completes the backwash process. In Great Britain, general air scour practice is air scour alone followed by wash water alone (Cleasby *et al.*, 1977; Robinson *et al.*, 1987). Still other methods involve the initial combination of air and water followed by water wash alone (Fitzpatrick, 1991).

During air scour, HSV and borescope pictures show particle detachment by two methods. Particles are released because of fluid shear forces caused by the flow of pore water after displacement by air. Also, particle contact results in abrasion, especially during collapse-pulsing, which scrapes deposits from the media and leaves them loose in the filter for removal. The difference in filter bed movement between air scour and water alone is described as erratic and violent with more rapid changes in the magnitude and direction of grain velocity (Fitzpatrick, 1991).

Summary

The species of manganese found in raw water sources can be soluble or particulate in several different oxidation states, which determines the type of water treatment necessary for removal. Conventional treatment includes oxidation and settling of manganese followed by filtration of any residual manganese particles, removal by manganese greensand, or sequestering soluble manganese in order to keep it in solution. However, further research has revealed a natural greensand effect due to the development of a $MnO_x(s)$ coating on anthracite coal filter media. The coating promotes sorption of soluble Mn(II) while the filter removes particulate $MnO_x(s)$ by conventional filtration. Free chlorine oxidizes the sorbed Mn(II) to create additional $MnO_x(s)$ coating and further catalyze the removal process. This natural greensand phenomenon takes place without strong chemical oxidants and does not require pressure filtration as manganese removal by greensand usually does.

Alkaline pH conditions promote sorption of soluble Mn(II), but acidic pH conditions hinder sorption. However, the addition of chlorine in filter-applied water causes oxidation of sorbed Mn(II) to a $MnO_x(s)$ coating which aids in further removal, even under acidic pH conditions. Chlorine does not oxidize Mn(II) before filtration but regenerates (i.e. oxidizes sorbed Mn(II)) the filter media for further sorption.

Development of a $MnO_x(s)$ coating increases filter media sizes only slightly, and density and specific gravity of the media remain virtually unaffected by the addition of a coating. Therefore, filtration for particle removal continues unhindered.

Hydrodynamic shear between filter backwash water and filter media grains is the method by which water backwash removes deposits from filter media. The fluidized filter media bed that has been found to have the most effective backwash capabilities has an expanded bed porosity of 0.7. Air scour has been a recent popular addition to the backwash scheme. Air scour promotes particle collisions and more effectively cleans filter media than backwash with water alone.

Methods and Materials

The methods and materials chapter presents the experimental approach by which the objectives of the project were addressed. The methods and materials chosen were developed based upon procedures, principles, and experiences found in the literature and were designed to advance technology concerning removal of soluble Mn(II) from raw water by sorption and oxidation on $MnO_x(s)$ coated filter media.

Specific subsections of the methods and materials chapter include the experimental layout, a description of the source water, preparation of stock solutions, media preparation, filter operation, backwash and backwash sample analysis, media sampling, air scour, a schedule of filter operation, and descriptions of the analytical methods.

Experimental Layout

Backwash studies on continuously regenerated manganese-oxide coated anthracite coal filter media were conducted at the Blacksburg-Christiansburg-VPI Water Authority treatment plant which provided the necessary water supply and adequate shelter for the apparatus. Three laboratory-scale plexiglass columns of height 6 feet and diameters of 6 inches, 3.5 inches, and 3 inches served to contain the 24 inches of anthracite coal under consideration as well as 6 inches each of supporting sand and gravel.

The experimental layout is shown in schematic form in Figure 5. The source water entered the constant head tank for chlorine addition and then the manganese mixing tank for soluble Mn(II) addition. From the manganese mixing tank, the water separated to the three filters at a typical hydraulic loading rate of 5 $^{gpm}/_{ft^2}$. Hose clamps controlled the flow to each filter, and Y-splitters served as flow diverters so that the water redistributed to the other two filters during backwash in the manner of a declining rate filter. The filters were operated with a significant excess (>1 $^{mg}/_{L}$) of free chlorine in the filter effluent. This

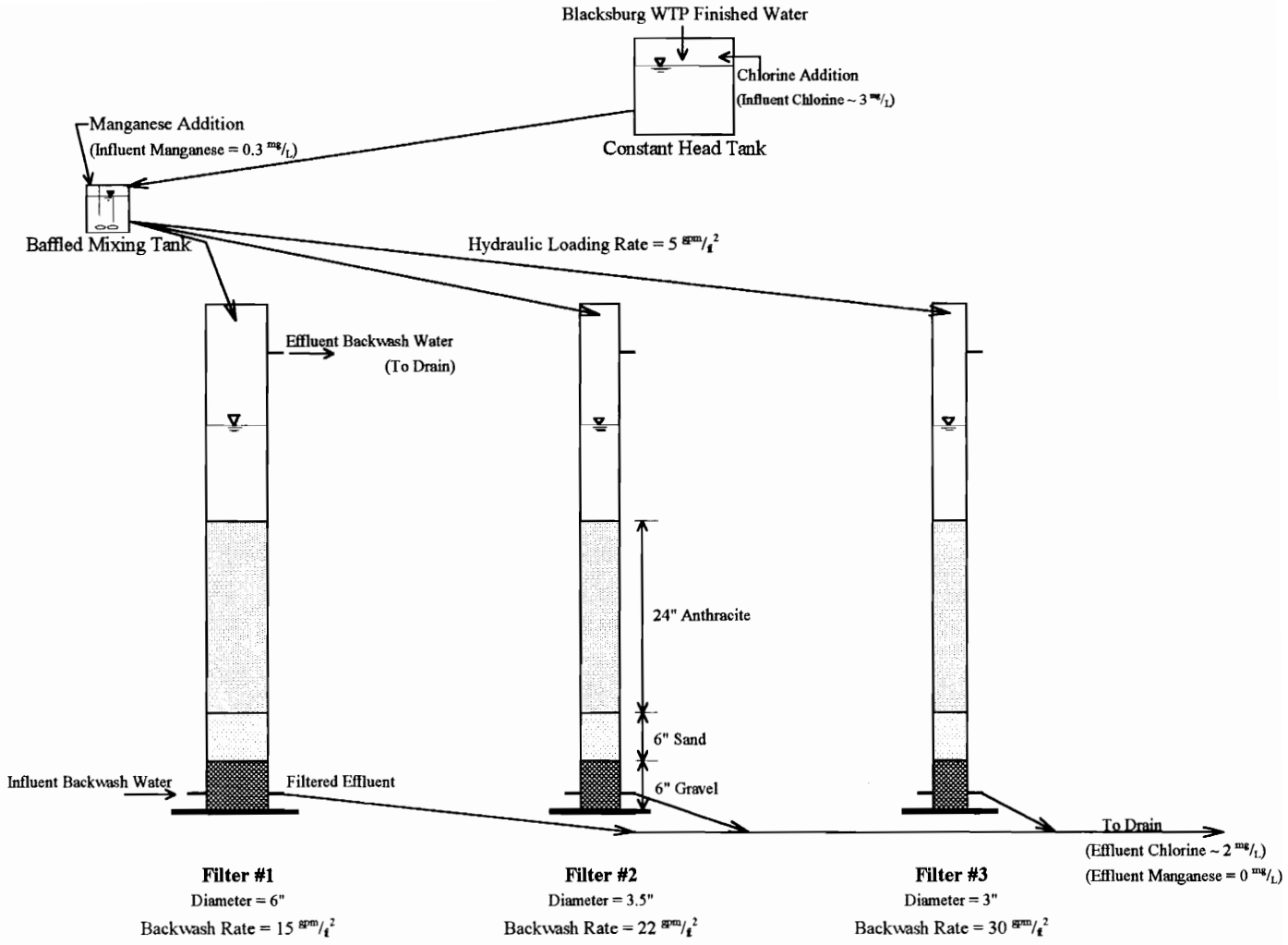

Figure 5: Experimental Filter Layout

resulted in essentially 100% Mn(II) removal. After application to the filter, the treated effluent escaped from each filter through a bottom port and was routed to the floor drain. Flow control valves at the end of the effluent lines maintained a constant head on top of each filter.

Source Water

The Blacksburg-Christiansburg-VPI Water Authority is a conventional rapid mix, flocculation, sedimentation, dual-media filtration plant using as its water source the New River. Chemicals added during rapid mix include polyaluminum chloride (PAX) as the coagulant, hydrofluosilicic acid for fluoride addition, and chlorine. After filtration, additional chlorine provides the final 1.7 $^{mg}/_{L}$ chlorine residual required to maintain an adequate oxidant level throughout the distribution system. Sodium hydroxide (NaOH) addition in the clear well counteracts the pH decrease associated with hydrofluosilicic acid addition for a final finished water pH of 8. Average finished water turbidity is 0.04 nephelometric turbidity units (NTU). Average finished water hardness for the duration of the experiment was 46.0 $^{mg}/_{L}$, and average alkalinity for the same time period was 45.8 $^{mg}/_{L}$ as $CaCO_3$.

The water source to the constant head tank was treatment plant finished water with a chlorine concentration of about 1.7 $^{mg}/_{L}$. Supplemental chlorine from a sodium hypochlorite bleach solution added in the constant head tank increased the chlorine concentration to 2 to 3 $^{mg}/_{L}$ to facilitate continuous regeneration of the media by immediately oxidizing the sorbed manganese. From the constant head tank, the influent water flowed to a baffled and magnetically stirred mixing tank for addition of a 590 $^{mg}/_{L}$ manganese solution (as Mn II), resulting in a 0.3 $^{mg}/_{L}$ influent manganese concentration to each filter. Both the chlorine and manganese solutions were added at a rate of 3 $^{mL}/_{min}$ by separate peristaltic pumps with size 13 pump heads and tubing.

Preparation of Stock Solutions

Both the manganese and chlorine chemical feed solutions were in five-gallon carboys that lasted for three days of filter operation. The soluble manganese solution was made from hydrous manganese chloride crystals of molecular formula $MnCl_2 \cdot 4H_2O$ and molecular weight 197.91 grams per mole. The chlorine feed solution was made by diluting 600 mL of 5.25% sodium hypochlorite bleach to a volume of 5 gallons with treatment plant finished water.

Since pH was a parameter under consideration, maintenance of the correct operating pH required addition of concentrated sulfuric acid (H_2SO_4) to the manganese feed solution so as to accommodate the pH adjustment of the entire finished water source. The supplemental chlorine solution pH was adjusted to the desired operating pH with sulfuric acid before addition to the water. When the water source became treatment plant filtered water, sodium hydroxide (NaOH) addition was required to increase the filtered water pH to the desired operating pH. Since addition of sodium hydroxide base to the manganese feed solution would have resulted in immediate precipitation of manganese solids due to a tremendous pH increase within the manganese feed solution, the necessary amount of 50% by weight sodium hydroxide solution was added to the supplemental chlorine solution to accommodate the pH adjustment of the entire treatment plant filtered water source.

Media Preparation

The anthracite for the manganese removal studies was collected from the Blacksburg, Christiansburg, VPI Water Authority dual media filters. After backwash, clean media (removed from the top six inches of the filters) was homogenized and separated into the volumes necessary for 24-inch anthracite depths within each pilot filter. Samples from each volume of media were taken for media characterization including

manganese extraction and sieve distribution analysis. The media remained submerged in water until placement within the columns.

The filter media configuration was constructed by initially adding new gravel and then new sand to a level of six inches each by gravity flow through water. This underdrain system was then backwashed at extremely high backwash rates in order remove impurities as well as fine sand that might interfere with studies on the anthracite. After this intense backwash, wet anthracite was added in the same manner to a level of 24 inches. The completed filters were then backwashed at their respective rates of 15 $^{gpm}/_{ft^2}$, 22 $^{gpm}/_{ft^2}$, and 30 $^{gpm}/_{ft^2}$ to remove extra impurities from the anthracite and to stratify the anthracite as would naturally occur during the first backwash.

Filter Operation

After media characterization and filter construction, the filter operating protocol was as follows. All three filters were in operation for four days at a hydraulic loading rate of 5 $^{gpm}/_{ft^2}$ and an influent manganese concentration of 0.3 $^{mg}/_{L}$. During the four days of operation, the hydraulic loading rate, influent and effluent manganese concentrations, pH, and influent and effluent chlorine concentrations were monitored. When it became evident through monitoring effluent manganese concentrations that manganese was not escaping any of the filters but was being completely removed within the filters, the effluent manganese and influent and effluent chlorine concentrations were monitored with less frequency. Influent and effluent chlorine concentrations were analyzed only to insure a greater influent chlorine concentration than stoichiometrically required for Mn(II) oxidation and to confirm a decreased chlorine concentration in the effluent after manganese oxidation within the filters. Typically, influent chlorine concentrations were between 2 and 3 $^{mg}/_{L}$ and effluent chlorine concentrations were between 1 and 1.7 $^{mg}/_{L}$. Manganese and chlorine feed solution pump rates were also checked periodically throughout each day.

Influent manganese concentrations were separated into three species: the total amount of manganese applied to the filter, the colloidal fraction, and the soluble fraction. Determination of the fraction of each species allowed comparison between respective pH values of the amount of soluble manganese available for sorption versus the amount of previously oxidized particulate manganese removed by deposition within the filter. Generally only a small percentage of influent manganese was particulate at either pH under consideration. After four days of operation, which was the typical length of operation of the Blacksburg-Christiansburg-VPI Water Authority filters, each filter was backwashed at its respective backwash rate (15 $^{gpm}/_{ft}^2$, 22 $^{gpm}/_{ft}^2$, and 30 $^{gpm}/_{ft}^2$).

Soluble Mn(II) sorption to MnO_x(s) and its subsequent oxidation to form additional manganese oxide is an autocatalytic reaction which accelerates with additional oxide coating. Since manganese deposition occurred on the sides of the plexiglass filter columns as well as within the manganese mixing tank, the sides of the columns were scrubbed with minimal media disturbance after each backwash to retard premature Mn(II) sorption on the apparatus and promote sorption and oxidation on the filter media. Acid waste containing hydroxylamine sulfate was beneficial in cleaning the baffled mixing tank and tubing after each backwash; the mixing tank and tubing to the filters required only a few minutes of contact with the acid waste solution to be rid of the brown manganese-oxide film that accumulated over the four-day loading period. The mixing tank and tubing were thoroughly rinsed before resuming filter operation to avoid adverse effects on the filter media from contact with hydroxylamine sulfate.

Backwash

After the four-day manganese loading period, each filter was backwashed for ten minutes at the rates listed in Table 3. Each filter was backwashed separately while the other two filters remained in service with the additional filter influent flow from the backwashed filter divided between them as in a declining rate filter system. Usually, the

Table 3: Backwash Parameters

Filter #	Filter Diameter (inches)	Backwash Rate ($^{gpm}/_{ft2}$)	Water Flowrate (gpm)
1	6	15	2.9
2	3.5	22	1.5
3	3	30	1.5

additional loading was too great for only two filters, and the filters that remained in service overflowed through their emergency overflow/backwash ports to the drain.

The backwash procedure for each filter was as follows. The influent water supply to the filter was turned off, and the water surface elevation in the filter was allowed to drain down to the surface level of the media. The effluent line was then plugged so that no additional water would escape and so that the backwash water would be forced back up through the filter instead of flowing out through the effluent line. A flowmeter (King Instrument Company, Huntington Beach, California) equipped with a valve between the finished water (backwash water) source and the backwash port measured and controlled the flow of backwash water to each filter. Fluidization of each filter was gradual so as not to disrupt the underdrain assembly and create excessive mixing between the sand and anthracite coal. Sample times began at zero minutes when the first effluent sample appeared out of the backwash port at the top of the plexiglass filter column after fluidization was complete. Backwash samples taken at the following times (minutes:seconds) created a profile of the amount and/or concentration of manganese released as a function of backwash progression: 0:00, 0:15, 0:30, 0:45, 1:00, 1:15, 1:30, 1:45, 2:00, 2:30, 3:00, 3:30, 4:00, 5:00, 6:00, 8:00, and 10:00 minutes. The frequency of samples decreased as backwash progressed because definition of a "spike" of manganese in the backwash water was desired, and the spike obviously occurred at the beginning of the backwash. As backwashing continued, the backwash water became cleaner, and sampling resulted only in defining the tail of the backwash profile.

In addition to timed samples, all backwash water was collected in a large basin for analysis of the entire mass of manganese released from each filter. The large basin was graduated which provided the value of the total volume of backwash water after backwash was complete. Triplicate samples of the homogenized backwash water then, indicated the concentration of manganese within the basin. Multiplication of the manganese concentration and the volume in the basin produced the total amount of manganese released from the media during backwash. Timed sample concentrations multiplied by the

sample volumes of 0.55 liters indicated the additional amount of manganese removed from the filters which was not accounted for in the analysis of the composite backwash water.

Backwash Sample Analysis

After all the filters were backwashed and reinstated, the backwash samples were transported to the Virginia Polytechnic Institute and State University Environmental Engineering Laboratory for separation and analysis. Initially, the backwash samples were separated for analysis of the soluble and colloidal fraction. If a soluble and colloidal fraction was detectable on the atomic absorption spectrophotometer, the samples were also separated for analysis of the soluble fraction. Preliminary backwash studies, however, indicated a virtually undetectable soluble and colloidal fraction, even at the first influent pH 6.0 condition. After several verifications of the undetectable soluble and colloidal fraction, separation through the 0.45 micron filter was abandoned, and analysis took place only on the total manganese fraction, which was essentially 100% particulate manganese oxide.

Media Sampling

After every third backwash, a representative depth sample from each filter defined a profile of manganese concentrations upon the filter media as a function of depth. After backwash, a coring device quickly inserted into the fluidized bed collected a sample throughout the depth of the filter. Samples from the coring device at three-inch intervals (extracted in triplicate as described in the Analytical Methods) completed the manganese mass balance through the time of the coring and indicated where in the filter the bulk of the influent manganese was being removed. Although sand was mixed with the deeper

media samples, an effort was made to extract only anthracite coal and prevent interference from any sand with minimal manganese oxide coating.

Air Scour

At the end of each set of operating conditions (i.e. completion of backwash studies at pH 6.0 and then again at pH 7.3), a simulation of air scour within each filter illustrated qualitatively the effect of air agitation upon the $MnO_x(s)$ coating. At the end of the final backwash, while the filter bed was still fluidized, a long, narrow glass tube with air stones attached to the end was inserted down through the media until it came to rest at the bottom of the filter. Three or four air stones were used for distribution of the air across the bottom of the filter. A large rubber stopper at the top of the glass tube aided in stabilizing the apparatus in the center of the filter. The upper end of the glass tube was attached through a valved air flow meter to a reversible vacuum pump that provided the air supply.

For the air scour experiments, the level of water on top of the filter was decreased to 1 to 1.5 feet to avoid filter eruption and loss of media. Air application was gradual and increased to a typical air scour flow rate of 3 standard cubic feet per minute (scfm) per square foot of filter area for each filter. Air scour alone lasted for four minutes. During the fifth and final minute, the air flow slowed to zero while the backwash water simultaneously began and increased to the rate respective to each filter, thus following the general operating protocol for practicing air scour. The backwash sampling procedure was the same as that described for a normal backwash. A final media core sample was collected after the air scour cycle and analyzed for $MnO_x(s)$ content. This allowed for a direct evaluation of air scouring on media $MnO_x(s)$ content.

Schedule of Filter Operation

The original conditions of filter operation included treatment plant finished water as the raw water source and an influent pH of 6.0. Under these conditions, several backwash cycles and corings took place before the final air scour study. At the termination of the pH 6.0 studies, a final core sample provided the manganese depth profile for the final mass balance on manganese and provided the media for the final sieve distribution analysis.

After completion of studies at pH 6.0, the original media was replaced with new media from the Blacksburg-Christiansburg-VPI Water Authority filters, which was also characterized by size distribution and manganese oxide coating analysis before a series of manganese loading and backwash studies at pH 7.3. The backwash studies at pH 7.3 began with treatment plant finished water and addition of sulfuric acid (H_2SO_4) in the manganese feed water for pH adjustment. However, because the utility began adding phosphoric acid to the finished water, the raw water source was changed to treatment plant filtered water after the first three backwash cycles and first coring. As a result, sodium hydroxide (NaOH) addition to the supplemental chlorine feed water became necessary to increase the pH of the filtered water to 7.3. After the treatment plant returned to its original operating procedure, the raw water source again became treatment plant finished water. Studies at pH 7.3 ended in the same manner as those at pH 6.0 with air scour and a final coring for extraction and sieve distribution analysis.

Analytical Methods

Plastic and Glassware Preparation

Before experimentation began, all plastic and glassware used in sampling, extracting, and preparing manganese standards was submerged in a 10% nitric acid bath for several hours for removal of residual contaminants. Thereafter, the plastic and glassware was acid washed as necessary according to the severity of manganese concentrations present in the contained solutions. Volumetric pipettes and flasks also underwent chromic acid cleansing to promote thorough release of their solutions. After acid-washing, all containers were rinsed once with tap water and three times with distilled water and were finally dried in the oven.

Standards and Analysis

Analysis for manganese concentrations took place on a Perkin-Elmer Model 703 Flame Atomic Absorption Spectrophotometer (AAS), Norwich, Connecticut with a manganese detection limit of 0.005 $^{mg}/_{L}$. Manganese standards between 0.1 $^{mg}/_{L}$ and 5 $^{mg}/_{L}$ and a blank were available to accommodate the range of possible Mn concentrations after dilution. Each standard was prepared from a 20 $^{mg}/_{L}$ manganese stock solution. All standards and blanks were prepared in 0.5% nitric acid solutions to discourage manganese oxidation and precipitation out of solution. All manganese standards and acid solutions were made with Milli-Q water (Millipore Corporation, Bedford, Massachusetts).

The most sensitive wavelength of 279.5 nanometers was used for all manganese analysis on the AAS. The AAS was standardized and checked at the beginning of operation. With the solution concentrations obtained on the AAS, the amount of manganese upon the media was determined using the following equation:

$$\frac{\text{Solution Concentration } (^{mg}/_{L}) \times 10 \text{ (dilution factor)} \times 0.25 \text{ L solution}}{\text{mass of media used in extraction (g)}} = \text{milligrams of Mn as Mn(II) per gram of media.} \quad [7]$$

The pH was initially measured with a Fisher Accumet digital pH meter and, later, with a Corning Model 7 pH meter equipped with a Fisher pH probe. The pH standards available for pH meter calibration were pH 4, 7, and 10.

Titrations

Since the treatment plant finished water was considerably buffered, potentiometric titration of 100 milliliters of water with 0.02 N H_2SO_4 according to Standard Method #102: Laboratory Apparatus, Reagents, and Techniques (*Standard Methods for the Examination of Water and Wastewater,* 1985) indicated the amount of acid necessary to decrease the pH of the treatment plant finished water to the desired pH. Titration, also, of 100 milliliters of chlorine solution indicated the amount of acid required to decrease the pH of the bleach solution to the operating pH. When the source water became filtered water, potentiometric titration of 100 milliliters of influent water with 0.025 N NaOH also indicated the amount of concentrated sodium hydroxide solution necessary to increase the pH of the plant-filtered water to the desired pH.

Extractions

Before oven-drying the media to obtain a dry weight media sample, each media sample was gently rinsed with distilled water until the rinse water was clear to remove any manganese oxide particulates not sorbed to the anthracite media grains. The amount of original manganese coating on the anthracite coal from service within the treatment plant filters and the additional quantity of manganese due to loading during pilot-scale experimentation was determined by extraction with hydroxylamine sulfate (HAS), a strong

reducing agent of molecular formula $(NH_2OH)_2{\cdot}H_2SO_4$. Approximately one gram of hydroxylamine sulfate was added to an accurately weighed quantity of media (goal of one gram by dry weight) in a 250 milliliter volume of 0.5% nitric acid solution. This provided the necessary environment for complete dissolution of the $MnO_x(s)$ coating. After sufficient contact time of at least four hours, the resulting manganese solution was diluted in a ratio of 1:10 with 0.5% nitric acid solution to decrease the manganese concentration to less than 5 mg/L, which enabled analysis within an accurate linear range on the AAS.

Sieve Distribution Analysis

The Geotechnical Division of the Civil Engineering Department allowed use of their sieves and sieve-shaker for the sieve-size distribution. A fifty-gram (dry weight) representative sample from each filter was separated between US Standard Sieves 4, 10, 14, 16, 18, 20, 40, and 200 according to general American Society for Testing and Materials procedures (*ASTM Designation D422-63, ASTM, 1964*). From the sieve analysis and resulting sieve size distribution, the original effective size (ES) and uniformity coefficient (UC) of the media were obtained from the following definitions:

Effective Size (D_{10})	=	Size in millimeters below which only 10% of the media (by weight) is smaller
Uniformity Coefficient ($^{D60}/_{D10}$)	=	Ratio of size below which 60% of the media (by weight) is smaller divided by the Effective Size

Manganese Speciation

Influent manganese samples were separated into three species: the total manganese concentration, the colloidal fraction, and the soluble fraction. The soluble and colloidal fraction was that portion of influent manganese able to pass through a 0.45 micron filter, and the soluble fraction was that portion of influent manganese able to additionally pass through a pressurized YM 30 Diaflo Ultrafiltration Membrane (Amicon, Inc., Beverly, Massachusetts.) The amount of particulate manganese applied to the filters was determined by subtracting the soluble manganese concentration from the total concentration. Under normal operating conditions, 95-99% of influent manganese was soluble Mn(II).

Hydroxylamine sulfate (HAS) and nitric acid addition insured complete dissolution of influent manganese for analysis on the AAS. Only a small amount of HAS (i.e. approximately 0.25 g HAS for a 250 milliliter volume and approximately 0.1 g for the 40 milliliter vials containing the filtered influent samples) was necessary to dissolve the 0.3 $^{mg}/_{L}$ manganese in the filter influent. Nitric acid (HNO_3) was desired just to reduce the pH of the sample to about 2 (i.e. about 5 drops HNO_3 for a 250 milliliter volume and about 2 drops for a 40 milliliter vial) to discourage oxidation and precipitation out of solution.

Backwash Sample Analysis

All backwash samples were collected in 550 mL volume plastic bottles for uniformity in sampling and insurance against sample breakage. After transport to the Civil Engineering laboratory, each 550 milliliter volume of backwash water was agitated for homogenization, and then about 300 milliliters of backwash sample was poured out to eliminate excessive acid waste. To the remaining volume of sample was added enough hydroxylamine sulfate to completely dissolve the particulate manganese (0.5 to 1 gram) and enough concentrated nitric acid (about 5 drops) to reduce the pH of the sample to pH

2, which discouraged oxidation and precipitation. After chemical addition, analysis began on the AAS. Few samples were within the accurate linear range of manganese concentrations for the AAS (i.e. below 5 $^{mg}/_{L}$) and required dilution with 0.5% nitric acid. Efficient 1:10 dilutions were accomplished with a Repipet Dilutor, Clinical and Research Instruments (Berkeley, California) containing the desired nitric acid solution.

Results and Discussion

The results and discussion chapter presents the experimental data gathered throughout the filtration study in a condensed format. Discussion regarding the data includes comparisons based upon different raw water conditions, comparisons with previous studies found in the literature, and observations that lead to recommendations regarding manganese removal in full-scale water treatment. Specific subsections relate to general filter performance for manganese removal, influent manganese characteristics, filter performance at various influent conditions, backwash efficiency comparisons based upon raw water conditions, the effect of backwash rate upon manganese-coated anthracite, oxide coatings at various filter depths, the effect of air scour on manganese oxide coatings, the effect of manganese oxide coatings on physical characteristics of anthracite coal filter media, an overall mass balance on manganese loading and accumulation on the filter media, and practical applications of the results in full-scale water treatment.

General Filter Performance for Manganese Removal

Previous studies involving sorption of soluble manganese (Mn(II)) to manganese oxide ($MnO_x(s)$) coated anthracite coal have proven sorption and surface catalyzed oxidation to be an effective Mn(II) removal method both in the laboratory and in full-scale water treatment. Frequent sampling of the influent and effluent of each pilot-scale filter validated the effectiveness of this type of manganese removal. Filter influent water with 0.3 $^{mg}/_{L}$ Mn(II) and greater than 1 $^{mg}/_{L}$ of free chlorine at pH 6.0, pH 7.3, and pH 7.3 in the presence of phosphates received efficient treatment under all three influent conditions.

Manganese concentration in the filter effluent was usually close to the atomic absorption spectrophotometer (AAS) detection limit of 0.005 $^{mg}/_{L}$. When the effluent

manganese concentration as Mn(II) was below the detection limit, the effluent concentration was assumed to be zero, and percent removal for that time period calculated as 100%. Under normal operating conditions (i.e. without the addition of phosphates), the average percent Mn removal for all three pilot filters was 99.0% $^{+}$/- 2.0% (of which 98.7% was soluble) at pH 6.0 and 98.5% $^{+}$/- 1.6% (of which 93.4% was soluble) at pH 7.3. Even in the presence of phosphate (a sequestering agent), Mn(II) removal by sorption and surface catalyzed oxidation was 97.9% $^{+}$/- 1.8% of the manganese concentration present in the influent water.

Manganese removal at this order of magnitude is efficient and cost-effective due to the use of free chlorine as the ultimate chemical oxidant. As a result, Mn(II) removal by $MnO_x(s)$ sorption and surface oxidation can be expected to compete favorably with other manganese removal techniques on the market.

Influent Manganese Characteristics

For each influent condition under consideration, the greatest percentage of influent manganese was in the soluble (Mn(II)) form. At pH 6.0 and at pH 7.3 in the presence of phosphate, soluble Mn(II) constituted greater than 98% of the influent manganese concentration; at pH 7.3 without phosphate, soluble Mn(II) comprised approximately 94% of the total manganese concentration in the filter influent. The small remaining portion of the manganese concentration was particulate (able to be retained on a 0.2 μm filter) at each influent pH condition. Information presented in Tables 4 and 5 summarize influent particulate manganese ($MnO_x(s)$) concentrations as a percentage of the total influent manganese concentration for influent conditions pH 6.0 and pH 7.3, respectively. Data contained in Table 6 describe the period of time during pH 7.3 influent conditions when phosphate was present in the filter-applied water. In the past, phosphates have been used to sequester soluble manganese to prevent oxidation and deposition in the distribution system. The phosphate addition had a similar effect on the filtration experiments by

Table 4: Amount of Particulate Influent Manganese ($MnO_x(s)$) at Influent pH 6.0

pH 6.0 Trial #	Amount of Mn Load to Filter in Particulate Form (% of total influent mass)		
	Filter #1	Filter #2	Filter #3
1	1.7%	0.5%	1.6%
2	1.2%	2.5%	1.6%
3	2.9%	1.1%	0.8%
4	0.8%	1.0%	0.8%
5	2.6%	3.1%	2.7%
6	1.3%	1.2%	0.5%
Average:	1.8%	1.6%	1.3%
Standard Deviation	0.8%	1.0%	0.8%
Overall Average:		1.6%	
Overall Standard Deviation:		0.9%	

Table 5: Amount of Particulate Influent Manganese ($MnO_x(s)$) at Influent pH 7.3 (without phosphate)

pH 7.3 Trial #	Amount of Mn Load to Filter in Particulate Form (% of total influent mass)		
	Filter #1	Filter #2	Filter #3
1	1.3%	1.7%	2.1%
2	7.5%	13.3%	18.5%
3	3.4%	10.1%	3.1%
11	1.9%	5.3%	4.7%
12	5.0%	5.0%	-
Average:	3.8%	7.1%	7.1%
Standard Deviation:	2.5%	4.6%	7.7%
Overall Average:		5.9%	
Overall Standard Deviation:		5.0%	

Table 6: Amount of Particulate Influent Manganese ($MnO_x(s)$) at Influent pH 7.3 in the presence of phosphates

pH 7.3 with phosphates	Amount of Mn Load to Filter in Particulate Form (% of total influent mass)		
Trial #	Filter #1	Filter #2	Filter #3
4	1.8%	1.8%	2.4%
5	1.5%	1.0%	3.7%
6	< 0.1%*	< 0.1%*	< 0.1%*
7	1.7%	0.3%	0.4%
Average:	1.3%	0.8%	1.6%
Standard Deviation:	0.9%	0.8%	1.7%
Overall Average:		1.2%	
Overall Standard Deviation:		1.1%	

*0.1% represents the minimum detection limit capability of the atomic absorption spectrophotometer.

maintaining a greater percentage of the influent manganese at influent pH 7.3 as soluble Mn(II) (shown in Table 6).

Kruskal-Wallis Multiple-Comparison Z-Value test results for evaluating the impacts of pH and the presence/absence of phosphates are contained in Table 7. These comparisons indicated no statistical difference (within a 95% confidence interval) between individual filters for the percent particulate manganese influent at each pH condition. Kruskal-Wallis Multiple-Comparison Z-Value test comparisons of the particulate influent manganese percentages for each treatment condition revealed no statistical difference (within a 95% confidence interval) between the percent of influent $MnO_x(s)$ particulates at pH 6.0 and the percent of influent $MnO_x(s)$ particulates at pH 7.3 in the presence of phosphates. However, the percentage of influent $MnO_x(s)$ particulates at pH 7.3 without phosphates was greater than that present in influent waters at pH 6.0 and pH 7.3 in the presence of phosphate. Regardless of the influent characteristics, though, the concentration of manganese in the filter effluent never exceeded 0.04 $^{mg}/_{L}$ during normal influent Mn(II) concentrations; manganese removal was continually efficient and thorough.

Filter Performance for Mn Removal Under Various Influent Conditions

Data presented in Figure 6 illustrate general manganese removal efficiency for each filter at the three filter influent conditions under consideration. Each column represents the average percent of total influent manganese removed over the duration of that influent water condition. The error bars extending above and below each column represent the standard deviation from the mean percent removal for each pH condition. The soluble and particulate influent manganese percentages with the corresponding total percent removal by filtration are compiled in Table 8 for each pilot filter at the three influent water

Table 7: Kruskal-Wallis Multiple-Comparison Z-Value Test Results Regarding the Percent Particulate Manganese ($MnO_x(s)$) Influent for each Filter Influent pH Condition

Condition	Average Percent Particulate Mass In ($\bar{x}$)	Comparison		Kruskal-Wallis Multiple Comparison Z-Value*	Comments
pH 6.0	$\bar{x}_{pH\ 6} = 1.55\%$	pH 6.0 vs.	pH 7.3 (with phosphates)	0.66	$\mu_{pH\ 6.0} = \mu_{pH\ 7.3\ w/phosphates}$ no statistical difference within 95% confidence interval
pH 7.3 (without phosphates)	$\bar{x}_{pH\ 7.3} = 5.91\%$	pH 6.0 vs.	pH 7.3 (without phosphates)	3.6	$\mu_{pH\ 7.3\ w/out\ phosphates} > \mu_{pH\ 6.0}$ percent influent particulates are greater at pH 7.3 without phosphates than at pH 6.0
pH 7.3 (with phosphates)	$\bar{x}_{pH\ 7.3\ w/phosphates} = 1.22\%$	pH 7.3 vs.	pH 7.3 (with phosphates)	3.89	$\mu_{pH\ 7.3\ w/out\ phosphates} > \mu_{pH\ 7.3\ w/phosphates}$ percent influent particulates are greater at pH 7.3 without phosphates than at pH 7.3 with phosphates

* Medians significantly different if z-value > 1.96 (regular test).

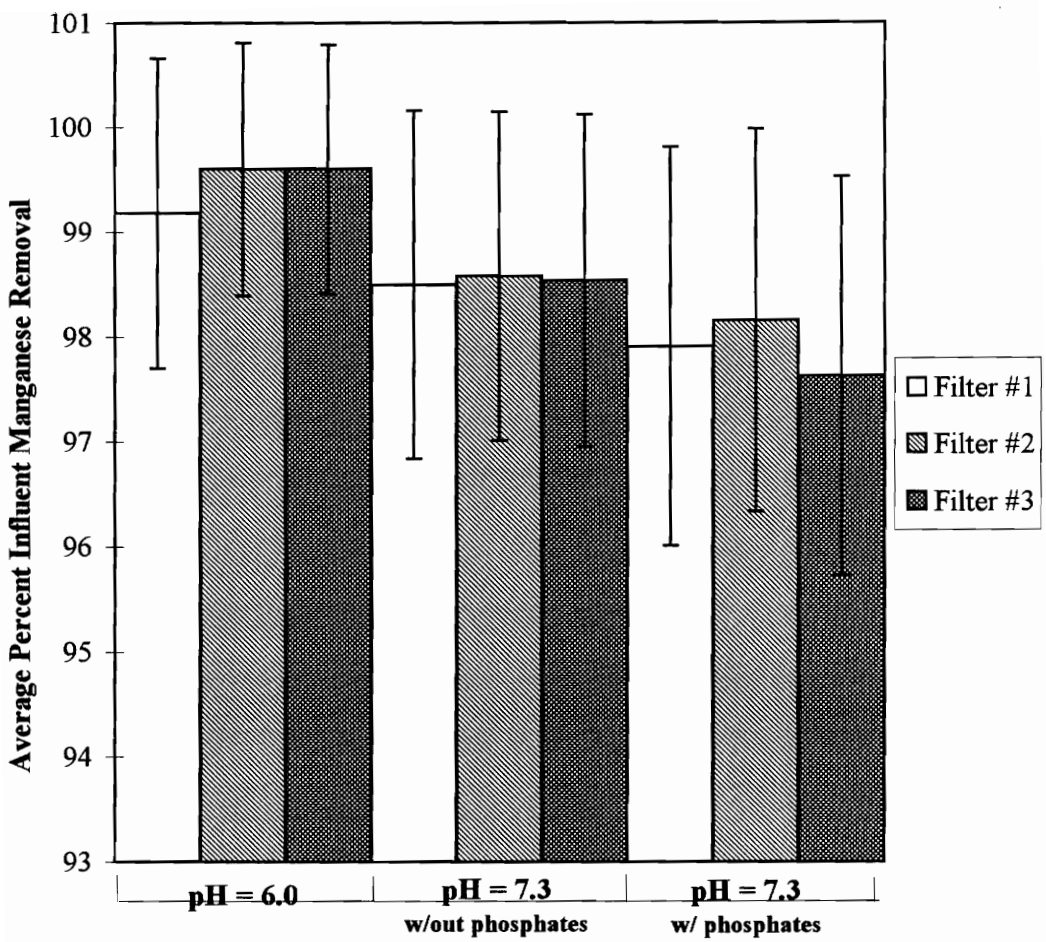

Figure 6: The Effect of Solution pH and presence/absence of Phosphates on the Percentage of Manganese Removed by Filtration

Table 8: Summary of Percent Mn (II) Influent, Percent $MnO_x(s)$ Influent, and the Percent of Total Influent Manganese Removal by Filtration

	Filter #1			Filter #2			Filter #3		
	pH 6.0	pH 7.3 (without phosphates)	pH 7.3 (with phosphates)	pH 6.0	pH 7.3 (without phosphates)	pH 7.3 (with phosphates)	pH 6.0	pH 7.3 (without phosphates)	pH 7.3 (with phosphates)
Percent Soluble Influent Mn(II) (%)	98.3	96.1	98.8	98.5	93.4	99.2	98.7	93.0	98.4
Percent Particulate Influent $MnO_x(s)$ (%)	1.7	3.9	1.2	1.5	6.6	0.8	1.3	7.0	1.6
Percent Manganese Removal by Filtration (%)	99.2	98.5	97.9	99.6	98.6	98.2	99.6	98.5	97.6

conditions. Statistical comparisons of the combined removal percentages of all three filters at the three influent water conditions are summarized in Table 9.

Kruskal-Wallis Multiple-Comparison Z-Value test comparisons of the influent manganese concentrations at the three influent pH conditions revealed no statistical difference (within a 95% confidence interval) in the influent concentrations. For this reason, statistical comparisons of manganese removal percentages for the three pH conditions are valid.

Both Table 8 and a visual interpretation of Figure 6 suggest a slight decrease in percent manganese removal from pH 6.0 to pH 7.3 to pH 7.3 with phosphates. Kruskal-Wallis Multiple-Comparison Z-Value comparisons in Table 9 indicate that percent removal at pH 6.0 was statistically greater (within a 95% confidence interval) than the percent removal at pH 7.3. Since a greater percentage of the influent manganese concentration was particulate at pH 7.3, the trend toward better removal at pH 6.0 suggests that sorption of Mn(II) is a slightly more effective treatment method than removal by particle filtration of $MnO_x(s)$.

The addition of phosphate at pH 7.3 did apparently sequester a portion of the Mn(II) (shown in Table 8 by the increased percent soluble manganese influent above that at pH 7.3 without phosphate). Data in Figure 6 suggest a small decrease in the average percent manganese removal by filtration, which indicates that the addition of phosphate at pH 7.3 also slightly inhibited Mn(II) sorption and/or oxidation upon the media. Table 9 confirms that percent removal at pH 6.0 is greater than percent removal at pH 7.3 with phosphate. However, contrary to tendencies possibly apparent in Figure 6, Kruskal-Wallis Multiple-Comparison Z-Value comparisons indicated no statistical difference (within a 95% confidence interval) between the average percent manganese removal at pH 7.3 and at pH 7.3 with phosphate.

Correlation of the influent manganese characteristics with filter performance in manganese removal suggests that the most efficient manganese removal occurred when the manganese was predominantly soluble Mn(II) in the presence of chlorine as the

Table 9: Kruskal-Wallis Multiple-Comparison Z-Value Test Comparing Average Percent Manganese Removal for each Influent pH Condition

Condition	Average Percent Manganese Removal ($\bar{x}$)	Comparison	Kruskal-Wallis Multiple Comparison Z-Value *	Comments
pH 6.0	$\bar{x}_{pH\ 6.0} = 99.5\%$	pH 6.0 vs. pH 7.3 (with phosphates)	4.42	$\mu_{pH\ 6.0} > \mu_{pH\ 7.3\ w/phosphates}$ percent manganese removal at pH 6.0 is greater than percent removal at pH 7.3 in the presence of phosphates
pH 7.3 (without phosphates)	$\bar{x}_{pH\ 7.3\ w/out\ phosphates} = 98.5\%$	pH 6.0 vs. pH 7.3 (without phosphates)	3.14	$\mu_{pH\ 6.0} > \mu_{pH\ 7.3\ w/out\ phosphates}$ percent manganese removal at pH 6.0 is greater than percent removal at pH 7.3 without phosphates
pH 7.3 (with phosphates)	$\bar{x}_{pH\ 7.3\ w/phosphates} = 97.9\%$	pH 7.3 (without phosphates) vs. pH 7.3 (with phosphates)	1.48	$\mu_{pH\ 7.3\ w/out\ phosphates} = \mu_{pH\ 7.3\ w/phosphates}$ no statistical difference within a 95% confidence interval

* Medians significantly different if z-value > 1.96 (regular test).

oxidant. Although acidic pH conditions (pH 6 to pH 7) are typically detrimental to manganese oxidation by chlorine in the bulk solution phase (Knocke *et al.*, 1988), these same conditions maintained the soluble Mn(II) form long enough for sorption to occur so that Mn(II) oxidation took place directly on the coated filter media. Alkaline pH conditions promote more rapid oxidation of Mn(II) to the $MnO_x(s)$ form that must be removed by the more inefficient particle capture within the filters. Additional constituents such as the phosphate did not prevent Mn(II) removal to below the maximum contaminant level (MCL) of 0.05 $^{mg}/_{L}$, but it did slightly interfere with sorption and/or Mn(II) oxidation.

Backwash After Manganese Application to Filters

Efficiency of Backwash in Removing Deposited $MnO_x(s)$ Based Upon Filter Influent Conditions

Figure 7 illustrates typical backwash response curves during filter backwash (filter influent conditions of pH 6.0 and pH 7.3 in the absence of phosphates). The data shown are the ratio of the manganese backwash concentrations released during the third backwash at 30 $^{gpm}/_{ft^2}$ to the total mass of manganese applied during the previous loading cycle at pH 6.0 and pH 7.3 without phosphate. Since the total mass of manganese applied to the filter was slightly different in each instance, the concentrations are shown as a ratio in order to normalize the data relative to the total mass of manganese applied during filtration.

Representative relative Mn concentrations in backwash water samples for the first three backwashes at a 30 $^{gpm}/_{ft^2}$ backwash rate are shown in Table 10 for pH 6.0 and pH 7.3 (no phosphates). Similar data for backwash rates of 15 $^{gpm}/_{ft^2}$ and 22 $^{gpm}/_{ft^2}$ are included in Appendix A, Table A-1. Only the first three trials were comparable between

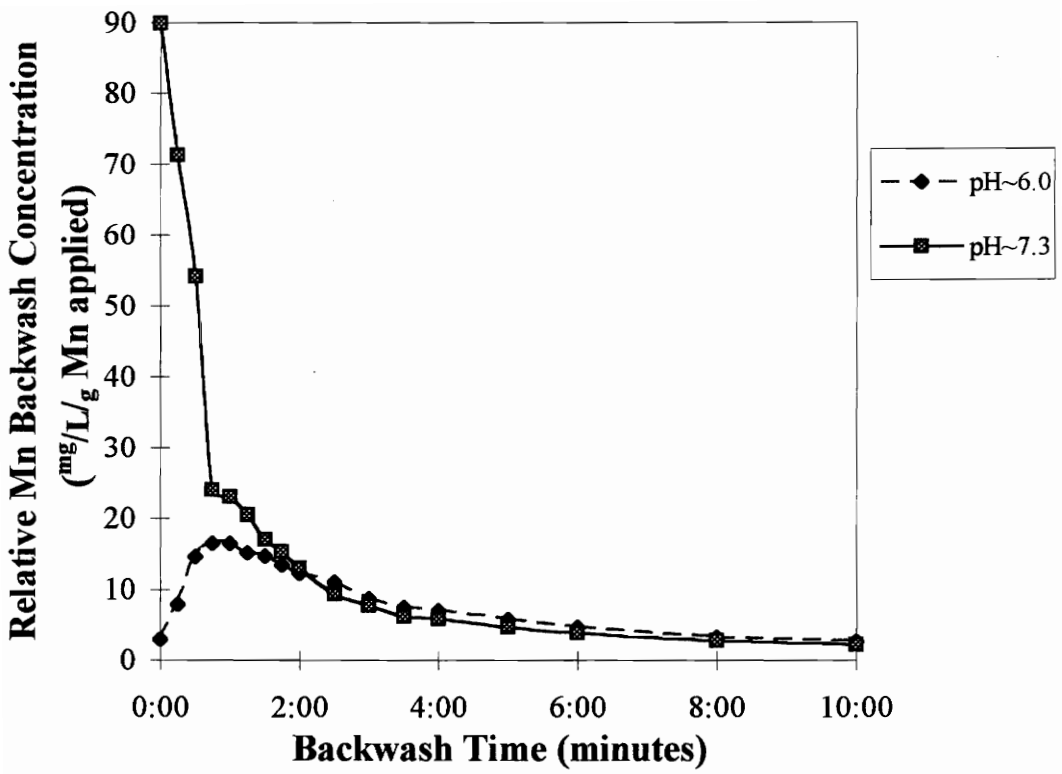

Figure 7: Effect of Influent pH on Manganese Release during Backwash @ $30^{gpm}/_{ft^2}$
(Third backwash for each influent pH condition, no phosphates present)

Table 10: Time-Based Manganese Backwash Concentrations Relative to the Total Influent Mass of Manganese after Influent pH 6.0 and pH 7.3 in the absence of phosphates ($^{mg}/_{L}/_{g}$ Mn applied to filter) (Backwash Rate = 30 $^{gpm}/_{ft^2}$)

		Backwash Time (minutes : seconds)																
Backwash #		0:00	0:15	0:30	0:45	1:00	1:15	1:30	1:45	2:00	2:30	3:00	3:30	4:00	5:00	6:00	8:00	10:00	grams Mn applied to filter during previous loading cycle
1	pH 6.0	4.1	2.1	0.8	0.9	1.0	0.8	0.9	0.9	0.9	0.9	0.8	1.0	0.8	0.8	0.7	0.6	0.6	1.6
	pH 7.3	20.2	24.0	12.0	12.0	9.3	7.2	5.7	5.3	4.9	3.8	3.2	2.7	2.2	1.8	1.4	1.0	0.8	1.3
2	pH 6.0	10.1	9.3	13.6	13.4	12.7	13.6	12.7	12.5	11.2	9.5	8.2	7.1	6.1	5.1	4.4	3.2	2.6	1.4
	pH 7.3	39.0	42.4	32.3	10.3	15.5	14.2	10.6	9.1	9.0	8.1	6.6	5.6	4.6	4.2	3.3	2.5	1.8	1.2
3	pH 6.0	2.3	6.4	11.9	13.4	13.4	12.3	11.9	10.9	9.9	8.9	7.0	6.1	5.6	4.6	3.8	2.6	2.1	1.6
	pH 7.3	89.5	70.9	53.9	23.9	22.9	20.4	16.9	15.2	12.9	9.3	7.7	6.2	5.7	4.4	4.0	2.7	2.1	1.1

the two pH conditions because phosphate in the influent water affected the fourth through the eighth trials at pH 7.3.

Manganese backwash concentrations at backwash rates of 15 $^{gpm}/_{ft}^2$ and 22 $^{gpm}/_{ft}^2$ after pH 6.0 loading conditions were generally steady, decreasing slightly toward the end of a backwash. Due to the more turbulent nature of the 30 $^{gpm}/_{ft}^2$ backwash rate, initial concentrations after pH 6.0 loading conditions were substantially greater than the concentrations at the lesser backwash rates. Manganese concentrations declined as the 30$^{gpm}/_{ft}^2$ backwash progressed, similar to the decline illustrated in Figure 7.

Black $MnO_x(s)$ clouds burst from the filter media at all backwash rates after pH 7.3 loading conditions, causing extreme initial backwash Mn concentrations as the first slug of manganese was released. As backwash progressed, manganese concentrations declined rapidly and leveled off (as illustrated in Figure 7).

For purposes of comparing the backwash concentrations of each influent pH condition, Table 10 and Table A-1 also list the amount of manganese applied during the filtration cycle preceding each backwash. Although the amount of manganese applied to the filters was different for each comparison shown, the amount applied at pH 7.3 was less than the amount applied at pH 6.0 in every instance except two. Therefore, the extreme backwash concentrations after pH 7.3 influent conditions are not attributed to excessive manganese influent concentrations above those at pH 6.0 but to the greater particulate manganese ($MnO_x(s)$) loading to the filters resulting from an alkaline pH.

The difference between the pH 6.0 and pH 7.3 influent conditions with regard to backwashing was in the backwashed manganese concentrations and the pattern of release of backwashed $MnO_x(s)$ from the filters. Initial backwash $MnO_x(s)$ concentrations after pH 7.3 loading conditions were greater than those after pH 6.0 loading conditions as shown in Table 10. $MnO_x(s)$ backwash concentrations after pH 7.3 influent conditions also declined rapidly during the first few minutes of backwashing compared to the gradual decrease or steady $MnO_x(s)$ backwash concentrations after pH 6.0 influent conditions. However, in most cases after two to four minutes of backwashing, $MnO_x(s)$ backwash

concentrations asymptotically approached zero for both pH 6.0 and pH 7.3 influent conditions.

During backwash at the completion of each filtration cycle, the appearance of the backwash water and the concentration of the backwash samples reflected the type of manganese loading upon the filter due to influent water conditions. Filter-applied water pH and the presence or absence of phosphate determined the ratio of Mn(II) to $MnO_x(s)$ in the filter influent and, thus, the ratio of Mn(II) adsorbed on the filter media to $MnO_x(s)$ deposited within the filters. The presence of phosphate at pH 7.3 and the acidic influent conditions at pH 6.0 allowed a greater percentage of influent manganese to remain soluble than at pH 7.3 without phosphate. As a result, at pH 6.0 and at pH 7.3 with phosphate, Mn(II) sorbed and oxidized on the anthracite coal filter media as a coating that was more resistant to removal during backwash than the loose particulate $MnO_x(s)$ trapped in the filter at pH 7.3 (no phosphate). Filter influent conditions of pH 7.3 without phosphate produced a greater particulate manganese ($MnO_x(s)$) load that was easily dislodged and removed during backwash. Therefore, at pH 7.3, a greater percentage of the manganese applied during filtration was removed during backwash than at pH 6.0 or at pH 7.3 in the presence of phosphate.

Typically, the appearance of the backwash water after influent condition pH 6.0 was brown with small, visible $MnO_x(s)$ flocs. The pH 7.3 influent condition, however, created a comparatively darker backwash with larger $MnO_x(s)$ flocs. The effect of phosphate application to the filters at influent pH 7.3 was an apparent strengthening of the oxide coating such that it was difficult to remove the coating during backwash. While normal backwashes at either pH 6.0 or pH 7.3 were dark brown or black, the addition of phosphates in the filter-applied influent caused the backwash water in the subsequent backwash to be dim and translucent. The manganese backwash concentrations and the total mass of manganese released from the filters during backwash after exposure to phosphates was 20% to 60% less than the manganese concentrations and total masses released without the presence of phosphates.

Figures 8, 9, and 10 illustrate the effects of the presence of phosphate at pH 7.3 in comparison to normal operation at pH 6.0 and pH 7.3 at each backwash rate. At a backwash rate of 15 $^{gpm}/_{ft}^2$ (shown in Figure 8), the amount of manganese released during backwash relative to the amount of manganese applied during filtration for pH 7.3 with phosphate was comparable to pH 6.0 but much less than pH 7.3 without phosphate. At 22 $^{gpm}/_{ft}^2$ and 30 $^{gpm}/_{ft}^2$ (Figures 9 and 10, respectively) relative manganese release at pH 7.3 with phosphate was less than that at both pH 6.0 and pH 7.3. In fact, the relative amount of manganese removed during backwash after influent conditions of pH 7.3 with phosphate did not increase with increasing backwash rate as it did under normal operating conditions. The relative amounts of manganese released in backwash during operation with phosphate stayed in the range of about 100 - 200 mg Mn backwashed per gram Mn applied for all three backwash rates.

The phosphate effects also interrupted an obvious trend that was developing during operation at pH 7.3. With each successive backwash during backwashes #1 through #3, the relative amount of manganese removed from the filter increased. However, addition of phosphate during filtration before backwash #4 caused a sudden and immediate decrease in the relative amount of manganese removed from the filters during backwash. The presence of phosphate in the influent water seemed to capture most of the manganese in the filter and did not allow it to escape during backwash, even though $MnO_x(s)$ continued to accumulate in the filter. After normal operation resumed and phosphate effects ceased, operation at pH 7.3 restarted the trend of increasing relative amounts of manganese released during backwash with each successive backwash, as backwashes 11 and 12 illustrate.

Backwash 8 is not shown in Figures 8, 9, and 10 because it was the transition from the presence of phosphate in the influent water back to normal operation at pH 7.3. During that time, the influent manganese characteristics (i.e. increased percent particulate $MnO_x(s)$ in filter applied water) indicated that phosphate was not present in the influent water. However, the backwash characteristics (i.e. decreased manganese concentrations

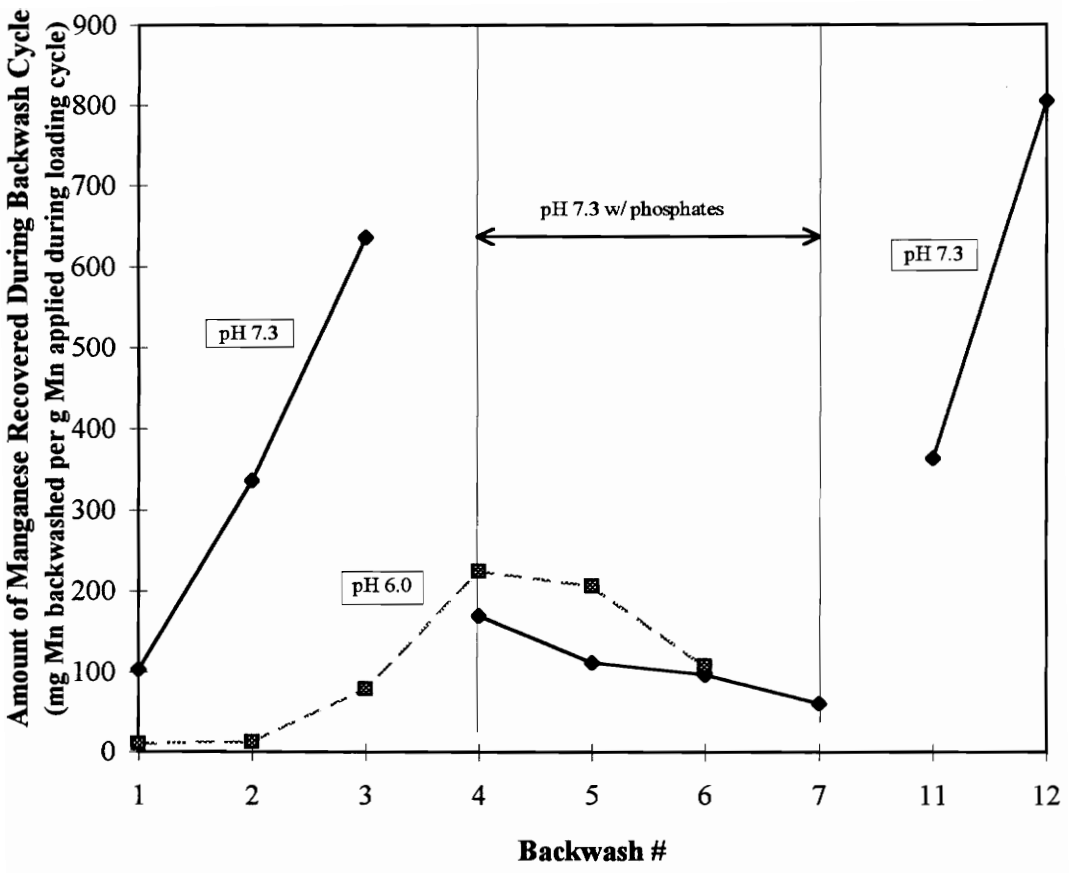

Figure 8: Comparison of total Mn release for influent pH 6.0 and pH 7.3 during backwash at 15 $^{gpm}/_{ft^2}$

(pH 7.3 shown with and without phosphate addition)

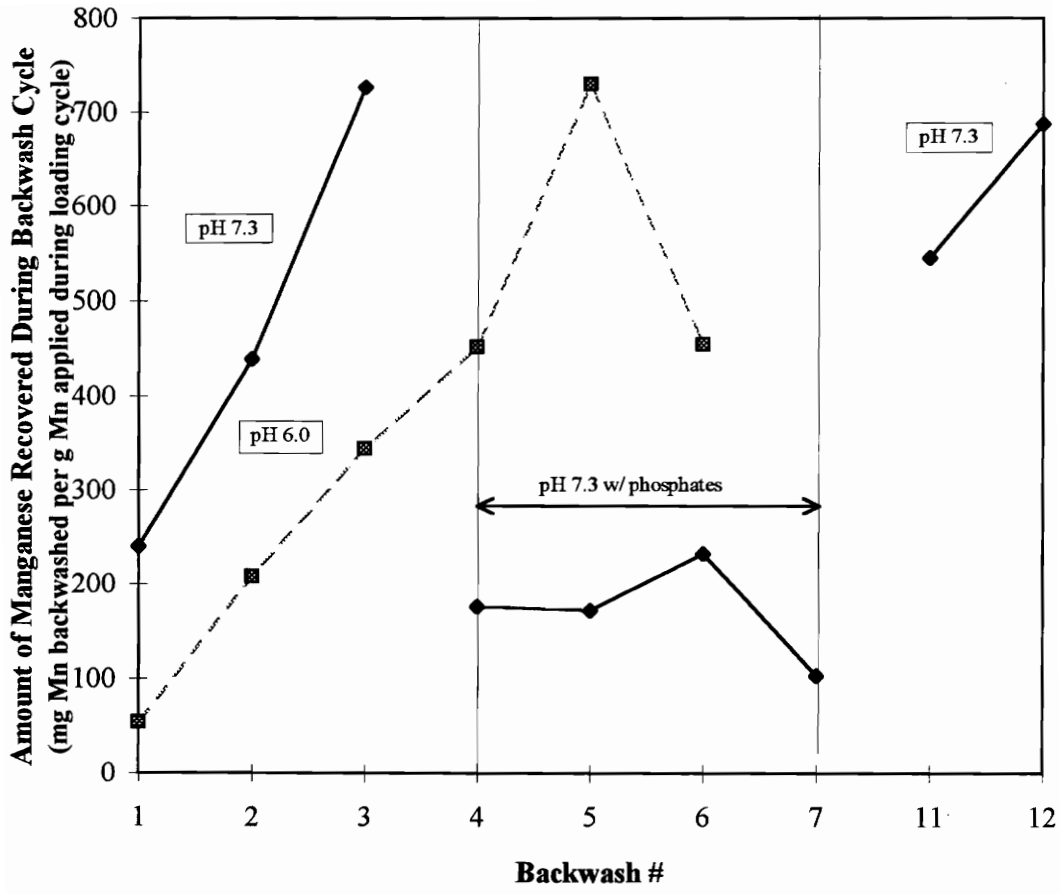

Figure 9: Comparison of total Mn release for influent pH 6.0 and pH 7.3 during backwash at 22 $^{gpm}/_{ft^2}$

(pH 7.3 shown with and without phosphate addition)

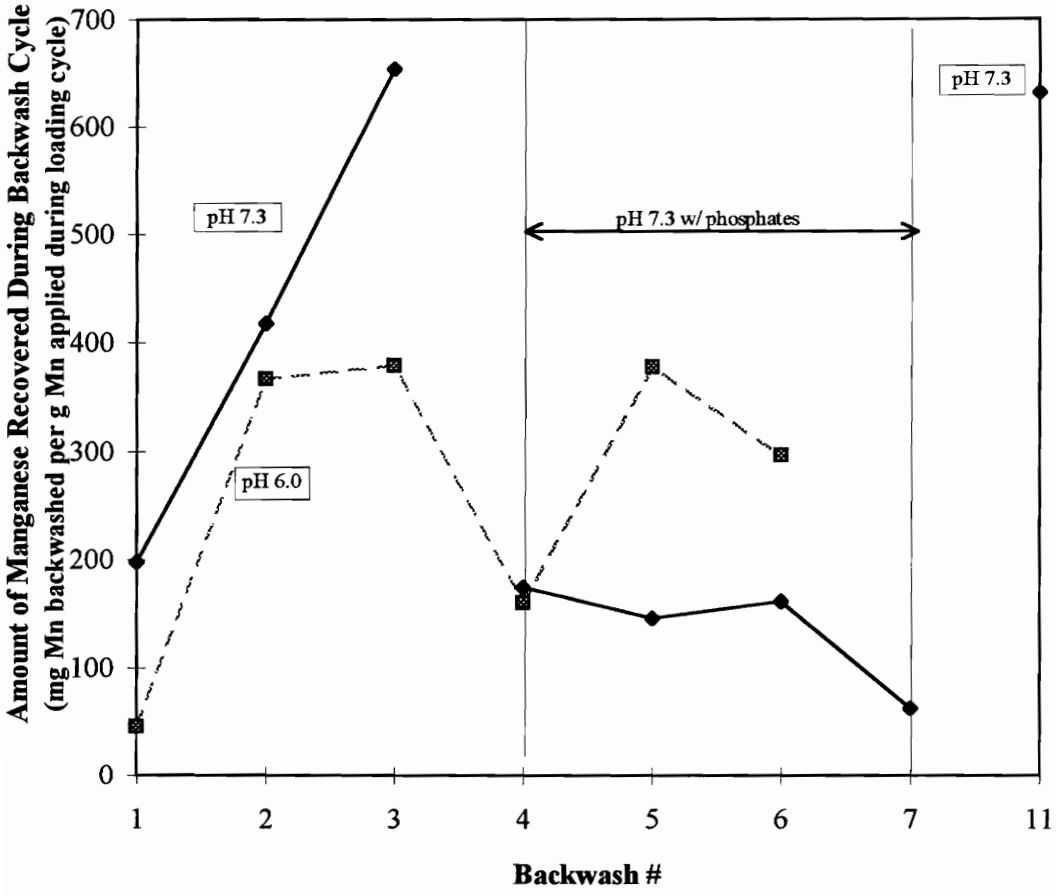

Figure 10: Comparison of total Mn release for influent pH 6.0 and pH 7.3 during backwash at 30 $^{gpm}/_{ft^2}$

(pH 7.3 shown with and without phosphate addition)

in backwash water, dim appearance of backwash water) indicated that phosphate apparently continued to influence the filter media in some manner. Backwashes 9 and 10 are not shown because of errors in filter operation, resulting in a large particulate $MnO_x(s)$ load to the filters that was not consistent with normal filter loading conditions. Backwash 12 is not shown in Figure 10 because the 30 $^{gpm}/_{ft^2}$ backwash rate filter (Filter #3) was taken out of service for air scour testing.

The information listed in Tables 11 and 12 is comparative data for manganese application to the filters and for backwash at each backwash rate during pH 6.0 and pH 7.3 without phosphate influent conditions. Table 13 lists loading and backwash data for the period during pH 7.3 studies when phosphate effects were predominant. Notice in Tables 11 and 13 that the percent of applied manganese that was removed during backwash was between 10% and 27% for the predominantly soluble manganese influent at pH 6.0 and pH 7.3 with phosphate. Backwash after pH 7.3 influent conditions, however, removed between 48% and 53% of the manganese applied to the filter.

Frequent analysis of the filter influent water during the manganese loading cycle determined the soluble (Mn(II)), colloidal, and particulate ($MnO_x(s)$) manganese fractions that made up the total influent manganese concentration at each influent condition. The influent manganese concentration was predominantly soluble Mn(II) at all pH conditions. Analysis of the backwash water, in turn, revealed that the entire manganese concentration in the backwash water was particulate $MnO_x(s)$ after every influent condition; all manganese cleaned from the filters during backwash was associated with a particulate $MnO_x(s)$ form. The estimated particulate mass of $MnO_x(s)$ applied to each filter during each loading cycle at each influent condition is listed in Tables 11, 12, and 13. Assuming that all particulate manganese applied to the filters during filtration was removed in the subsequent backwash, the percentage of backwashed $MnO_x(s)$ that was initially particulate in the filter influent is also tabulated.

The estimated total influent $MnO_x(s)$ mass to each filter as well as the percent of total influent manganese in the form of $MnO_x(s)$ is given at the bottom of Tables 11, 12,

Table 11: Mass of Manganese Applied to Filters (total and particulate) and Mass of Manganese Removed in Subsequent Backwash during pH 6.0 Influent Conditions

pH 6.0 Backwash #	Total Manganese Loading to Filters (mg)			$MnO_x(s)$ Loading to Filters (mg as Mn)			Total Manganese Recovered in Backwash Water (mg as Mn) Backwash Rate			Percentage of $MnO_x(s)$ present in Backwash Water that can be Attributed to Particulate $MnO_x(s)$ Loading to Filter [1]		
	Filter #1	Filter #2	Filter #3	Filter #1	Filter #2	Filter #3	15 gpm/ft^2 (Filter #1)	22 gpm/ft^2 (Filter #2)	30 gpm/ft^2 (Filter #3)	Filter #1 (15 gpm/ft^2)	Filter #2 (22 gpm/ft^2)	Filter #3 (30 gpm/ft^2)
1	5910	1800	1570	101	9	25	62.4	54	71.9	100%	16.7%	34.8%
2	6100	2150	1370	73	54	22	78	208	503	93.6%	26.0%	4.4%
3	6330	2390	1570	185	27	12	504	344	596	36.7%	7.9%	2.0%
4	5530	1960	1930	46	20	16	1240	452	309	3.7%	4.4%	5.2%
5	4840	1440	1390	126	44	37	996	730	526	12.7%	6.0%	7.0%
6	6760	2100	1510	88	25	7	727	455	448	12.1%	5.5%	1.6%
Sum Total:	35,500	11,800	9,340	619	179	119	3610	2240	2450			
Percent of Total Mass In:				1.7%	1.5%	1.3%	10.2%	19.0%	26.2%			
Composite[2] Percentage of Backwashed $MnO_x(s)$ Initially Particulate in Filter Influent:										17.1%	8.0%	4.9%

(1) Percentage of $MnO_x(s)$ present in backwash water that can be attributed to particulate $MnO_x(s)$ loading to filter = $\frac{MnO_x(s) \text{ loading to filter (mg as Mn)}}{\text{Total manganese recovered in backwash water (mg as Mn)}}$

(2) Composite percentage is compiled over all six backwash cycles.

Table 12: Mass of Manganese Applied to Filters (total and particulate) and Mass of Manganese Removed in Subsequent Backwash during pH 7.3 (without phosphate) Influent Conditions

pH 7.3 (w/out phosphates) Backwash #	Total Manganese Loading to Filters (mg)			MnO_x(s) Loading to Filters (mg as Mn)			Total Manganese Recovered in Backwash Water (mg as Mn) Backwash Rate			Percentage of MnO_x(s) present in Backwash Water that can be Attributed to Particulate MnO_x(s) Loading to Filter [1]		
	Filter #1	Filter #2	Filter #3	Filter #1	Filter #2	Filter #3	15 gpm/ft^2 (Filter #1)	22 gpm/ft^2 (Filter #2)	30 gpm/ft^2 (Filter #3)	Filter #1 (15 gpm/ft^2)	Filter #2 (22 gpm/ft^2)	Filter #3 (30 gpm/ft^2)
1	6020	2020	1260	76	35	26	620	485	249	12.3%	7.2%	10.4%
2	5030	1690	1240	378	225	229	1690	742	518	22.4%	30.3%	44.2%
3	4780	1610	1070	163	163	33	3040	1170	700	5.4%	13.9%	4.7%
11	6450	2290	1630	120	121	77	2350	1250	1030	5.1%	9.7%	7.5%
12	9150	2660		477	132		7370	1830		6.5%	7.2%	
Sum Total:	31,400	10300	5200	1210	676	365	15100	5480	2500			
Percent of Total Mass In:				3.9%	6.6%	7.0%	48.1%	53.2%	48.1%			
Composite[2] Percentage of Backwashed MnO_x(s) Initially Particulate in Filter Influent:										8.0%	12.3%	14.6%

(1) Percentage of MnO_x(s) present in backwash water that can be attributed to particulate MnO_x(s) loading to filter = $\frac{\text{MnOx(s) loading to filter (mg as Mn)}}{\text{Total manganese recovered in backwash water (mg as Mn)}}$

(2) Composite percentage is compiled over all five backwash cycles.

Table 13: Mass of Manganese Applied to Filters (total and particulate) and Mass of Manganese Removed in Subsequent Backwash during pH 7.3 in the presence of phosphates Influent Conditions

pH 7.3 w/ phosphates Backwash #	Total Manganese Loading to Filters (mg)			$MnO_x(s)$ Loading to Filters (mg as Mn)			Total Manganese Recovered in Backwash Water (mg as Mn) Backwash Rate			Percentage of $MnO_x(s)$ present in Backwash Water that can be Attributed to Particulate $MnO_x(s)$ Loading to Filter [1]		
	Filter #1	Filter #2	Filter #3	Filter #1	Filter #2	Filter #3	15 gpm/ft^2 (Filter #1)	22 gpm/ft^2 (Filter #2)	30 gpm/ft^2 (Filter #3)	Filter #1 15 gpm/ft^2	Filter #2 22 gpm/ft^2	Filter #3 30 gpm/ft^2
4	6130	1980	1380	112	36	33	1040	348	241	10.8%	10.3%	13.7%
5	6760	2100	1540	99	21	57	754	361	225	13.1%	5.8%	25.3%
6	7480	2170	1640	< DL[2]	< DL[2]	< DL[2]	722	505	265	< DL[2]	< DL[2]	< DL[2]
7	6200	1870	1440	107	6	6	378	193	91	28.3%	3.1%	6.6%
Sum Total:	26600	8120	6000	318	63	96	2890	1410	822			
Percent of Total Mass In:				1.2%	0.8%	1.6%	11%	17%	14%			
Composite[3] Percentage of Backwashed $MnO_x(s)$ Initially Particulate in Filter Influent:										11.0%	4.5%	11.7%

(1) Percentage of $MnO_x(s)$ present in backwash water that can be attributed to particulate $MnO_x(s)$ loading to filter = $\frac{MnO_x(s) \text{ loading to filter (mg as Mn)}}{\text{Total manganese recovered in backwash water (mg as Mn)}}$

(2) DL = Detection Limit

(3) Composite percentage is compiled over all four backwash cycles.

and 13. At pH 6.0 and at pH 7.3 with phosphate, the percent of influent manganese that was in the form of $MnO_x(s)$ was 1.5% and 1.2%, respectively. At pH 7.3 without phosphate, however, the percent of influent manganese in the form of $MnO_x(s)$ was 5.8%, which corresponded with previous research findings that manganese oxidation by free chlorine is kinetically more favorable under alkaline pH conditions (Knocke *et al.*, 1989).

The total mass and percent of manganese backwashed from each filter and the composite percentage of backwashed $MnO_x(s)$ that was initially particulate in the filter influent are also given at the bottom of Tables 11, 12, and 13. Figures 11, 12, and 13 show the percent of manganese recovered during each backwash after each influent pH condition. The percent of backwashed $MnO_x(s)$ that was initially particulate in the influent was 10.0% at pH 6.0, 11.6% at pH 7.3 without phosphate, and 9.1% at pH 7.3 with phosphate (the averages of the composite percentages given for each filter at the bottom of Tables 11, 12, and 13). Hypothetically, the greater percentage of $MnO_x(s)$ influent at pH 7.3 should indicate a greater percent of backwashed $MnO_x(s)$ that was initially particulate in the influent. However, the percent of backwashed $MnO_x(s)$ that was initially particulate is similar for all three influent water conditions. Two explanations resolve the apparent contradiction. First, backwashing does not clean all of the deposits from the filters. For example, in filter #1 during backwash #1 at pH 6.0, the estimated mass of influent $MnO_x(s)$ was greater than the mass of $MnO_x(s)$ cleaned from the filter during backwash. Therefore, the percent of backwashed $MnO_x(s)$ that was initially particulate in the influent was 100%. Although the total influent $MnO_x(s)$ mass at pH 6.0 was less than the influent $MnO_x(s)$ mass at pH 7.3, the mass of $MnO_x(s)$ released during backwash after pH 6.0 was also less than the mass of $MnO_x(s)$ released during backwash after pH 7.3 so that the ratios and percentages were similar at both conditions.

Second, backwashing after pH 7.3 (no phosphate) cleaned a greater percentage of the influent manganese from the filter than backwashing after pH 6.0 and pH 7.3 with phosphate. When influent $MnO_x(s)$ was removed by particle capture within a filter, that particle also became a sorption site for influent Mn(II) like the $MnO_x(s)$ coating on the

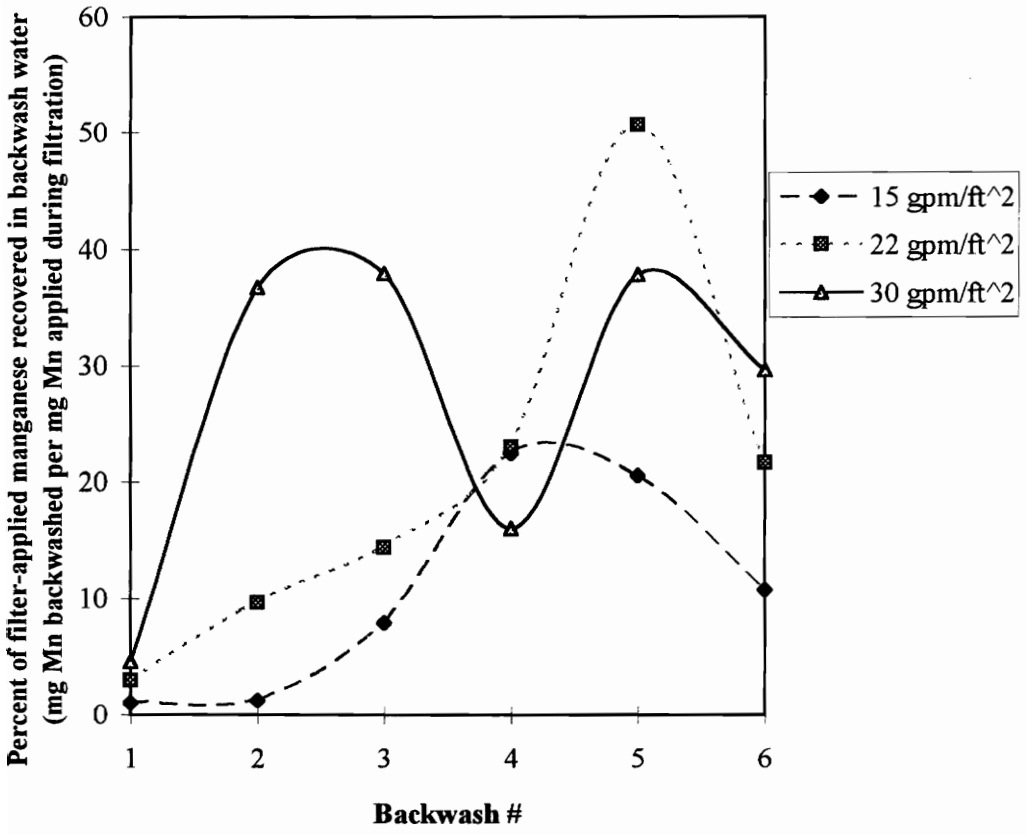

Figure 11: Percent of Filter-Applied Manganese Released During Backwash after Influent pH 6.0 Loading Conditions

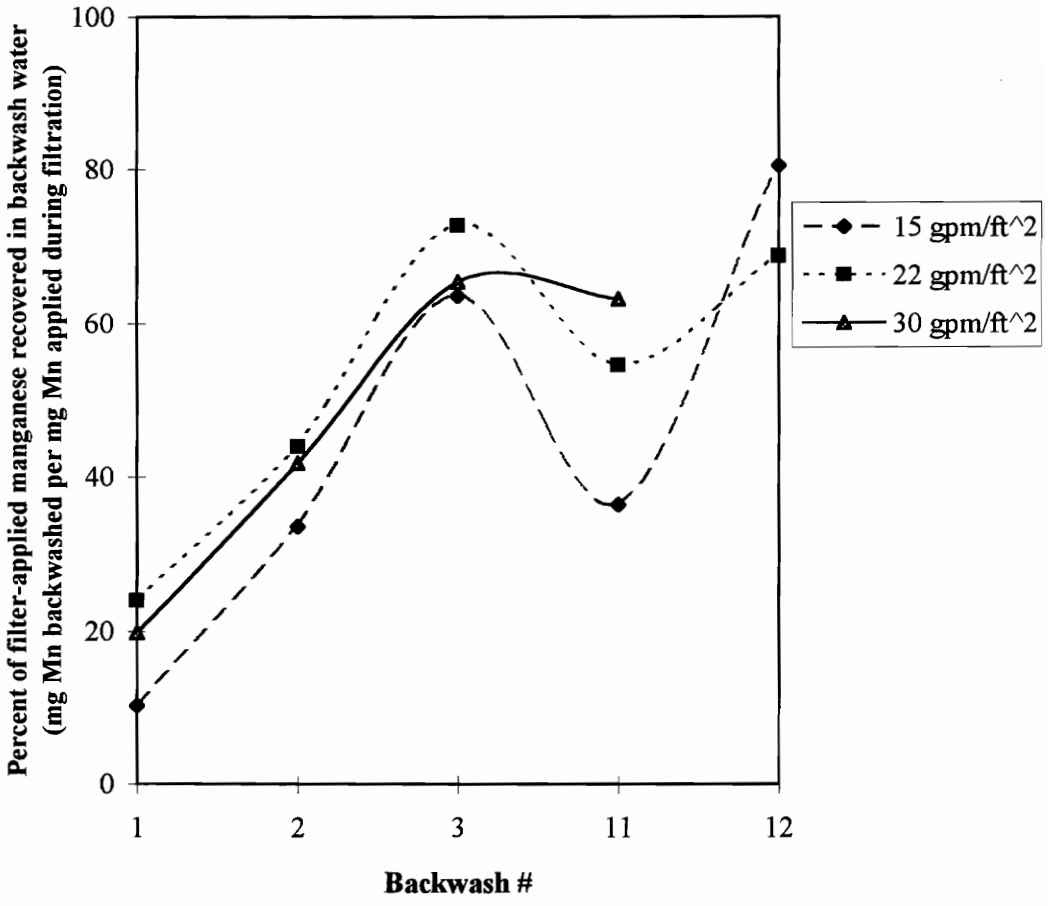

Figure 12: Percent of Filter-Applied Manganese Released During Backwash after Influent pH 7.3 without phosphate Loading Conditions

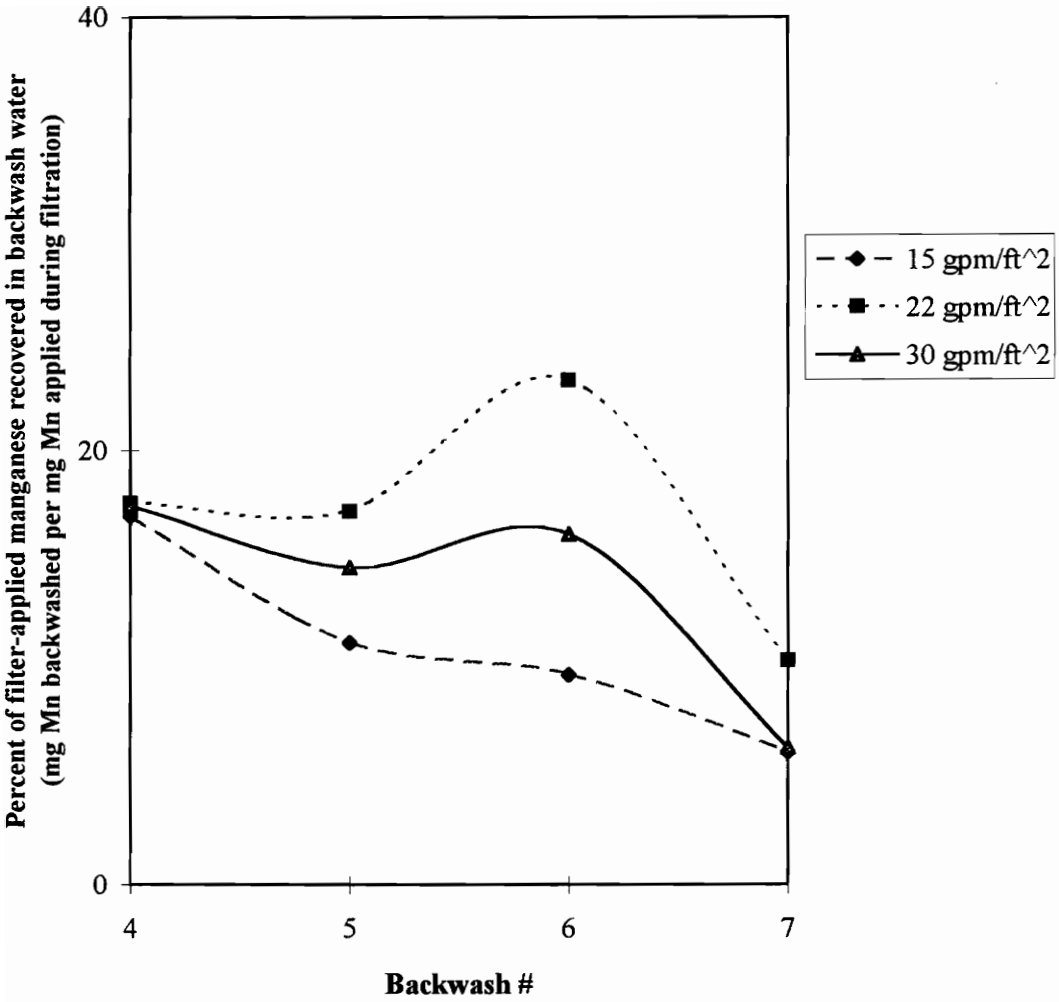

Figure 13: Percent of Filter-Applied Manganese Released During Backwash after Influent pH 7.3 in the presence of phosphates Loading Conditions

anthracite coal. As a result, the unattached particles increased in size by continuing sorption and oxidation during filtration. When the particles were backwashed from the filter, then, they potentially carried out much of the initially soluble manganese that might otherwise have remained sorbed and oxidized to the oxide-coated filter media. Although the mass of influent particulate $MnO_x(s)$ removed during backwash was greater at pH 7.3 than at pH 6.0 or pH 7.3 with phosphate, the total mass of $MnO_x(s)$ removed during backwash at pH 7.3 was correspondingly greater than that removed at pH 6.0 and pH 7.3 with phosphates, which also caused the ratio of influent $MnO_x(s)$ to backwashed $MnO_x(s)$ to be similar.

Effect of Backwash Rate on Manganese Backwash Concentrations

Comparison of the effect of backwash rates in the range of 15 to 30 $^{gpm}/_{ft}^2$ upon oxide-coated anthracite coal was a primary objective of the filtration study. After the first few filtration and backwash cycles, it became clear that most of the removable manganese oxide washed out of the filter early at all backwash rates so that the final several minutes of sampling only defined a tail of decreasing manganese concentrations.

Figure 14 is a typical time-based backwash response curve comparing true manganese concentrations of the three experimental backwash rates after an influent loading condition of pH 7.3 without phosphate. All three backwash rates produced a spike of manganese concentrations at the outset of backwashing that diminished within three minutes of backwashing. Backwash at 30 $^{gpm}/_{ft}^2$ yielded the greatest spike, but the manganese concentrations diminished more quickly than the concentrations at 15 $^{gpm}/_{ft}^2$ or 22 $^{gpm}/_{ft}^2$. Backwash at 22 $^{gpm}/_{ft}^2$ resulted in the second largest spike which, in turn, diminished more steeply than the manganese concentrations at 15 $^{gpm}/_{ft}^2$. However, all three backwash rates approached the same asymptote as Figure 14 illustrates. After an initial slug of manganese, each manganese backwash concentration curve settled into a gradual decrease that approached zero coincident with the other backwash rate curves.

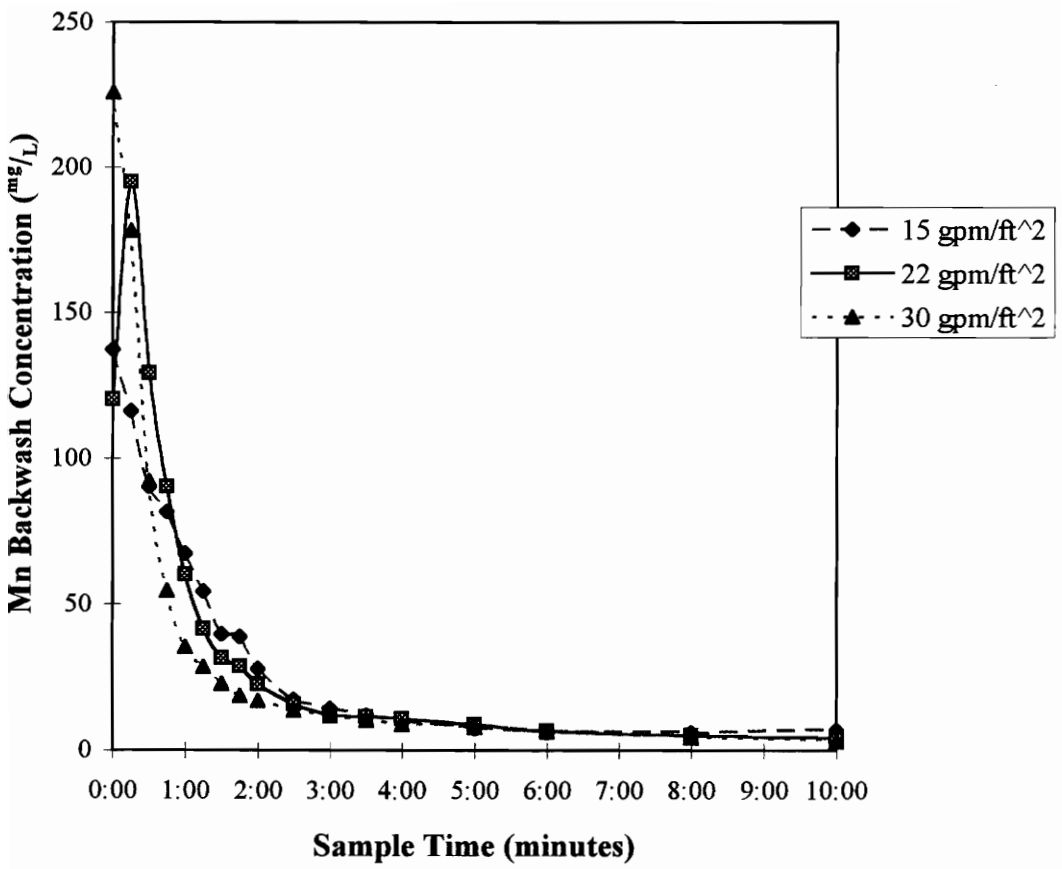

Figure 14: Mn Concentrations in Backwash Based Upon Backwash Rate after Influent pH 7.3 without phosphate

The data in Figure 14 are true manganese concentrations in milligrams per liter as they were washed from each filter. The data in Figure 15, however, are backwashed manganese concentrations relative to the amount of manganese applied to the filter during the previous loading cycle. Because the filters had different surface areas, filtration rates of 5 $^{gpm}/_{ft^2}$ at concentrations of 0.3 $^{mg}/_{L}$ Mn(II) did not produce the same mass of manganese applied to each filter. For the particular filtration cycle shown, the mass of Mn(II) applied to each filter was 6.45 grams, 2.29 grams, and 1.63 grams for backwash rates of 15 $^{gpm}/_{ft^2}$, 22 $^{gpm}/_{ft^2}$, and 30 $^{gpm}/_{ft^2}$, respectively. Since the filter surface area was smaller for the greater backwash rate filters, the total mass of Mn(II) applied to each filter decreased with increasing backwash rate. Even so, the initial backwash manganese concentrations were greater at the increased backwash rates.

The relative backwashed manganese concentrations in Figure 15 show a more defined spike separation between the backwash rates but give the same trends as described for Figure 14. The normalized data in Figure 15 also indicate how a true concentration backwash response curve might have appeared if the filters had the same surface area. The data in Figure 14, though, emphasize the contrast between the backwash rates since the greater backwash rates produced greater true manganese concentrations, even though the total Mn(II) applied during filtration was notably less.

Cumulative amounts of manganese released during backwash relative to the mass of Mn(II) applied during filtration for each backwash rate at influent pH 6.0 and pH 7.3 are shown in Figures 16 and 17, respectively. Figure 16 indicates that after pH 6.0 influent conditions, the greater backwash rates yielded greater amounts of manganese per square foot of filter area. Also, the cumulative manganese release curves were steeper for greater backwash rates, indicating that the rate of increase in the amount of manganese backwashed from the filters was greater for increased backwash rates.

In contrast to Figure 16, data presented in Figure 17 indicate a greater manganese release during backwash at 22 $^{gpm}/_{ft^2}$ than at 30 $^{gpm}/_{ft^2}$ for the first several backwashes after pH 7.3 loading conditions. The curves representing the three backwash rates tracked each

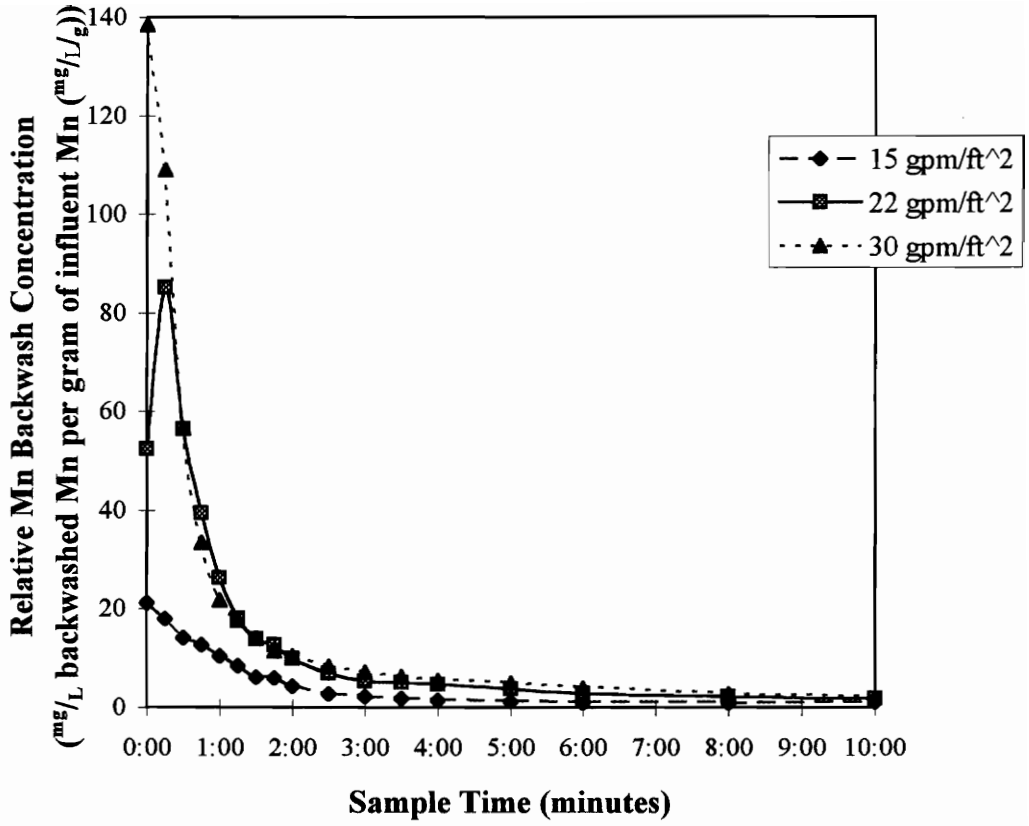

Figure 15: Relative Mn Concentrations in Backwash Based Upon Backwash Rate after Influent pH 7.3 without phosphate Loading Conditions

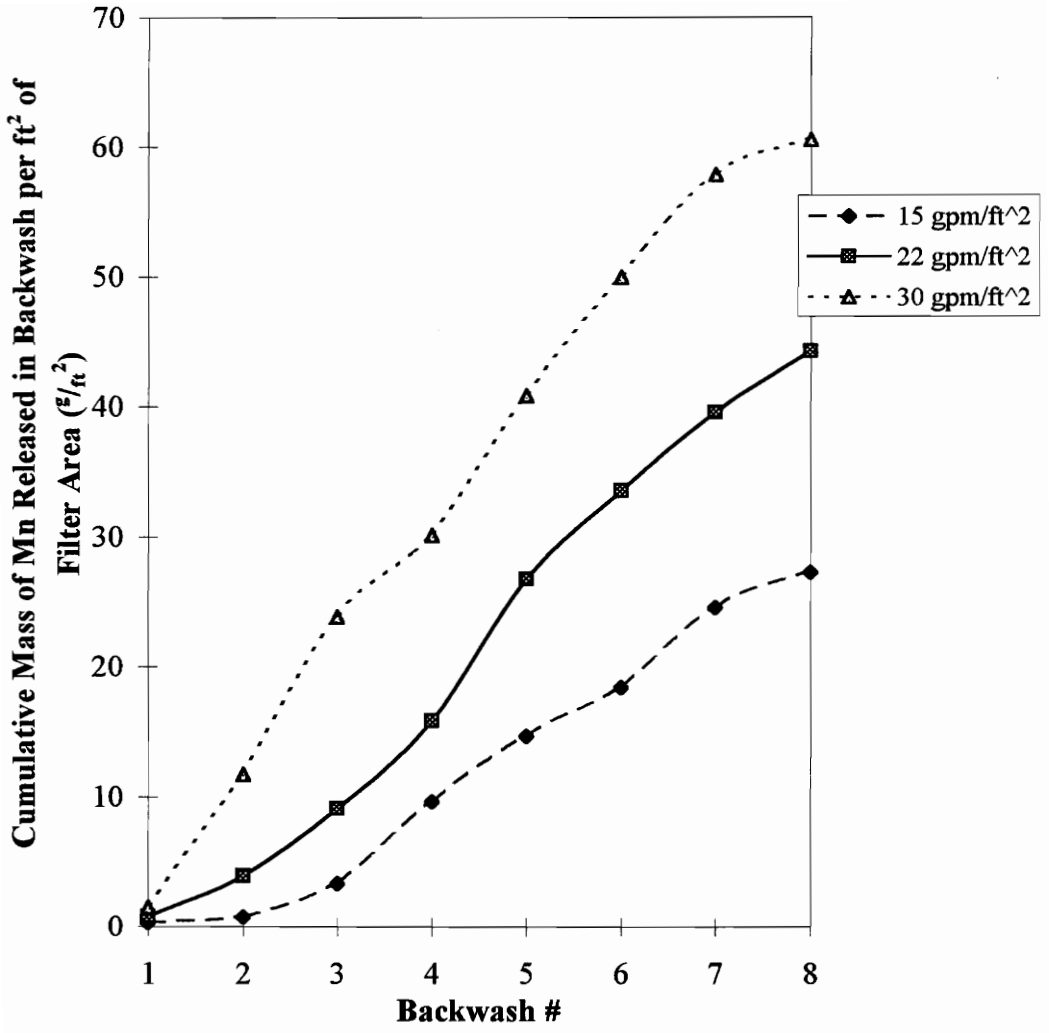

Figure 16: Cumulative Manganese Released at each Backwash Rate during Filter Influent pH 6.0 Loading Conditions

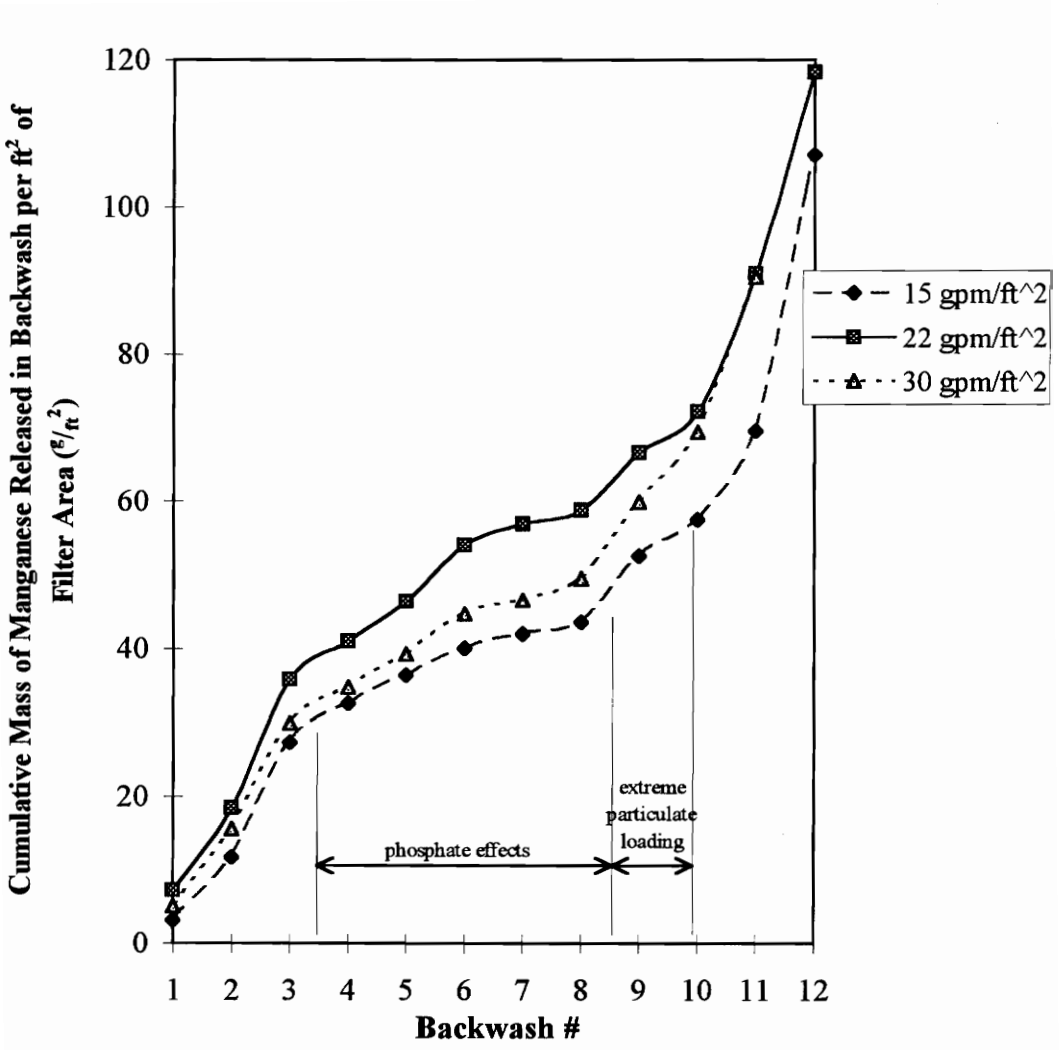

Figure 17: Cumulative Manganese Released at each Backwash Rate during Filter Influent pH 7.3 without phosphate Loading Conditions

other closely during the pH 7.3 loading condition due, in part, to the duration of phosphate effects. Apparently the mass of manganese released during backwash at 22 $^{gpm}/_{ft}^2$ was initially greater than the mass released during backwash at 30 $^{gpm}/_{ft}^2$, and the backwashes that followed at 30 $^{gpm}/_{ft}^2$ did not overcome that difference. By backwash #11, the cumulative mass of manganese released per square foot of filter at 30 $^{gpm}/_{ft}^2$ was approximately equal to that released at 22 $^{gpm}/_{ft}^2$.

MnO_x(s) Coating Amounts at Various Filter Media Depths

Frequent depth profiles throughout experimentation at pH 6.0 and pH 7.3 indicated a continual oxide accumulation upon the anthracite coal despite regular backwashing. The media coring data in Figures 18 and 19 illustrate MnO_x(s) accumulation upon the media subjected to a 15 $^{gpm}/_{ft}^2$ backwash rate. The media coring data in Figures 20 and 21 indicate a similar response for the 30 $^{gpm}/_{ft}^2$ backwash rate. The length of time between each coring or media depth sampling was three filtration and backwash cycles so that Mn(II) application to the filters was similar between each depth profile study.

The depth studies pictured in Figures 18 through 21 may be compared based upon pH condition or backwash rate. Oxide accumulation differences based upon influent pH may be seen by comparing Figure 18 to Figure 19 and Figure 20 to Figure 21. Figures 18 and 20 show oxide accumulation at influent pH 6.0 throughout the depth of the filter. Although the majority of Mn(II) sorption and oxidation took place within the top six inches of media, a substantial portion of the deeper anthracite also increased in MnO_x(s) concentration. In comparison, data contained in Figures 19 and 21 indicate minimal MnO_x(s) accumulation deep in the filter relative to the accumulation at the top of the filter. This may be explained by the more alkaline pH condition (pH 7.3) promoting both greater Mn(II) sorption capacity (Morgan and Stumm, 1964) as well as faster surface oxidation of

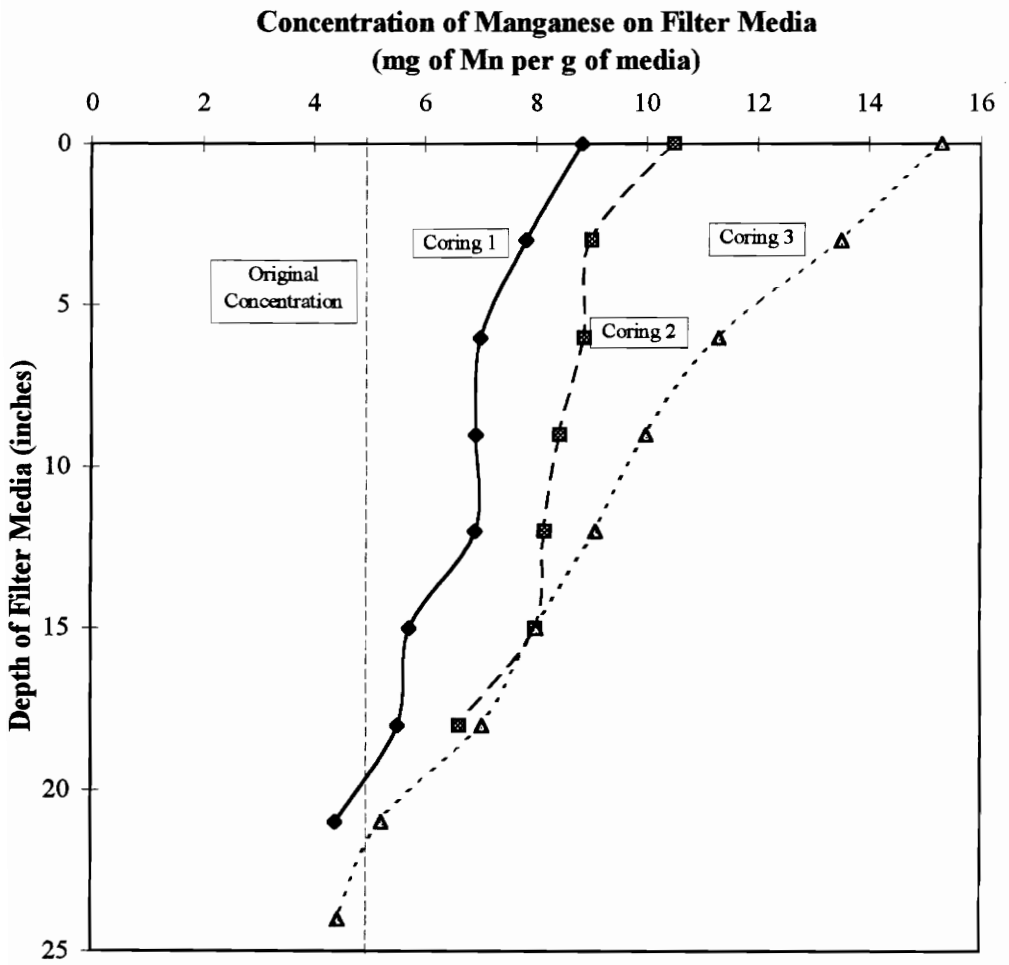

Figure 18: Progression of $MnO_x(s)$ Coating Accumulation for Filter #1 (Backwash Rate: 15 $^{gpm}/_{ft^2}$; Filter Influent pH 6.0 Loading Conditions)

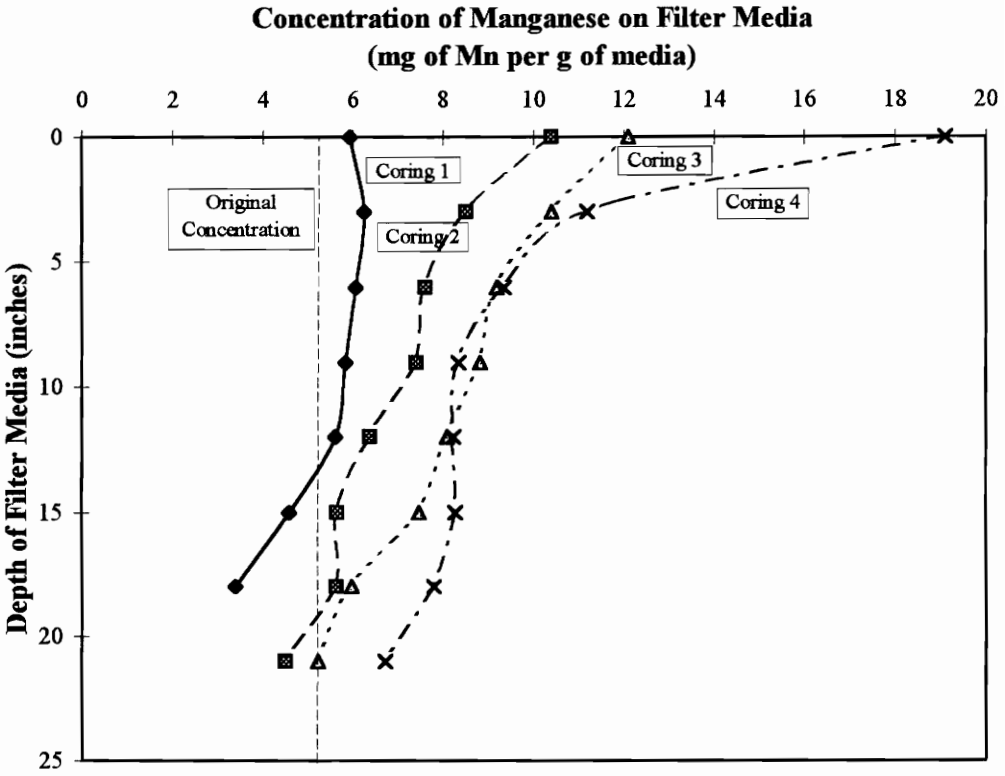

Figure 19: Progression of $MnO_x(s)$ Coating Accumulation for Filter #1 (Backwash Rate: 15 $^{gpm}/_{ft^2}$; Filter Influent pH 7.3 Loading Conditions; presence of phosphate in the influent affected backwash studies for coring 2 and 3)

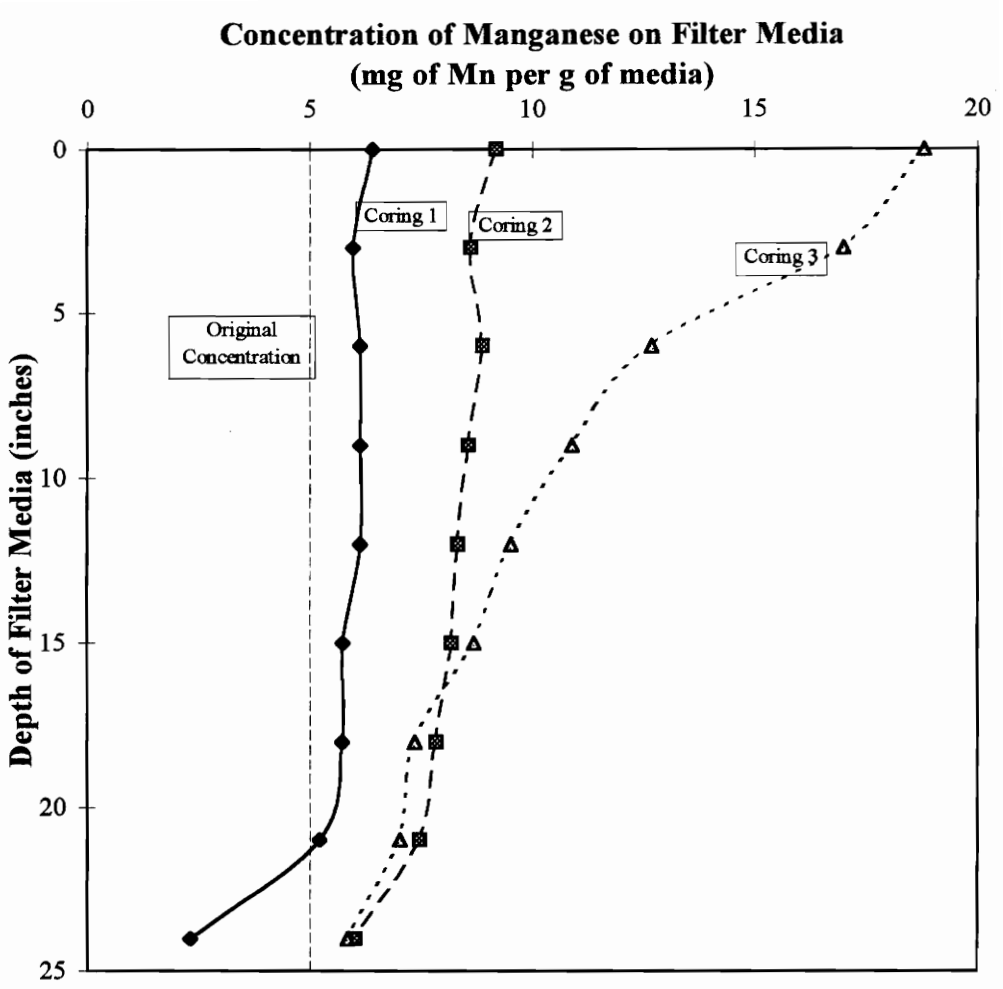

Figure 20: Progression of $MnO_x(s)$ Coating Accumulation for Filter #3 (Backwash Rate: 30 $^{gpm}/_{ft^2}$; Filter Influent pH 6.0 Loading Conditions)

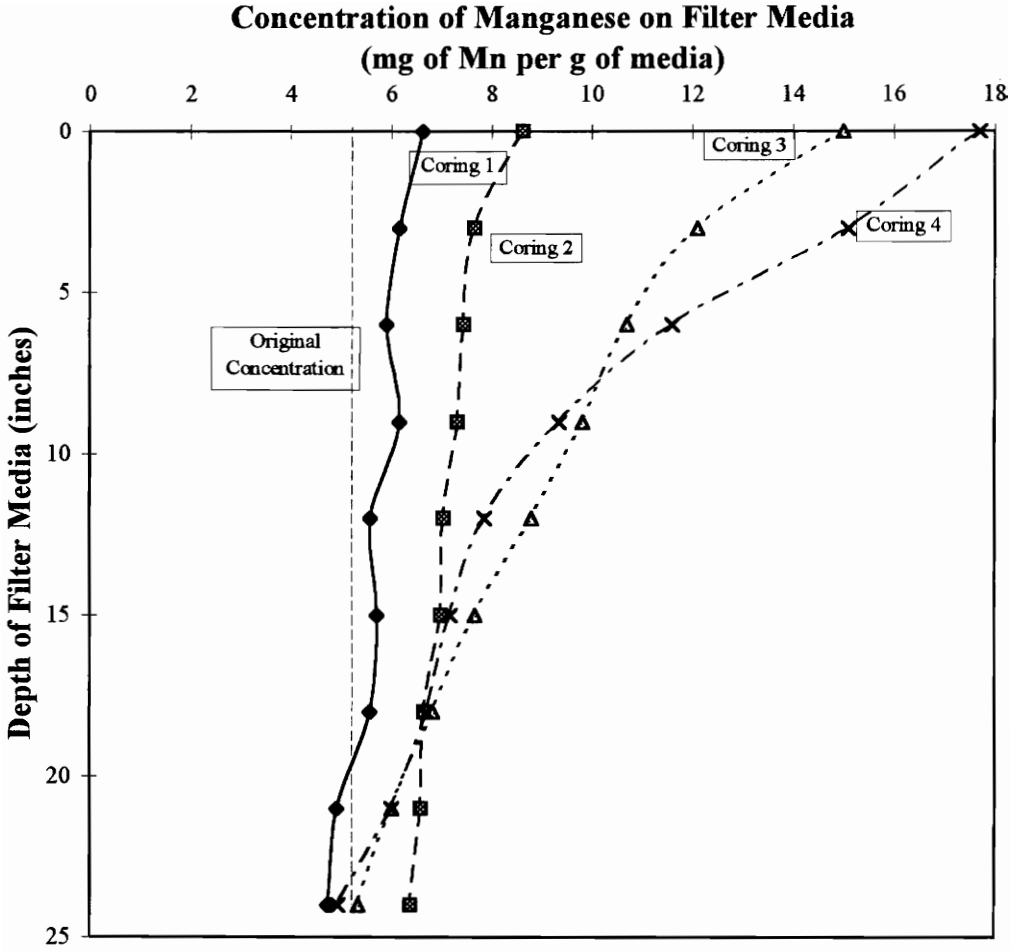

Figure 21: Progression of MnO_x(s) Coating Accumulation for Filter #3 (Backwash Rate: 30 $^{gpm}/_{ft^2}$; Filter Influent pH 7.3 Loading Conditions; presence of phosphate in the influent affected backwash studies for coring 2 and 3)

sorbed Mn(II). Rapid oxidation at pH 7.3 maintained available sorption sites at the top of the filter that removed most of the Mn(II) before it reached the deeper sorption sites. Oxidation at pH 6.0 was presumed kinetically slower. Sorption sites were not as readily available at the top of the filter, and some Mn(II) removal had to take place at deeper sorption sites throughout the filter (Coffey, 1990).

The anthracite under study at pH 6.0 also retained more of its oxide coating than the media under study at pH 7.3. The third and last coring at pH 6.0 revealed greater $MnO_x(s)$ coating concentrations than the third coring at pH 7.3 at all filter depths. The more acidic pH 6.0 maintained a greater percentage of Mn(II) influent that adsorbed to and oxidized on the media. Alkaline conditions of pH 7.3 promoted more pre-filter Mn(II) oxidation to $MnO_x(s)$ creating particulate solids that were removed from the influent by particle filtration. The settled particles were easily backwashed from the filter after influent pH 7.3, but the extensive oxide coating that developed at influent pH 6.0 was more resistant to removal by backwashing and, thus, remained on the media.

The data presented in Table 14 include the total manganese mass loaded onto each filter during the last filtration cycle and the manganese mass released during the final backwash before air scour. Several hypothetical deductions may be inferred from the data in Table 14 combined with previous backwash data and pH studies in the literature. The influent pH conditions may have determined the status of the $MnO_x(s)$ coating; influent pH 6.0 promoted Mn(II) sorption and oxidation upon the media while influent pH 7.3 allowed more oxidation to $MnO_x(s)$ before filtration, resulting in settled particles not sorbed to the media. These settled $MnO_x(s)$ particles may have become competitive Mn(II) sorption sites so that the soluble influent Mn(II) associated itself with the filtered $MnO_x(s)$ particles rather than the $MnO_x(s)$ coating on the anthracite filter media. If this supposition is correct, then the early stages of particulate $MnO_x(s)$ removal are similar to filter ripening, in which normal filtration for turbidity removal improves with the addition of a few particles after backwash that aid in catching further turbidity-causing particles. In the same way, filtered $MnO_x(s)$ particles not chemically attached but contained within the pore

Table 14: Additional Effect of Air Scour Over Water Backwash for $MnO_x(s)$ Removal from Filter Media

	pH ~ 6.0			pH ~ 7.3 (no phosphate)		
	15 $^{gpm}/_{ft^2}$	22 $^{gpm}/_{ft^2}$	30 $^{gpm}/_{ft^2}$	15 $^{gpm}/_{ft^2}$	22 $^{gpm}/_{ft^2}$	30 $^{gpm}/_{ft^2}$
Mn Mass In in Final Filtration Cycle (mg as Mn)	22900	6720	5090	9150	2660	1630
Mn Mass Out in Final Backwash (mg as Mn)	536	315	131	7370	1830	1030
Additional Mn Mass Out Due to Air Scour (mg as Mn)	1720	630	271	4400	877	469
Percent Increase in Mn Mass Out Due to Air Scour	320%	200%	210%	60%	48%	46%

spaces of $MnO_x(s)$ coated media became an available $MnO_x(s)$ surface for removal of the influent soluble Mn(II). As a result, more of the soluble influent Mn(II) may have been removed during backwash with the free $MnO_x(s)$ particulates instead of being retained as a coating on the media. Examination of the $MnO_x(s)$ mass amounts present in the final backwash (Table 14) reveals that water backwash alone removed a greater amount of the manganese applied at influent pH 7.3 than applied at influent pH 6.0.

If this "filter ripening" effect is viable, potassium permanganate ($KMnO_4$) could be used at the beginning of a filtration cycle to produce $MnO_x(s)$ particles that would be retained in the filter. Mn(II) removal by sorption would improve at the beginning of filtration due to $MnO_x(s)$ being deposited in the pore spaces of the filter and providing initial sorption sites. Further research to investigate these hypotheses would involve preloading a filter with free particulate $MnO_x(s)$ before filtration of soluble Mn(II). Comparison of a backwash, then, between the $MnO_x(s)$ particulate preloaded filter and a $MnO_x(s)$-coated-media-only filter after the same soluble Mn(II) loading would indicate how much of the incoming Mn(II) was released in backwash due to sorption onto the free $MnO_x(s)$ particles rather than sorption onto the coated media.

Oxide accumulation differences based upon backwash rate were not as distinct as the differences based upon pH conditions. During the first two coring periods (i.e. six loading and backwash cycles), the lower backwash rate displayed a greater oxide accumulation, as expected, since a greater backwash rate theoretically removed more of the oxide coating. However, after the first two coring periods, backwash rate no longer distinguished the media with regard to surface $MnO_x(s)$ concentration. Instead, $MnO_x(s)$ accumulated upon the media at similar rates for all backwash rates.

The Effect of Air Scour on $MnO_x(s)$ Coatings

The air scour experiments performed at the completion of filter operation at pH 6.0 and at pH 7.3 were designed to qualitatively determine the effect of air scour upon $MnO_x(s)$ coatings. Air scour represents the upward flow of air bubbles through filter media that causes individual media grains to collide, producing a scrubbing or scouring effect (Amirtharajah, 1988). The abrasive forces resulting from increased media contact are useful for removing filtered turbidity-causing particles entrapped in the media. However, this scrubbing mechanism could potentially prove detrimental to Mn(II) removal by sorption and oxidation by scouring the $MnO_x(s)$ coating from the filter media, thus removing Mn(II) sorption sites from the filter. Removing sorption sites from the filter could result in decreased Mn(II) removal from filter-applied water by sorption until the $MnO_x(s)$ coating sufficiently reestablished itself.

Data presented in Table 14 compare the mass of manganese released from the filter during the final water backwash to the additional mass removed due to air scour and its subsequent backwash. No additional manganese was applied to the filter between the final backwash and air scour, but the total mass of manganese applied to each filter in the final filtration cycle is included in Table 14.

Air scour enhanced $MnO_x(s)$ removal from the filter at every pH condition and backwash rate. The percent increase in mass out indicates that air scour was most effective in the filters with the lowest backwash rate and an acidic influent pH. The 15 $^{gpm}/_{ft^2}$ water backwash rate in filter #1 was generally the most inefficient backwash rate due to the large size of the filter coupled with the slowest backwash rate. $MnO_x(s)$ removal from the filter due to air scour increased by 320% at pH 6.0 and 60% at pH 7.3 over $MnO_x(s)$ removal due to water backwash alone. The percent increase in mass out was less drastic for greater backwash rates. The amount of $MnO_x(s)$ removed increased by approximately 200% at influent pH 6.0 and 47% at influent pH 7.3 for both backwash

rates of 22 $^{gpm}/_{ft^2}$ and 30 $^{gpm}/_{ft^2}$. The distinction in the percent increase between the 22 $^{gpm}/_{ft^2}$ backwash rate and the 30 $^{gpm}/_{ft^2}$ backwash rate was insubstantial.

Comparison of air scour effects with respect to pH (Table 14) reveals that air scour better enhanced $MnO_x(s)$ removal from the media at influent pH 6.0 than at influent pH 7.3. Since, hypothetically, a considerable amount of manganese at influent pH 7.3 either was particulate $MnO_x(s)$ in the influent or associated itself with filtered $MnO_x(s)$ particles, more of that applied manganese was effectively removed from the filter during regular water backwash. The data in Table 14 confirm that water backwash removed a greater amount of manganese applied at influent pH 7.3 than applied at influent pH 6.0. As a result, the media at pH 6.0 retained a relatively thicker coating susceptible to enhanced abrasion during air scour. Even so, air scour removed a greater additional mass of manganese from the pH 7.3 media, possibly because the coating formed at pH 7.3 was more easily detached than the coating formed at pH 6.0. The data required to support a comparison between the ease of removal of a coating formed at pH 6.0 versus a coating formed at pH 7.3, though, would be a coring sample between the final water backwash and the air scour study and a coring sample after the air scour study at both influent pH 6.0 and at pH 7.3. Only the studies at pH 7.3 included a coring sample at both times; the studies at pH 6.0 included a coring sample only after the air scour study.

Figures 22 and 23 are typical media depth profiles showing the manganese concentration upon influent pH 7.3 media immediately prior to and following air scour. The profiles confirm that air scour is most effective at the top of the filter bed where the motion of the media is most violent and sporadic (Cleasby *et al.*, 1977). A substantial portion of the oxide coating (2 to 5 $^{mg\ Mn}/_{g\ media}$) was removed from the media that was within the top 3 to 4 inches of the filter bed. However, air scour effects on media $MnO_x(s)$ concentration below the first few inches of media were minimal; typically less than one milligram of $MnO_x(s)$ as Mn per gram of media was removed.

Comparison of the media depth profiles before and after air scour with respect to backwash rate indicate that air scour has a more marked effect on the $MnO_x(s)$ coated

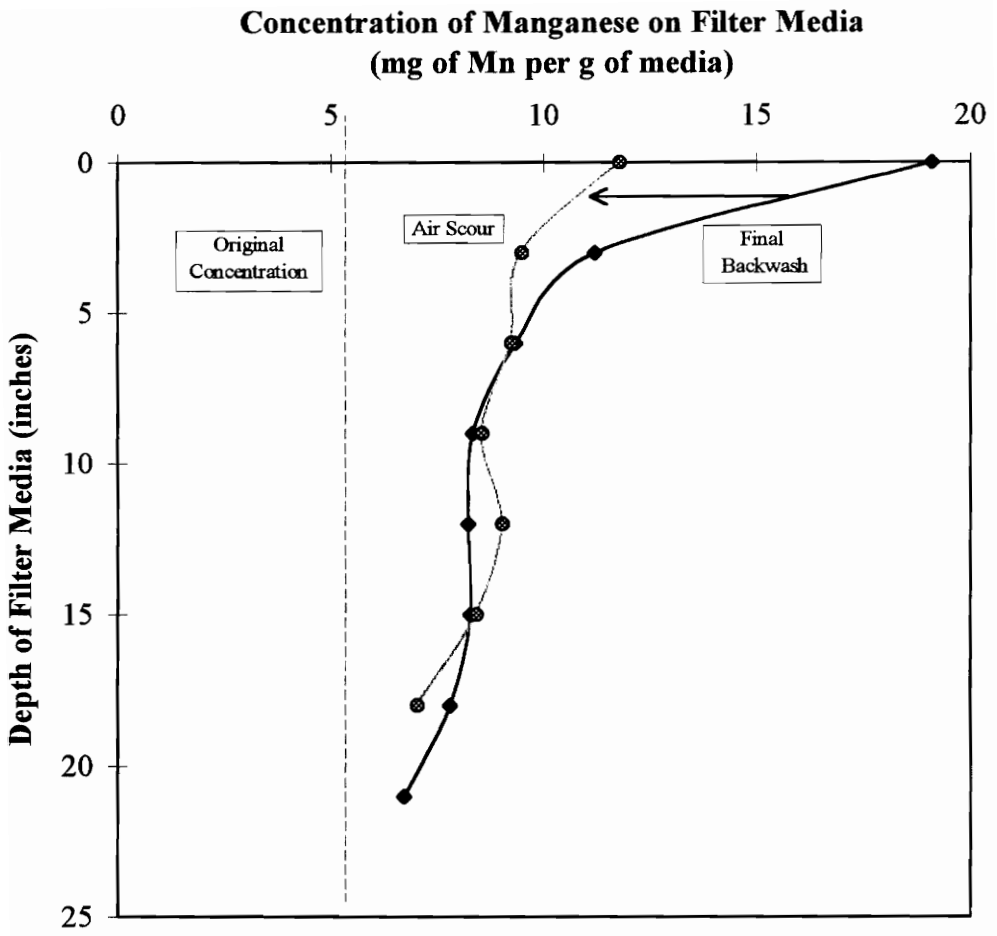

Figure 22: Effect of Air Scour on $MnO_x(s)$ Coating
Filter #1: Backwash Rate = 15 $^{gpm}/_{ft^2}$
Influent pH ~ 7.3

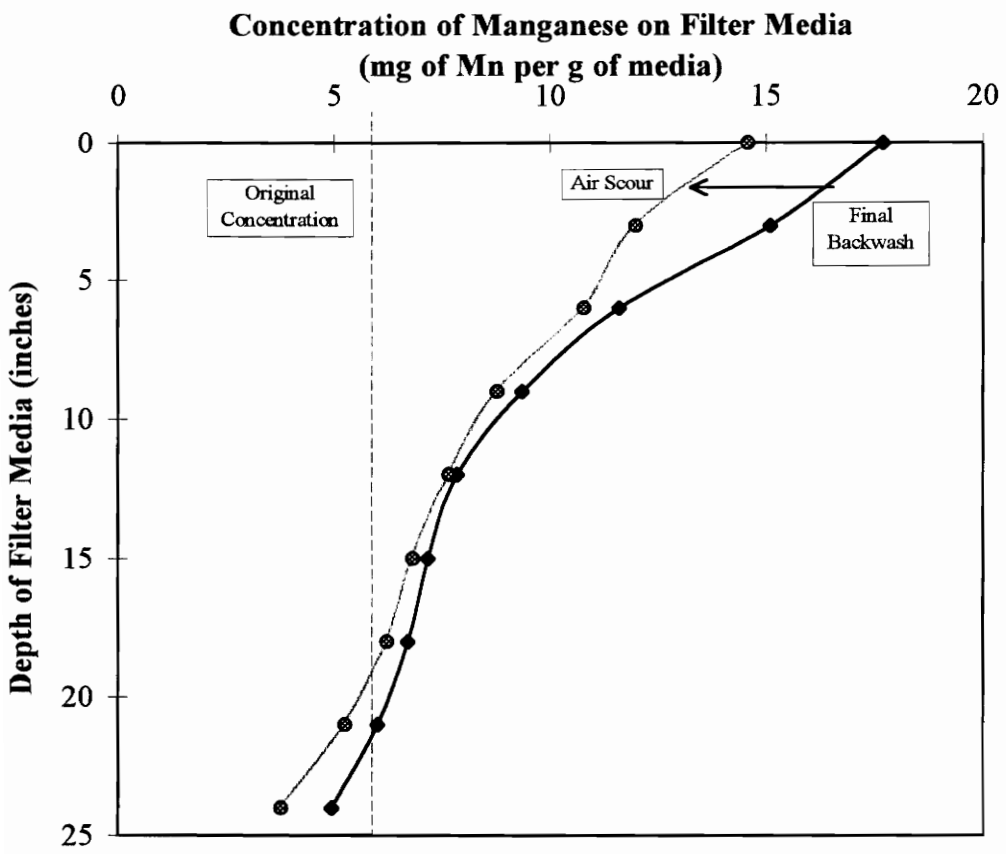

Figure 23: Effect of Air Scour on $MnO_x(s)$ Coating
Filter #3: Backwash Rate = 30 $^{gpm}/_{ft^2}$
Influent pH ~ 7.3

media continually subjected to the slower backwash rate. Air scour removed 5 $^{mg\ Mn}/_{g\ media}$ from the top media layer of Filter #1 with backwash rate 15 $^{gpm}/_{ft^2}$ as opposed to 3.5 $^{mg\ Mn}/_{g\ media}$ from the top media layer of Filter #3 with backwash rate 30 $^{gpm}/_{ft^2}$.

Figure 24 presents data from an air scour/backwash study on anthracite which was similar to that on which backwash studies began. The air scour study on this original Blacksburg filter media began with a less extensive oxide coating than the actual media used for the continual backwash studies. The initial $MnO_x(s)$ concentration upon the anthracite used in continual backwash studies was approximately 5 $^{mg\ as\ Mn}/_{g\ media}$. The $MnO_x(s)$ concentration upon the original Blacksburg anthracite was 3.41 $^{mg\ as\ Mn}/_{g\ media}$, which was equivalent to a total of 8.36 g Mn contained in the filter. The resulting backwash manganese concentrations after air scour of this original media were 10 to 100 times less than normal backwash manganese concentrations after a regular manganese filtration cycle. The total mass of manganese removed due to air scour and backwash was 5.67 mg for a percent $MnO_x(s)$ release from the original anthracite of 0.07%. The sparse $MnO_x(s)$ coating on this original Blacksburg anthracite was less susceptible to abrasion and breakage (even during air scour) than the extensive $MnO_x(s)$ coating that developed during the filtration studies because it was thin and probably patchy upon the media. Therefore, air scour was less effective in removing the $MnO_x(s)$ coating from the media. Although these results are merely qualitative, they suggest that even though air scour can remove a substantial portion of $MnO_x(s)$ coating from filter media, it does not endanger the coating such that filter influent Mn(II) removal would cease. The amount of $MnO_x(s)$ coating remaining on the filter media after air scour should be more than sufficient to promote sorption of Mn(II) and continue the desired Mn(II) removal.

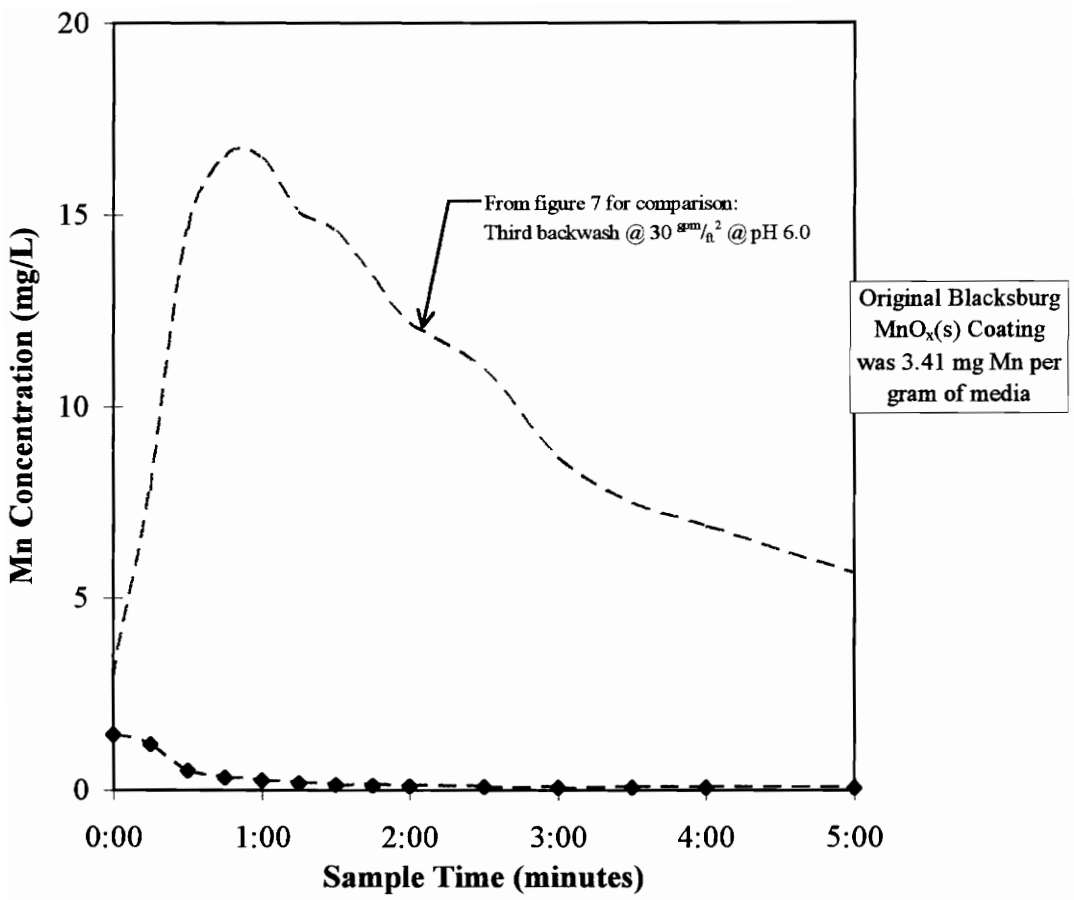

Figure 24: Blacksburg Media Air Scour Backwash
Backwash Rate: 30 $^{gpm}/_{ft^2}$

Effect of $MnO_x(s)$ Coating on the Physical Characteristics of Anthracite Coal

During large-scale filter design and media selection, special consideration is given to the size and shape of filter media in order to promote optimal filtration. Thus, development of any sort of $MnO_x(s)$ surface coating or buildup raises a concern that the carefully selected media grain sizes will increase, creating larger void spaces and increasing the likelihood that small particles will escape filtration. Grain size distribution analyses (ASTM sieve analyses) were performed on $MnO_x(s)$ coated anthracite and on uncoated (i.e. extracted) anthracite to investigate the effects of a coating on media size.

The results of the sieve analyses for the anthracite used in filtration and backwash studies at influent pH 7.3 are illustrated in Figures 25 through 27. Since the top 6" to 8" of media displayed the greatest $MnO_x(s)$ accumulation over the course of the filtration studies, only that portion of the filter media underwent sieve analyses so that notable grain size differences could be more easily identified. Both the coated and uncoated (extracted) anthracite were obtained in the same coring sample so that the sieve analyses would be comparable. Filters #1 and #2 each had an oxide concentration of approximately 12 $^{\text{mg MnOx(s) as Mn}}/_{\text{g media}}$ on the smallest media at the surface of the filter bed, and the oxide concentration at the surface of Filter #3 was approximately 14.5 $^{\text{mg MnOx(s) as Mn}}/_{\text{g media}}$.

Figures 25 through 27 demonstrate the virtually immeasurable effect of the stated amount of $MnO_x(s)$ coating upon media size. However, the three figures indicate a slight media size increase throughout the top eight inches of each filter by the leftward shift of the line toward larger grain diameters. Table 15 lists D_{60}, D_{10} (effective size), and the uniformity coefficient ($UC = {}^{D60}/_{D10}$) for the media used in influent pH 7.3 filtration studies. Note the slight size increase (especially of the effective size) within the top eight inches of each filter. D_{60} was similar between the coated and the uncoated media. The

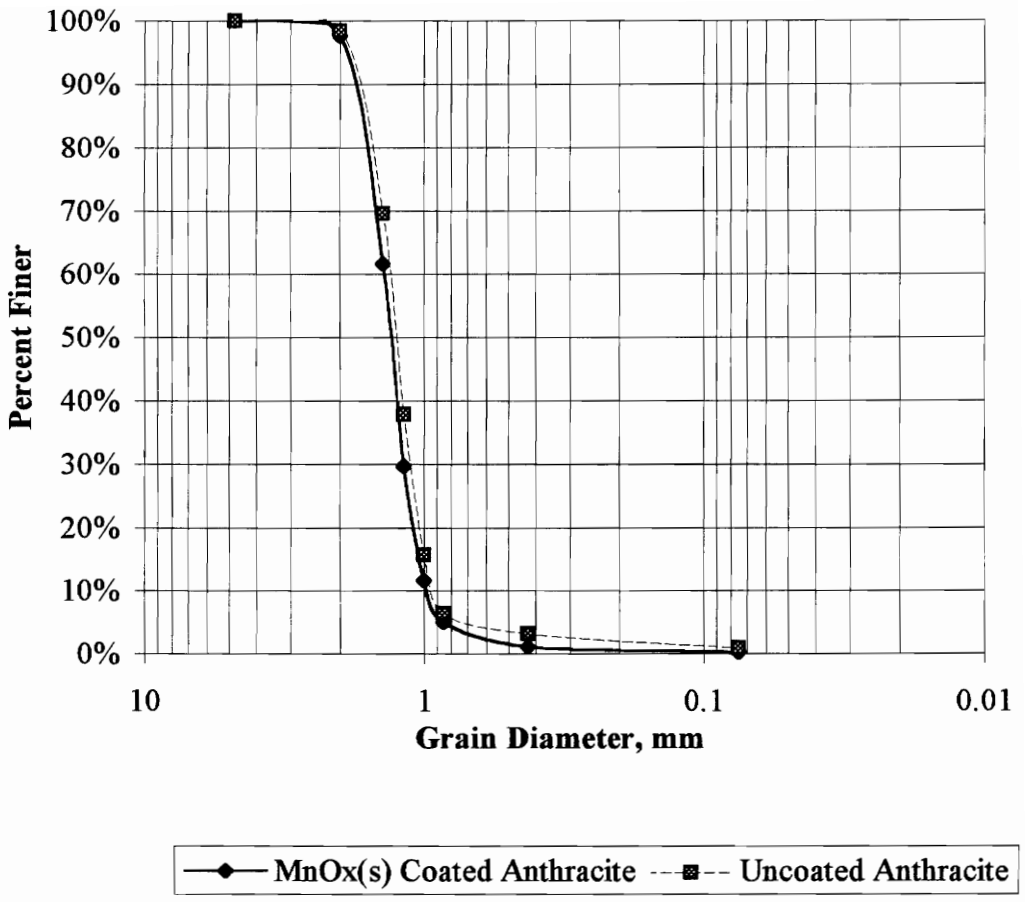

Figure 25: Grain Size Distribution Comparison for Filter #1: Upper 8" Anthracite Coal (Influent pH = 7.3,with and without phosphate; Backwash Rate = 15 $^{gpm}/_{ft^2}$)

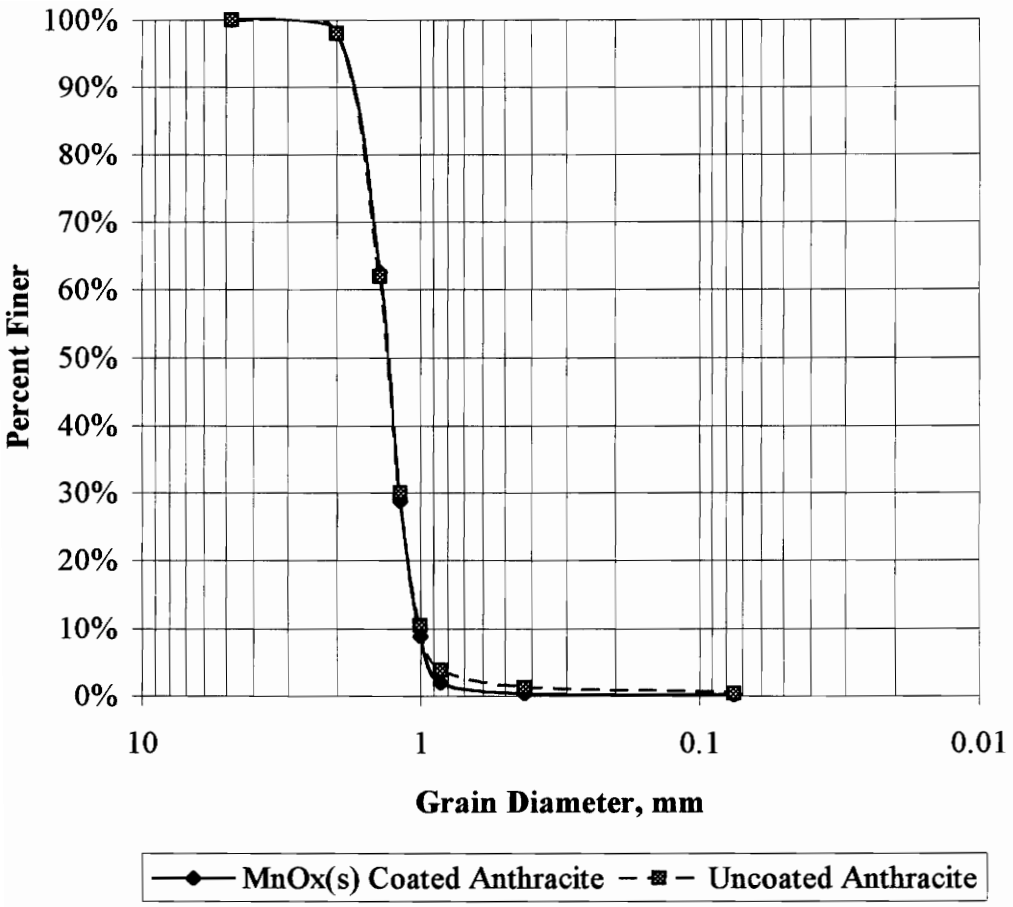

Figure 26: Grain Size Distribution Comparison for Filter #2: Upper 8" Anthracite Coal (Influent pH = 7.3,with and without phosphate; Backwash Rate = 22 $^{gpm}/_{ft^2}$)

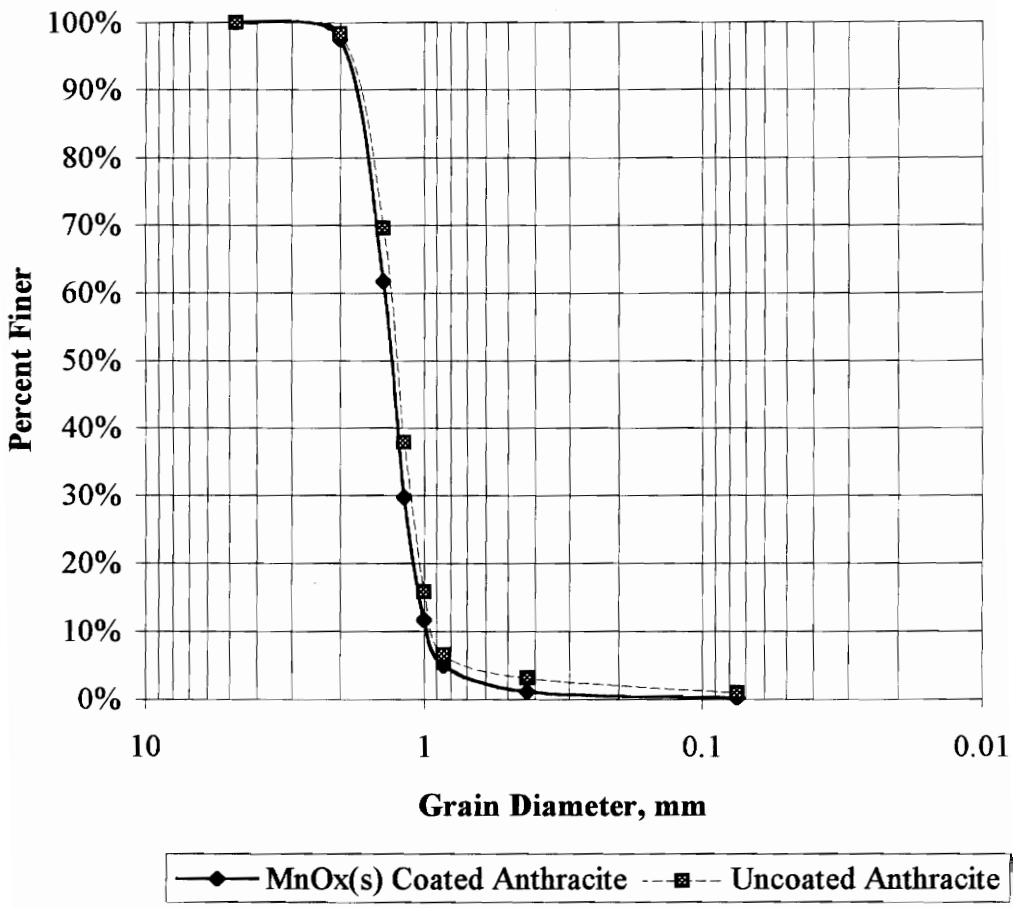

Figure 27: Grain Size Distribution Comparison for Filter #3: Upper 8" Anthracite Coal (Influent pH = 7.3, with and without phosphate; Backwash Rate = 30 $^{gpm}/_{ft^2}$)

Table 15: Gradation Characteristics (D_{60}, D_{10} (effective size), and Uniformity Coefficient (UC)) for Anthracite Coal following influent pH 7.3 studies (with and without phosphate)

Media Description		D_{60} (mm)		D_{10} (mm)		UC ($^{mm}/_{mm}$)	
		Uncoated	Coated	Uncoated	Coated	Uncoated	Coated
Filter #1	Upper 8"	1.40	1.50	0.98	0.99	1.43	1.52
	Middle 8"	1.60	1.60	0.99	0.98	1.62	1.63
	Lower 8"		1.60		0.75		2.13
Filter #2	Upper 8"	1.50	1.50	1.00	1.10	1.50	1.36
	Middle 8"	1.60	1.60	0.93	0.98	1.72	1.63
	Lower 8"		1.70		0.70		2.43
Filter #3	Upper 8"	1.40	1.40	0.95	1.00	1.47	1.4
	Middle 8"		1.70		1.10		1.55
	Lower 8"		1.70		0.65		2.62

relatively slight relational change between D_{60} and D_{10} also resulted in a similar uniformity coefficient between the coated and uncoated media.

Theoretical size effects of an $MnO_x(s)$ coating on a 1 mm diameter sphere of anthracite coal are illustrated in Figure 28. Starting with an uncoated spherical filter media particle of diameter 1.000 mm, the theoretical diameter of that particle was calculated as the amount of $MnO_x(s)$ coating increased from 0 to 100 $^{mg\ Mn}/_{g\ media}$. Even with 100 $^{mg\ MnOx(s)\ as\ Mn}/_{g\ media}$ of oxide coating on the one millimeter media particle, the theoretical spherical diameter increased to only 1.026 mm. In a sieve analysis, the 1.000 mm media particle, which would be retained on a US Standard Sieve No. 18 with 1.00 mm openings, would have to increase to 1.18 mm in diameter to be retained on the next largest consecutive US Standard Sieve No. 16 with 1.18 mm openings. This diameter increase would theoretically correspond to a $MnO_x(s)$ coating concentration of 800 $^{mg\ MnOx(s)\ as\ Mn}/_{g\ media}$. Even with extensive $MnO_x(s)$ coatings on the media, the slight media diameter increase shown in Figure 28 indicates that the coatings have a minor effect on media shape and size and should not seriously impact the media characteristics for particle filtration.

The media used in influent pH 6.0 filtration and backwash studies was not separated into three layers for sieve distribution analysis. Consequently, any difference in size was undetectable due to the averaging effect of a composite sample; the original and final effective size and uniformity coefficient were similar for all three filters.

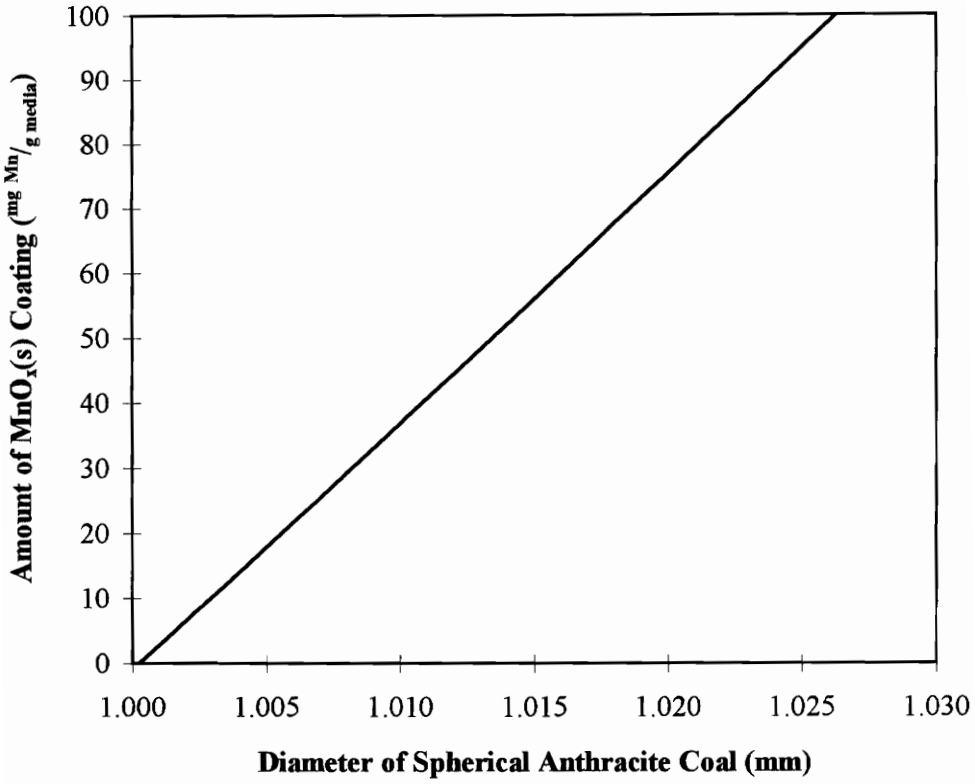

Figure 28: Theoretical Size Effects of Various $MnO_x(s)$ Coating Concentrations on a 1 mm Diameter Sphere of Anthracite Coal

Overall Mass Balance

One of the objectives of the pilot-filter study was to establish a manganese mass balance for each pH condition and backwash rate. The general equation for any mass balance is:

$$\text{Mass In} = \text{Mass Out} + \text{Accumulation}. \qquad [8]$$

During the filtration experiments, the mass in was the amount of manganese applied to each filter during filtration mode, the mass out was the amount of manganese removed due to backwashing each filter plus the amount that escaped in the filter effluent (routinely equal to zero), and the accumulation was the amount of manganese that sorbed and oxidized on the filter media and remained in the filter despite backwashing.

Throughout the sorption and oxidation studies at pH 6.0 and pH 7.3, measurements were made of the concentration of manganese applied to each filter, the manganese content in the filter effluent, and the amount of manganese released during backwash to determine the "mass in" and "mass out," respectively, for an overall manganese mass balance at each pH condition. The media coring samples taken between every three filtration and backwash cycles completed the manganese mass balance as the accumulation within each filter. Table 16 contains data regarding the theoretical amount of manganese accumulation within each filter and the amount determined by media sampling at each coring. The theoretical amount of manganese accumulation in each filter at each coring was determined by adding the net amount of manganese applied during filtration to the amount of manganese originally contained in the filter and subtracting the portion removed by backwash. Table 16 also includes the percent difference in the theoretical and measured manganese accumulation. Negative percentages indicate that the measured amount of manganese was greater than the theoretical amount. The numerical values listed in Table 16 for Filter #3 at influent pH 7.3 filtration conditions are illustrated in Figure 29.

Table 16: Overall Mass Balance for Influent pH 6.0 and pH 7.3 (with and without phosphates) Filtration Conditions

Filtration Condition	Coring #	Theoretical Amount of $MnO_x(s)$ as Mn Accumulation in Filter (g)			Amount of $MnO_x(s)$ as Mn Accumulation in Filter Determined by Media Sampling (g)			% Difference in Theoretical and Measured $MnO_x(s)$ Accumulation		
		Filter #1	Filter #2	Filter #3	Filter #1	Filter #2	Filter #3	Filter #1	Filter #2	Filter #3
Preliminary Studies (pH varied)	1	70.5	23.0	12.3	57.1	25.1	13.9	19%	-8%	-12%
pH 6.0	2	92.5	30.3	21.2	62.6	22.8	20.1	32%	25%	5%
	3	102	32.6	23.2	90.7	33.8	26.2	11%	-4%	-11%
	4	133	42	28.1	78.7	32.6	27.1	41%	22%	4%
pH 7.3	1	63.8	20.6	15.5	40.4	19.0	14.0	37%	8%	10%
	2	81.6	25.7	19.3	59.5	22.7	17.5	27%	12%	9%
	3	97.7	31	22.9	71.8	23.3	22.1	27%	25%	3%
	4	110	33.3	24.4	81.0	25.3	23.0	26%	24%	6%
(after air scour)	5	103	32.4	24.0	66.4	25.6	20.4	36%	21%	15%

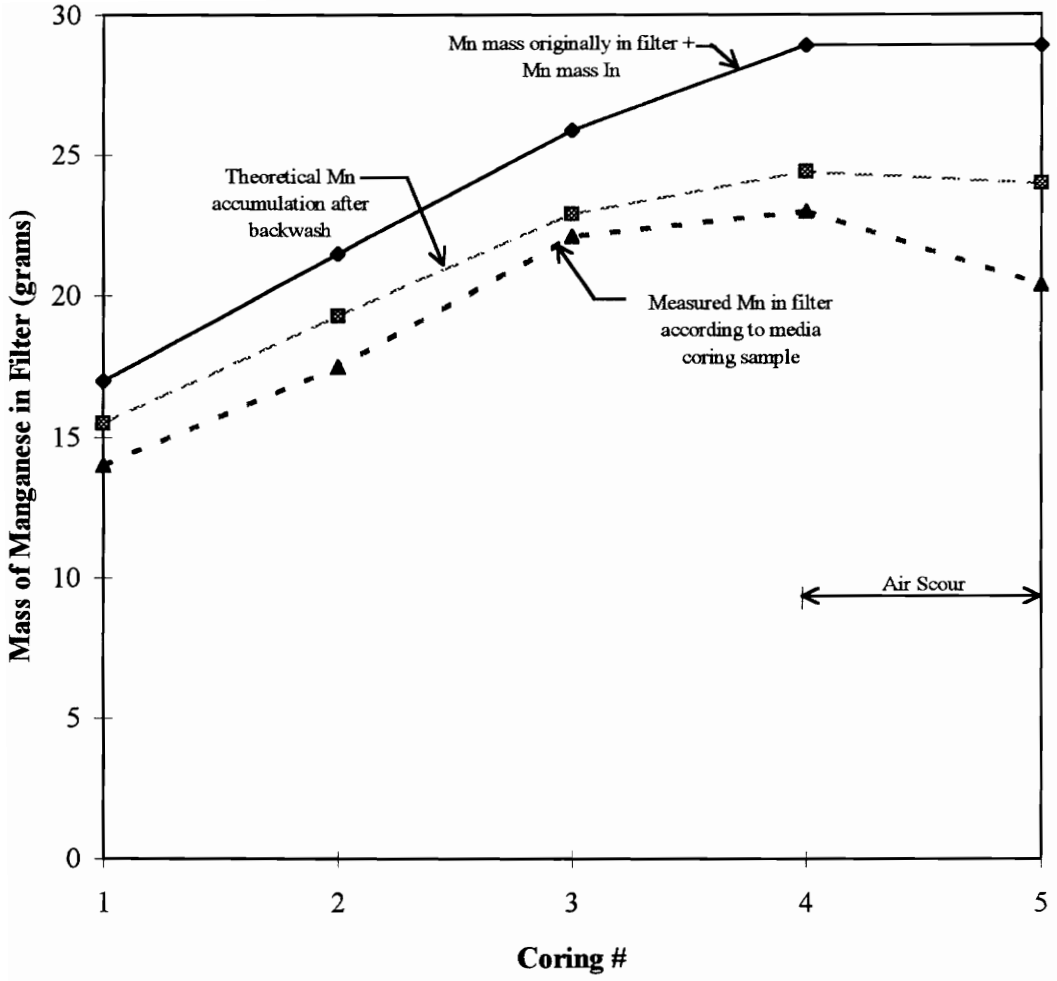

Figure 29: Mass Balance at each Coring for Filter #3 (Backwash Rate: 30 $^{gpm}/_{ft^2}$; Influent pH 7.3, with and without phosphate)

In most cases, the measured manganese accumulation was less than the theoretical manganese accumulation. The theoretical accumulation, though, was calculated from the experimental difference in the mass of manganese released during backwash and the mass of manganese added during filtration. A considerable potential for error in estimating the amount of manganese added during filtration existed due to the frequency of maintenance required for the filters and the uncertainty of pilot system changes between influent sample times. Although filter influent conditions were monitored two or three times daily, the cause and timing of any changes between those sample times were often unknown.

Frequently, the advent of a pilot system change involved a decrease or halt of chemical feed due to a pump slowing down, losing suction prime, or breaking. Many times the pilot system feed water lost pressure and the filter loading rate decreased drastically. If the manganese feed stopped, the mass of manganese added to each filter was estimated by calculating the amount of Mn(II) feed solution used and distributing it among the filters according to their flowrates. If the feed solution pump rate decreased or if the filter loading rate decreased, the mass of manganese added to each filter was estimated by averaging the influent conditions at the sample times before and after the system change to calculate an estimated amount of manganese applied to each filter. Other system changes occurred between the filters themselves. For instance, although the flowrates to individual filters were controlled, sometimes the flowrate to Filter #3 would arbitrarily increase, thereby decreasing the flowrate to Filters #1 and #2 and causing Filter #3 to overflow. Again, the mass of manganese added to each filter was estimated by averaging the influent conditions at the sample times before and after the system change. The problem with averaging the influent conditions was that the averaging effect assumed that the system change occurred half-way between the two monitoring times or that the change occurred gradually over some duration of the period between samples, both of which are probably incorrect assumptions. Calculating the theoretical manganese accumulation within each filter from the difference in the mass of manganese released

during backwash and the mass of manganese added during filtration, then, contributed uncertainty to both the "mass in" and "mass out" components of the mass balance.

The theoretical manganese accumulation tended to be greater than the measured manganese accumulation (as illustrated in Figure 29) which suggests one of the following:

1. The techniques used for estimating influent manganese during uncertain loading times, instead, overestimated the amount of manganese applied to each filter during those times.
2. The method of testing the amount of manganese removed from the filter during backwash actually underestimated the mass removed.
3. Some of the filter-applied manganese did, indeed, escape in the filter effluent despite frequent sampling that indicated negligible effluent manganese concentrations. In this case, the manganese supposedly retained in the filter would not have been available for removal from the filter by backwashing.
4. The techniques used for coring (sampling the filter media) and/or analyzing the concentration of manganese on the media underestimated the total amount of manganese contained in the filter.
5. The thin $MnO_x(s)$ coating that accumulated on the sides of the filter columns and was removed by cleaning the filters with a brush after backwash actually contained a significant amount of coating that was unaccounted for in the mass balance.

Of the five potential sources of error, the first, fourth, and fifth are the most probable causes of differences in the mass balance. The second and third potential sources of error would have resulted from unreliable laboratory analyses, which were the most controlled and statistically correct aspect of the project. The entire volume of backwash water for each filter was collected and analyzed in triplicate samples so that there was no uncertainty associated with an unknown amount of manganese lost between timed backwash samples. The effluent manganese concentrations were negligible in almost

every case, which is consistent with previous research regarding the efficiency of soluble Mn(II) removal by sorption and oxidation (Coffey, *et al.*, 1993; Knocke, *et al.*, 1988; Knocke *et al.*, 1989; Knocke *et al.*, 1991). Therefore, the second and third listed potential sources of error were the least probable causes of discrepancies in the mass balance. In fact, the most likely sources of error that contribute uncertainty to the mass balance are those associated with upsets in the pilot system and/or obtaining too infrequent influent samples and unrepresentative depth samples rather than the laboratory analysis techniques.

The techniques used for estimating the total influent manganese mass were accurate at the moment of each filter influent sample. However, the filters ran continuously and influent manganese concentration samples were taken an average of once every eight to twelve hours. The likelihood that the average of two samples spanning an eight to twelve hour loading period was a true representation of the actual loading conditions during that loading period is slight, especially in the case of a pilot system change, described earlier. Automatic sampling of each filter influent manganese concentration and metering the filter loading rate would have been the only remedy to shorten the length of time between influent samples for a more accurate estimation of the total influent mass of manganese.

From the fourth potential source of error, the technique used for coring the filter media was more likely the cause of error than the method of analyzing the concentration of manganese on the media. The quality of representation of the media coring sample to the actual manganese accumulation profile throughout the depth of the filter seemed to depend upon how well the media bed fluidized during backwash. Filter #1, the largest filter with the least backwash rate (15 $^{gpm}/_{ft^2}$), was the most difficult filter to backwash. Although the underdrain system consisted of six inches of gravel that did not move during backwash, small "currents" were obvious in the fluidized bed instead of a uniform fluidization across the surface area of the filter. The resulting media coring sample was more shallow than the actual anthracite filter bed depth. An orifice plate designed to disperse the water evenly and placed within the gravel underdrain would have been

beneficial in distributing the backwash water across the entire filter area for a more uniform fluidization of the media. The lack of uniform fluidization may have caused the filter coring device to miss some of the media when it was quickly inserted into to the filter. The smaller diameter filter columns were easier to backwash and had more uniform fluidization.

During the course of a filter loading cycle, a thin brown coating would gradually accumulate upon the sides of the filter columns. Since the object of the filtration studies was to promote accumulation upon the media, the coating was periodically (after backwash) brushed from the filter walls so as not to promote sorption and oxidation on the walls instead of on the media. However, much of the $MnO_x(s)$ side coating was probably lost in the brush or in water that spilled from the filter column during cleaning, from which the fifth potential source of error comes. As a result, that portion of $MnO_x(s)$ coating remained undetected in the mass balance since it would have been classified as part of the accumulation term but was lost to the filter walls.

One further potential source of error in estimating both the amount of manganese removed during backwash and the accumulation of manganese on the anthracite was the dilution required for manganese concentration analysis on the atomic absorption spectrophotometer (AAS). Accurate analysis on the AAS required manganese concentrations below 5 $^{mg}/_{L}$. Since the manganese concentrations in each backwash and media coring sample extraction were always unknown, dilutions were performed based upon previous dilution experience and the appearance of the sample. However, if one dilution was not sufficient to decrease the manganese concentration to below 5 $^{mg}/_{L}$, further dilutions were necessary for analysis of the sample. Each dilution compounded the potential for error in analysis of the sample.

Practical Applications to Full-Scale Water Treatment

Soluble Mn(II) Removal

Optimizing a water treatment scheme for soluble manganese removal by sorption and oxidation on filter media is uncomplicated and convenient. Raw water should be treated with the appropriate coagulants and then subjected to rapid mixing, flocculation, and sedimentation. If the intent is to remove soluble Mn(II) by sorption and oxidation in the filters, the use of strong oxidants such as ozone (O_3) or potassium permanganate ($KMnO_4$) is not recommended for oxidation or disinfection before application to the filters. Such oxidants will oxidize soluble Mn(II), thus forming particulate $MnO_x(s)$. However, mild doses of chlorine in raw water to prevent bacteria and algae growth within the flocculation and sedimentation basins is acceptable.

Drastic pH adjustments of the raw water are not recommended for removing soluble Mn(II) by sorption and oxidation. Alkaline pH conditions ($pH > 9$) cause soluble manganese to oxidize and precipitate out of solution. Acidic pH conditions ($pH < 5.5$) jeopardize the sorption process so that soluble manganese could potentially pass through the filters. Also, an acidic environment has the tendency to reduce $MnO_x(s)$ to Mn(II) and could potentially redissolve the oxidized media coating back into the filter water and allow manganese to escape the filter.

Chlorine should be added just ahead of the filters for disinfection and Mn(II) oxidation upon contact with the filter media. Enough chlorine should be used that a minimum 1 $^{mg}/_{L}$ residual free chlorine is present in the filter effluent. After filtration, additional oxidants may be added to satisfy concentration and contact time requirements and to maintain residual disinfection capabilities in the distribution system. By postponing disinfection until after sedimentation, organics and other constituents in the raw water

have an opportunity to be removed in sedimentation instead of reacting with chlorine to form chlorinated organics such as trihalomethanes.

One advantage of removing manganese from raw water by soluble Mn(II) sorption and oxidation onto $MnO_x(s)$-coated filter media is the redundancy provided naturally in the depth of the filter. Because the majority of Mn(II) sorption takes place in the upper regions of the filter, deeper regions of the filter may be considered "stand-by" sorption capacity for Mn(II) removal. If the media at the top of the filter was not sufficiently regenerated (i.e. chlorine concentration was 0 $^{mg}/_{L}$ or too low for rapid oxidation), and all of the sorption sites at the top of the filter were occupied, the sorption reaction would migrate downward through the filter and soluble Mn(II) removal would continue on the deeper $MnO_x(s)$-coated media. Mn(II) removal would continue in this manner until all the available sorption sites throughout the filter were occupied, by which time any complications with the oxidant feed should be recognized and corrected. Soluble Mn(II) removal by sorption may continue for several hours or days without regeneration of the media, dependent upon the extent of the $MnO_x(s)$ coating present on the filter media and the filter-applied water Mn(II) concentration and pH.

Backwashing may be considered a beneficial rate-of-growth controller for the $MnO_x(s)$ coating. Backwash generates a media surface disruption that removes some of the $MnO_x(s)$ coating. However, a sufficient amount of coating remains after backwash to continue soluble Mn(II) sorption and oxidation. Typical full-scale filter system media $MnO_x(s)$ coatings will also accumulate less rapidly than the coating that developed in the pilot-scale filter system under study. Raw water manganese concentrations will not usually be greater than 0.3 $^{mg}/_{L}$ and should involve shorter time periods than the pilot study. Also, backwashes on full-scale systems are typically required more often than once every three to four days, which was the frequency of backwash for the pilot-scale filters. The $MnO_x(s)$ coating in full-scale filters will probably be disturbed more frequently, resulting in a decrease in the overall rate of $MnO_x(s)$ coating accumulation.

Although the qualitative air scour study did not remove all of the $MnO_x(s)$ coating from the filter media, utilities that intend to practice both soluble Mn(II) removal by sorption and oxidation and regular air scour as part of the backwash scheme should be aware of the potential for air scour to have a detrimental effect on the $MnO_x(s)$ coating.

Particulate $MnO_x(s)$ Removal

Manganese solids (particulate $MnO_x(s)$) present in raw water require a different approach to manganese removal than soluble manganese. When manganese is already oxidized, it is not recommended to redissolve the manganese by adding chemicals or adjusting the pH just so that the manganese may be removed in the filters. Such actions are expensive and would jeopardize other treatment processes and probably inhibit sorption and oxidation, allowing manganese to escape the filters. Instead, the goal in removing influent $MnO_x(s)$ solids should be to cause the solids to adhere to one another and coagulate with other turbidity-causing agents during flocculation so that they settle out during sedimentation. Manganese particles and colloids that do not settle will be removed in the filters. However, as much $MnO_x(s)$ removal as possible should be accomplished during sedimentation to minimize the risk of colloidal manganese escaping filtration.

Summary

Generally, the pilot scale filter system functioned as predicted and even exceeded expectations for soluble manganese removal from filter applied water. Mn(II) removal by sorption and oxidation was neat and predictable with no threat of extreme headloss due to filter clogging or solids breakthrough due to shearing of filtered particles. $MnO_x(s)$ removal by particle filtration was sufficient to meet treated water standards, but the filtered water quality after removing soluble Mn(II) was more desirable, and the filters functioned more smoothly. $MnO_x(s)$ coatings also remained on the media despite regular backwashing, whereas a large amount of filtered $MnO_x(s)$ particles were removed from the filter during backwash. As a result, the $MnO_x(s)$ coating accumulated more readily upon the media when the influent manganese was in the soluble Mn(II) form. Greater backwash rates and air scour dislodged and removed more $MnO_x(s)$, whether as filtered particles or coatings, but neither cleaning technique was sufficiently harmful to the media so as to jeopardize the $MnO_x(s)$ coating required for sorption and oxidation. Also, due to the $MnO_x(s)$ coatings accumulating on the filter media, the size of the media increased slightly. However, the slight increase in filter media size occurred only in the smallest size media (located in the upper few inches of the filter). It is doubtful that this slight increase in media size would adversely impact media performance for particle removal. A mass balance on the system was difficult to quantify due to the uncertainty associated with a large pilot system.

Manganese removal from raw water may be accomplished easily using several techniques. The most reliable method of sorption and oxidation on $MnO_x(s)$-coated filter media also involves the least maintenance and fewer chemicals than any of the traditional methods of removal. For this reason, manganese removal by sorption and oxidation is economical and should be considered as an alternative to traditional manganese removal techniques.

Conclusions

The following conclusions may be formulated from the results of the research and experimentation presented in the preceding chapters:

1. Neutral or slightly acidic filter influent pH conditions ($6 \leq pH \leq 7$) inhibit Mn(II) oxidation before filtration, thus promoting sorption and oxidation of Mn(II) on $MnO_x(s)$ coated filter media. The result is a $MnO_x(s)$ coating that adheres well to filter media. Alkaline filter influent pH allows some Mn(II) oxidation before filtration, which results in significant manganese removal by $MnO_x(s)$ particle filtration. Although this is a comparable treatment method, the filtered $MnO_x(s)$ particles interfere with the formation of a uniform coating and are easily removed in backwash so that the $MnO_x(s)$ coating is not retained as efficiently on the media.
2. The primary intent of the $MnO_x(s)$ coating on the filter media was to remove influent soluble Mn(II) from filter-applied water. However, particulate $MnO_x(s)$ that was removed by particle filtration contributed to the $MnO_x(s)$ surface area within the filter and, thus, provided additional sorption sites for soluble Mn(II) removal.
3. Increases in fluid backwashing rate tended to produce greater amounts of $MnO_x(s)$ release from filter media for the duration of these backwash operations. However, backwashing did not result in complete $MnO_x(s)$ release from the media surface; rather, there was always sufficient $MnO_x(s)$ retained to permit efficient soluble Mn(II) removal after filtration operations were restarted.

4. Air scour removed a significant portion of the accumulated $MnO_x(s)$ coating at the top of the filter. However, it posed no threat to the bulk of the $MnO_x(s)$ coating present throughout the depth of the filter during the qualitative air scour study.
5. Minimal physical changes in effective size or uniformity coefficient due to a $MnO_x(s)$ coating on filter media were observed. This would imply that a $MnO_x(s)$ coating does not compromise the integrity of a filter for normal operation, headloss, and particle removal.
6. Development of a mass balance on manganese loading, backwash, and accumulation within the filter was difficult because of the uncertainties and magnitude of a pilot-scale system.

Based upon the findings of this research, sorption and oxidation of soluble Mn(II) is a rugged, dependable removal technique that is not easily upset and works within a reasonably wide range of raw water influent conditions. Because the process is easily integrated into existing facilities or new facilities, it is an economical and competitive alternative to removal of soluble Mn(II).

References

Amirtharajah, A. "Optimum Backwashing of Sand Filters." *Journal of the Environmental Engineering Division, ASCE,* Vol. 104, 917-932 (1978)

Amirtharajah, A., "Some Theoretical and Conceptual Views of Filtration." *Research and Technology, Journal AWWA,* Vol. 80, No.12, 36-46 (1988)

Bratby, J. R. "Optimizing Manganese Removal and Washwater Recovery at a Direct Filtration Plant in Brazil." *Research and Technology, Journal AWWA,* Vol. 80, No. 12, 71-81 (1988)

Buevich, Y. A., and Markov, V. G., "Pseudo-turbulent Diffusion of Particles in Homogeneous Suspensions." *International Chemical Engineering*, Vol. 10, No. 4, 570-575 (1970)

Camp, T. R., Grater, S. D., and Conklin, G. F. "Backwashing of Granular Filters." *Journal of the Sanitary Engineering Division, Proceedings of the American Society of Civil Engineers*, Vol. 97, 903-926 (1971)

Cleasby, J. L., Arboleda, J., Burns, D. E., Prendiville P. W., and Savage, E. S. "Backwashing of Granular Filters." *Research, Journal of the American Water Works Association,* Vol. 69, 115-126 (1977)

Cleasby, J. L., Stangl, E. W., and Rice, G. A. "Developments in Backwashing of Granular Filters." *Journal of the Environmental Engineering Division, ASCE,* Vol. 101, 713-727 (1975)

Coffey, B. M., Knocke, W. R., and Gallagher, D. L. "Modeling and Prediction of Soluble Manganese Removal by Oxide-Coated Media Filtration." *Journal of the Environmental Engineering Division, ASCE*, Vol. 119, 679-694 (1993)

Coffey, B. M. (1990). *Removal of Soluble Iron and Manganese from Groundwater by Chemical Oxidation and Oxide-Coated Multi-Media Filtration.* Masters Thesis, Virginia Polytechnic Institute and State University, Blacksburg, Virginia, 115 pages.

De Vitre, R. R., Buffle, J., Perret, D., and Baudat, R., "A Study of Iron and Manganese Transformations at the O_2/S(-II) Transition Layer in a Eutrophic Lake (Lake Bret, Switzerland): A Multimethod Approach." *Geochimica et Cosmochimica Acta,* Vol. 52, 1601-1613 (1988)

Edwards, S. E., and McCall, G. B. "Manganese Removal by Break-Point Chlorination: Experiences at Montebello Filters, Baltimore, MD." *Water & Sewage Works*, Vol. 93, 303-305 (1946)

Fitzpatrick, C. S. B., "Detachments of Deposits by Fluid Shear During Filter Backwashing." *Water Supply,* 177-183 (1991)

Griffin, A. E. "Significance and Removal of Manganese in Water Supplies." *Journal AWWA,* Vol. 52, 1326-1334 (1960)

Hoehn, R. C., Novak, J. T., and Cumbie, W. F. "Effects of Storage and Preoxidation on Sludge and Water Quality." *Research and Technology, Journal AWWA*, Vol. 79, No. 6, 67-75 (1987)

Huang, J. Y. C., and Basagoiti, J. "Effect of Solids Property on Rates of Dislodgment." *Journal of Environmental Engineering,* Vol. 115, 3-19 (1989)

Johnson, R. L., and Cleasby, J. L., "Effect of Backwash on Filter Effluent Quality." *Journal of the Sanitary Engineering Division*, ASCE, Vol. 92, No. SA1, Proceedings Paper 4692, 215-228 (1966)

Junta, J. L., and Hochella, Jr., M. F. "Manganese (II) Oxidation at Mineral Surfaces: A Microscopic and Spectroscopic Study." *Geochimica et Cosmochimica Acta,* Vol. 58, No. 22, 4985-4999 (1994)

Knocke, W. R., Hamon, J. R., and Thompson, C. P. "Soluble Manganese Removal on Oxide Coated Filter Media." *Research and Technology, Journal AWWA,* Vol. 193, No. 12, 65-70 (1988)

Knocke, W. R., Occiano, S., and Hungate, R., Removal of Soluble Manganese from Water by Oxide-Coated Filter Media (1989). AWWA Research Foundation and the American Water Works Association.

Knocke, W. R., Occiano, S. C., and Hungate, R. "Removal of Soluble Manganese by Oxide-Coated Filter Media: Sorption Rate and Removal Mechanism Issues." *Research and Technology, Journal AWWA,* Vol. 83, 64-69 (1991)

LaZerte, B. R., and Burling K. "Manganese Speciation in Dilute Waters of the Precambrian Shield, Canada." *Water Research*, Vol. 24, No. 9, 1097-1101 (1990)

Merkle, P. B., Knocke, W. R., Gallagher, D., Junta-Russo, J., and Solberg, T., "Characterizing Filter Media Mineral Coatings." *Journal American Water Works Association*, Vol. 88, No. 12, 62-73 (1996)

Morgan, J. T., and Stumm, W. "Colloid-Chemical Properties of Manganese Dioxide." *Journal of Colloid Science*, Vol. 19, 347-359 (1964)

Murray, J. W., Dillard, J. G., Giovanoli, R., Moers, H., and Stumm, W. "Oxidation of Mn (II): Initial Mineralogy, Oxidation State and Ageing." *Geochimica et Cosmochimica Acta,* Vol. 49, 463-470 (1985)

O'Connor, J. T. (1971). "Iron and Manganese." in: *Water Quality and Treatment.* McGraw Hill, New York, New York, 378-396.

Robinson, R. B., Dart, F. J., Pisarczyk, K., Singer, P. C., and Sung, W. "Committee Report: Research Needs for the Treatment of Iron and Manganese." *Research and Technology, Journal AWWA,* Vol. 79, No. 9, 119-122 (1987)

Standard Methods for the Examination of Water and Wastewater, 16th edition (1985). American Public Health Association (APHA), American Water Works Association (AWWA), Water Pollution Control Federation (WPCF).

Stumm, W., and Morgan, J. T. (1970). *Aquatic Chemistry.* Wiley Interscience, A Division of John Wiley & Sons, Inc., New York, New York, 583 pages.

Tobriason, J. E., and O'Melia, C. R. "Physicochemical Aspects of Particle Removal in Depth Filtration." *Research and Technology, Journal AWWA,* Vol. 80, No. 12, 54-64 (1988)

Zabrodsky, S. S. (1966). *Hydrodynamics and Heat Transfer in Fluidized Beds.* The MIT Press, Massachusetts Institute of Technology, Cambridge, Massachusetts.

Bibliography

Bhargava, D. S., and Onja, C. S. P. "A New and Rational Model for Backwash Velocity." *Transactions of the Institution of Engineers, Australia: Civil Engineering*, Vol. 32, No. 4, 187-198 (1990)

"Down to the Nitty-Gritty." *Chemical Engineer (London)*, Vol. 484, 27-28 (1990)

Johnson, R. L., and Cleasby, J. L. "Effect of Backwash on Filter Effluent Quality." *Journal of the Sanitary Engineering Division, Proceedings of the American Society of Civil Engineers (ASCE)*, Vol. 92, 215-228 (1966)

Merkle, P. B., Knocke, W. R., and Gallagher, D. L. "Filter Media Mineral Coatings: Filtration Theory and Practice." Unpublished Report. Department of Civil Engineering, Virginia Polytechnic Institute and State University, Blacksburg, Virginia.

Qureshi, N. "The Effect of Backwashing Rate on Filter Performance." *Research and Technology, Journal AWWA*, Vol. 74, No. 5, 242-248 (1982)

Walker, J. D. "High Energy Flocculation and Air-and-Water Backwashing." *Journal of the American Water Works Association*, Vol. 60, No. 3, 321-330 (1968)

Viraraghavan, T., Winchester, E. L., Brown, G. J., Wasson G. P., and Landine R. C. "Removing Manganese From Water at Fredericton, N. B., Canada." *Management and Operations, Journal AWWA*, Vol. 79, No. 8, 43-48 (1987)

Appendix A

Table A-1: Time-Based Manganese Backwash Concentrations Relative to the Total Influent Mass of Manganese after Influent pH 6.0 and pH 7.3 in the absence of phosphates ($^{mg}/_{L}/_{g}$ Mn applied to filter)

[Supplemental to Results and Discussion, Table 10: Time-Based Manganese Backwash Concentrations Relative to the Total Influent Mass of Manganese after Influent pH 6.0 and pH 7.3 in the absence of phosphates ($^{mg}/_{L}/_{Mn}$ applied to filter) (Backwash Rate = 30 $^{gpm}/_{ft^2}$)]

Table A-1: Time-Based Manganese Backwash Concentrations Relative to the Total Influent Mass of Manganese after Influent pH 6.0 and pH 7.3 in the absence of phosphates ($^{mg}/_{L}$/$_{g}$ Mn applied to filter)

Backwash Rate: 15 $^{gpm}/_{ft}{}^{2}$

		Backwash Time (minutes : seconds)																	grams Mn applied to filter during previous
	Backwash #	0:00	0:15	0:30	0:45	1:00	1:15	1:30	1:45	2:00	2:30	3:00	3:30	4:00	5:00	6:00	8:00	10:00	loading cycle
1	pH 6.0	0.04	0.22	0.07	0.07	0.09	0.08	0.07	0.09	0.1	0.1	0.09	0.1	0.08	0.1	0.09	0.1	0.1	5.9
	pH 7.3	1.5	1.5	1.5	1.4	1.5	1.5	1.2	1.2	1.0	0.9	1.1	1.0	0.9	1.0	0.7	0.7	0.6	6.0
2	pH 6.0	0.2	0.2	0.4	0.3	0.3	0.3	0.4	0.4	0.4	0.4	0.4	0.3	0.4	0.4	0.2	0.2	0.2	6.1
	pH 7.3	10.1	10.1	8.0	5.9	5.0	4.9	4.4	4.4	4.1	3.4	3.3	2.9	2.8	2.2	1.7	1.4	1.3	5.0
3	pH 6.0	0.1	0.3	0.5	1.0	0.8	0.7	0.6	0.6	0.6	0.6	0.7	0.9	1.0	0.7	0.6	0.6	0.9	6.3
	pH 7.3	27.0	19.2	17.7	17.3	16.4	13.2	11.0	10.6	7.8	5.9	5.4	4.3	3.4	2.9	2.7	1.6	1.4	4.8

Backwash Rate: 22 $^{gpm}/_{ft}{}^{2}$

		Backwash Time (minutes : seconds)																	grams Mn applied to filter during previous
	Backwash #	0:00	0:15	0:30	0:45	1:00	1:15	1:30	1:45	2:00	2:30	3:00	3:30	4:00	5:00	6:00	8:00	10:00	loading cycle
1	pH 6.0	0.6	0.9	1.0	0.8	0.6	0.6	0.5	0.5	0.5	0.5	0.5	0.5	0.5	0.5	0.5	0.5	0.5	1.8
	pH 7.3	5.1	7.3	11.2	17.5	14.7	12.8	10.0	8.4	7.0	5.8	4.5	3.9	3.5	2.7	2.4	1.8	1.3	2
2	pH 6.0	1.7	1.6	1.5	1.5	1.7	1.5	1.6	1.6	1.7	1.7	1.7	1.8	1.6	1.7	1.6	1.7	1.5	2.1
	pH 7.3	16.7	20.7	26.3	23.4	21.6	20.1	18.3	16.0	14.1	11.1		7.6	6.8	5.2	4.1	3.1	2.4	1.7
3	pH 6.0	1.6	2.2	2.8	2.7	2.8	2.9	2.9	2.9	2.9	2.8	3.0	3.0	2.7	2.5	2.2	2.1	2.0	2.4
	pH 7.3	44.3	48.6	52.4	47.3	36.4	34.3	31.0	26.1	24.3	20.5	14.2	11.2	8.4	6.6	5.0	4.0	2.8	1.6

Appendix B

Statistical Methods

Appendix B

Statistical Methods

Kruskal-Wallis nonparametric one way analysis of variance (ANOVA) and Kruskal-Wallis Multiple-Comparison tests were the primary statistical analyses performed on the data collected during the pilot-scale filtration experiments. Preliminary statistical testing indicated that the data were not normally (Gaussian) distributed, so a nonparametric test was chosen instead of the standard parametric analysis of variance. The Kruskal-Wallis ANOVA tests if the underlying population median of each of the categories is the same. If this hypothesis is rejected, the multiple comparison test is used to identify which categories are different from the other categories. These tests were used for the following purposes in this project:

1. To ensure that the influent manganese concentrations were statistically the same between the three filters. Because the influent manganese concentrations were the same, comparisons between filters for manganese removal, $MnO_x(s)$ accumulation, and other comparisons were valid.
2. To assess the differences and similarities of the influent characteristics and filter performance for manganese removal for the three pH regimes explored. The differences discovered between the influent and removal characteristics for each pH, such as the amount of particulate $MnO_x(s)$ load to the filters and the percent of total influent manganese removed by the filters, helped explain many of the anomalies uncovered during the research.

NCSS version 6.0 (NCSS Statistical Software, Kaysville, Utah) software was used to perform the analyses. Exhibits B-1 and B-2 indicate the analysis performed to generate the information for Results and Discussion, Table 9: Kruskal-Wallis Multiple-Comparison

pH 6 (pH 6)	pH 7.3WO (pH 7.3 without phosphates)	pH 7.3W (pH 7.3 with phosphates)
95.97	97.10	95.90
99.26	98.63	96.08
97.40	99.24	95.39
100.00	97.72	95.60
100.00	94.32	96.94
100.00	97.18	99.09
100.00	100.00	99.36
100.00	97.81	99.67
100.00	100.00	99.66
96.38	100.00	100.00
100.00	99.26	99.36
100.00	99.20	96.97
100.00	100.00	96.68
100.00	96.66	95.35
100.00	98.32	96.04
100.00	98.84	96.88
100.00	98.85	100.00
100.00	94.90	100.00
96.44	97.73	100.00
100.00	100.00	99.61
100.00	97.15	100.00
100.00	100.00	98.23
100.00	100.00	96.19
100.00	100.00	95.93
100.00	99.44	94.44
100.00	99.49	95.95
100.00	99.67	96.59
	98.74	99.64
	97.26	99.14
	98.36	98.01
	95.09	99.67
	97.10	100.00
	100.00	98.42
	98.02	
	100.00	
	100.00	
	99.75	

Exhibit B-1: Data for Table 9: Kruskal-Wallis Multiple Comparison Z-Value Test Comparing Average Percent Manganese Removal for each Influent pH Condition

Analysis of Variance Report

Page	1
Database	F:\NCSS60\CROWE2.S0
Time/Date	00:24:47 01-29-1997
Response	pH6,pH7.3WO,pH7.3 W

Tests of Assumptions Section

Assumption	Test Value	Prob Level	Decision (0.05)
Skewness Normality of Residuals	-3.0615	0.002202	Reject
Kurtosis Normality of Residuals	-0.3125	0.754661	Accept
Omnibus Normality of Residuals	9.4707	0.008779	Reject
Modified-Levene Equal-Variance Test	8.9641	0.000273	Reject

Box Plot Section

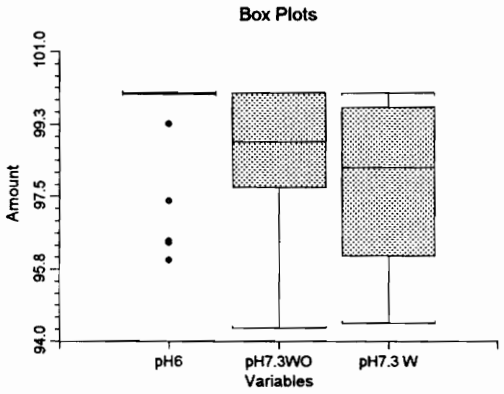

Kruskal-Wallis One-Way ANOVA on Ranks
Hypotheses
Ho: All medians are equal.
Ha: At least two medians are different.

Test Results

Method	DF	Chi-Square (H)	Prob Level	Decision(0.05)
Not Corrected for Ties	2	18.8562	0.000080	Reject Ho
Corrected for Ties	2	20.16717	0.000042	Reject Ho

Number Sets of Ties	5
Multiplicity Factor	59322

Exhibit B-2: NCSS version 6.0 Analysis for Table 9: Kruskal-Wallis Multiple-Comparison Z-Value Test Comparing Average Percent Manganese Removal for each Influent pH Condition

Analysis of Variance Report

Page	2
Database	F:\NCSS60\CROWE2.S0
Time/Date	00:24:47 01-29-1997
Response	pH6,pH7.3WO,pH7.3 W

Group Detail

Group	Count	Sum of Ranks	Mean Rank	Z-Value	Median
pH6	27	1832.50	67.87	4.1010	100
pH7.3WO	37	1711.50	46.26	-0.7538	98.85
pH7.3 W	33	1209.00	36.64	-3.1066	98.23

Kruskal-Wallis Multiple-Comparison Z-Value Test

Variable	pH6	pH7.3WO	pH7.3 W
pH6	0.0000	3.1377	4.4226
pH7.3WO	3.1377	0.0000	1.4763
pH7.3 W	4.4226	1.4763	0.0000

Regular Test: Medians significantly different if z-value > 1.9600
Bonferroni Test: Medians significantly different if z-value > 2.3940

Exhibit B-2 (continued): NCSS version 6.0 Analysis for Table 9: Kruskal-Wallis Multiple-Comparison Z-Value Test Comparing Average Percent Manganese Removal for each Influent pH Condition

Z-Value Test Comparing Average Percent Manganese Removal for each Influent pH Condition. Exhibit B-1 contains the data necessary to perform the analysis.

Exhibit B-2 contains the results of the comparison between each set of data. The table of values under "Kruskal-Wallis Multiple-Comparison Z-Value Test" indicate if the data sets are the same. For each comparison, if the z-value is greater than 1.96, then the medians are significantly different.

VITA

Andrea Lea Crowe was born in Memphis, Tennessee on June 14, 1971. After living in Memphis for most of her childhood, she moved with her family to Cookeville, Tennessee in 1984. She graduated from Cookeville High School in 1989 and went to Tennessee Technological University, Cookeville, Tennessee. She pursued extracurricular interests in music while obtaining a Bachelor of Science degree in Civil Engineering by May, 1994.

Andrea entered graduate school as a Via Scholar at Virginia Polytechnic Institute and State University in the fall of 1994. She spent much research time at the Blacksburg, Christiansburg, VPI Water Authority, where her pilot system was located. After the data collection for her research was completed, Andrea started her first full-time job with Black & Veatch, Charlotte, North Carolina in February, 1995. She completed the requirements for a Master of Science Degree in Environmental Engineering in January, 1997.

At the time of completion of her thesis, Andrea was working for Black & Veatch in Greenville, South Carolina.

Andrea L. Crowe